Title
Development of Carbonate Clumped-Isotope Paleothermometry for Application to Paleozoic Fossils

Author
Petrizzo, Daniel Anthony

Publication Date
2013

Peer reviewed|Thesis/dissertation

UNIVERSITY OF CALIFORNIA

Los Angeles

Development of Carbonate Clumped-Isotope Paleothermometry for Application to Paleozoic Fossils

A dissertation submitted in partial satisfaction of the requirements for the degree Doctor of Philosophy in Geology

by

Daniel Anthony Petrizzo

2013

ABSTRACT OF THE DISSERTATION

Development of Carbonate Clumped-Isotope
Paleothermometry
for Application to Paleozoic Fossils

by

Daniel Anthony Petrizzo
Doctor of Philosophy in Geology
University of California, Los Angeles, 2013
Professor Bruce N. Runnegar, Chair

Making precise measurements of clumped-isotopes in CO_2 (reported as Δ_{47}) is resource-intensive and time-consuming. Instrument and time-related variability of measured Δ_{47} values have hindered inter-laboratory calibration efforts. Additionally, clumped-isotopes measured in Paleozoic fossils suggest ancient marine temperatures and/or ocean isotopic compositions that are difficult to accept at face value.

This dissertation describes a strategy for measuring Δ_{47} on a conventional mass spectrometer, with the usual CO_2 set of three Faraday collectors by "multicollector peak hopping" (MPH). The MPH method involves directing $m/z = 46$ and $m/z = 47$ ion beams into the

Faraday cups used for *m/z* = 44 and *m/z* = 45, and then calculating Δ_{47} from sample $\delta^{13}C$, $\delta^{18}O$, and measured $^{47/46}CO_2^+$. This method includes a protocol for correcting ion-beam intensities for secondary electrons in order to remove Δ_{47} dependence on $\delta^{47}CO_2$.

Measurements of Δ_{47} in CO_2 liberated from modern bivalved mollusc shells demonstrate that electron scatter has a significant influence on Δ_{47} values. As this effect is similar in magnitude to the pairwise differences between carbonate temperature calibrations that were made using different instruments, it is possible that electron scatter is responsible for these discrepancies. The observed relationship between Δ_{47} and growth temperature preserved in modern mollusc shell is very close to theoretical predictions for Δ_{47} in calcite.

Measurements of Δ_{47} in CO_2 liberated from shells of the Permian bivalved mollusc *Eurydesma cordatum* yield paleotemperatures that are too high to conform with geologic indicators for near-freezing water temperatures, yet too low to represent maximum burial temperatures. Cycles in $\delta^{18}O$ that are in-phase with growth bands suggest that this fossil did not exchange oxygen isotopes with water after the precipitation of the carbonate, meaning that ^{13}C-^{18}O bonds were re-ordered at low temperature in the absence of significant amounts of fluid. It is suggested that original seawater was present in trace amount, enough to catalyze ^{13}C-^{18}O bond re-ordering, but without affecting $\delta^{18}O$ of the shell. Such subtle alteration eludes detection with current screening methods. Unless the role of geologic processes in altering Δ_{47} is better understood, successful application of clumped-isotope paleothermometry to Paleozoic fossils may be limited.

The dissertation of Daniel Anthony Petrizzo is approved.

Edward D. Young

Edwin A. Schauble

Raymond V. Ingersoll

David K. Jacobs

Bruce N. Runnegar, Committee Chair

University of California, Los Angeles

2013

DEDICATION

I dedicate this dissertation to Hilary and Dominic.

Contents

List of Tables and Figures

Acknowledgements

I would like to thank my advisor Bruce Runnegar for his time and patience. He was always supportive and encouraging of my work with clumped-isotopes. His example as a researcher and teacher — in both the field and the classroom — over the seven years that I have known him has been invaluable. I cannot thank him enough for the opportunity I have had to work with him.

I would also like to thank Professor Edward Young for providing me access to an open and collaborative stable isotope laboratory environment in which to learn and experiment. His boldness, enthusiasm, and willingness to try almost any experiment was in large part the inspiration for my education in mass spectrometry. In addition, his participation as a co-author and code writer was critical to the sections of this dissertation that have been submitted for publication.

I would like to thank Professor Edwin Schauble and Professor Ray Ingersoll for great editorial suggestions concerning this dissertation, but more importantly, for providing me with insight into their geological/geochemical research, and also sage advice and encouragement over several years.

I would also like to express my gratitude to Karen Ziegler and Laurence Yeung for their support in the laboratory. Karen's technical knowledge was a great help to me, and she ordered and tracked virtually every part of the systems we constructed to liberate, extract, and purify CO_2

from carbonates. Laurence Yeung's technical knowledge, positive attitude, and great sense of humor were a tremendous resource for me during the most trying times in the laboratory.

Finally, I would like to thank Lauri Holbrook, Kathleen Micham, Rick Fort and Issaku Kohl for all different types of support of this research. You may not remember everything you did to help me, but I want you to know I remember and appreciate all of it.

Funding for this research came from both the Department of Earth and Space Sciences at University of California, Los Angeles, and the NASA Astrobiology Institute.

Curriculum Vitae

Name:	Daniel Anthony Strong Petrizzo

Presentations:

December 7, 2011	American Geophysical Union Fall Meeting Presentation title: "Clumped-Isotope Temperatures From Known and Proposed Paleozoic Glacial Intervals Suggest that Oceans Were Depleted in $\delta^{18}O$"
August 9, 2011	Clumped-Isotope Workshop, Imperial College London Presentation title: "A 'Direct Method' for Measuring Δ_{47} in Calcitic Fossils Indicates Cold Tropical Sea Surface Temperatures During A Large Silurian $\delta^{13}C$ Excursion"

University Education:

2004 – 2007	Undergraduate studies (non-degree seeking) at Pasadena City College, Glendale Community College and University of California, Los Angeles Coursework equivalent to Bachelor of Science in Geology
1992 – 1996	Undergraduate studies at University of Florida Degree awarded: Bachelor of Arts (History)
1991 – 1992	Undergraduate studies at University of South Florida

School Education:

1988 – 1991	Bloomingdale Senior High School (Valrico, Florida)
1986 – 1988	Pearl River High School (Pearl River, NY)
1983 – 1986	Pearl River Middle School (Pearl River, NY)
1978 – 1983	Franklin Avenue Elementary School (Pearl River, NY)

During the years 1996–2003 I lived and worked in Manhattan. I was an executive in the technology sector employed by several corporations that provided cellular phone service (1996–1997), commercial internet connectivity (1997–2000), database software (2000-2001), and professional technical services to the financial sector (2001–2003). While I found this work to be financially rewarding, I felt unfulfilled, and abandoned that career to attempt a more rewarding career as a scientific researcher and educator.

Chapter 1

Introduction

"It would be interesting indeed to know not only the mean temperature but also the variations of temperature on an ancient beach or in the forests where coal was deposited and whether a prehistoric animal had warm blood or not. However, too much optimism is not justified, for all the thermometers may be destroyed."

– Harold C. Urey, 18th December 1946. Liversidge Lecture delivered before the Chemical Society in the Royal Institution, London (Urey, 1947).

1.1 OXYGEN ISOTOPE THERMOMETRY AND DIFFICULTIES WITH OXYGEN ISOTOPE THERMOMETRY

Since Urey (1947) first suggested the idea of leveraging the thermodynamic properties of isotopic substances for use as paleothermometers, the oxygen isotopic composition of biogenic marine carbonates has been widely used to estimate past ancient ocean temperatures (e.g., Urey et al., 1951). However, there are three inherent liabilities of this proxy when applied to fossils: 1) by itself, the paleothermometer has difficulty detecting instances when precipitation in disequilibrium with seawater has occurred, 2) the oxygen isotopic composition of the water that the minerals formed in must be known, and 3) the fossils must have maintained oxygen isotopic fidelity despite having experienced subsequent geologic processes that include exposure to geothermal heat from burial and/or intrusive igneous activity, and geochemical reactions with subsurface fluids.

The first of these potential complications has been constrained by measuring oxygen isotope ratios in the skeletons of modern organisms that grew at known temperatures. Living foraminiferans, ahermatypic corals, brachiopods, bryozoans, molluscs, fish and most echinoderms are known to precipitate calcium carbonate in isotopic equilibrium with seawater, while hermatypic corals, echinoids and arthropods do not (Wefer and Berger, 1991). It is generally assumed that ancient relatives of living organisms precipitated their skeletons using similar mechanisms, and therefore should maintain equilibrium or disequilibrium precipitation accordingly, but this is impossible to know with certainty.

The second difficulty with applying the oxygen isotope paleothermometer to ancient fossils, knowing the isotopic composition of the precipitating fluid, is intractable (cf. Adkins and Schrag, 2003 concerning estimation of much more recent marine $\delta^{18}O$). However, the safest assumption is that high-temperature and low-temperature exchange between seawater and silicates, thought to control the oxygen isotopic composition of oceans on long timescales (Muehlenbachs and Clayton, 1976), has been relatively stable over Earth's long history. Measurements of oxygen isotope ratios in Precambrian ophiolites support this concept (Holmden and Muehlenbachs, 1993; but see Ivany and Runnegar, 2010). Additionally, water-rock exchange rates are thought to allow for a maximum change of ~ 1 ‰ per 10^8 years (Walker and Lohmann, 1989), so variations occurring during the relatively short Phanerozoic (~ 5 x 10^8 years) could not have been very large (5‰). In the modern ocean, latitudinal gradients of ~ 2.0 ‰ (Atlantic Ocean) and ~ 1.5 ‰ (Pacific Ocean) are due to increased evaporation in the tropics, and higher contributions from freshwater runoff at high latitudes (LeGrande and Schmidt, 2006). In the

longer term, oceanic $\delta^{18}O$ is further affected by the presence of a significant volume of continental ice, which is isotopically light and therefore drives oceanic $\delta^{18}O$ towards higher values. Oceanic $\delta^{18}O$ is assumed to be – 1 ‰ SMOW on an ice-free Earth, and + 1 ‰ SMOW during the Last Glacial Maximum (LGM) compared with the present average of 0‰. Finally, local and regional variability can have the greatest effect. Enrichment in ^{18}O is significant in highly evaporative estuaries, such as the Hamelin Pool end of Shark Bay, Western Australia ($\delta^{18}O$ > +5 ‰ SMOW; see Chapter 5) and the Mediterranean Sea ($\delta^{18}O$ ~ +3 ‰ SMOW; Gat et al., 1996), whereas freshwater contributions from isotopically light ice melt or river runoff can drive oxygen isotope ratios to significantly lower values.

The third uncertainty, isotopic fidelity, is also difficult to constrain. Marine fossils may exchange oxygen atoms with sea or meteoric water before, during, and after burial. This can be particularly problematic for fossils of warm-water pelagic animals, as oxygen isotope ratios may indicate water temperatures that are cooler than the actual growth temperatures if annealing, Ostwald ripening, or partial recrystallization takes place in cold bottom waters (Pearson, 2012). Exchanging oxygen isotopes with seawater at any significant burial depth will result in temperatures that will almost certainly be higher than the original shell growth temperatures. Finally, even long-buried fossils can encounter and exchange oxygen isotopes with isotopically light water (at any elevated temperature) in the form of phreatic lenses that migrate through carbonate-cemented sandstones and silts (Knauth and Kennedy, 2009). In short, post-mortem carbonate/water exchange at almost any time will compromise the fidelity of the paleothermometer.

Combining visual inspection of shell microstructures using scanning electron microscopy (SEM) and cathodoluminescense (CL) with measurements of trace element (Fe, Sr, Mn) content is often used to screen fossils for evidence of alteration. SEM inspection can reveal modification of original shell microstructure, while CL may reveal potential zones of altered mineral enriched in Fe and Mn (Azmy et al., 1998; Samtleben et al., 2001). Interaction with subsurface water is known to increase the concentration of Fe and Mn, and decrease concentrations of Sr in carbonates. A positive correlation between skeletal $\delta^{13}C$ and $\delta^{18}O$, presumably resulting from exchange with isotopically light terrestrial water (that also contains isotopically light carbon from biomass) is often used to assess the relative quality of preservation of individual shells within stratigraphically associated assemblages (Azmy, et al., 1998; Knauth and Kennedy, 2009). However, these tests only provide certainty in the case of positive results; a minimum amount of alteration may never be established using these criteria.

1.2 A NEW APPROACH: CLUMPED-ISOTOPE THERMOMETRY

Urey (1947) also suggested that slight mass differences between di-atomic and tri-atomic molecules containing multiple isotopic substitutions could also be useful for paleothermometry if they could be accurately measured, something not possible in the 1950s. Eiler and Schauble (2004) demonstrated that the proportion of CO_2 molecules containing more than a single heavy isotope of carbon and/or oxygen (multiply substituted isotopologues or clumped isotopes; i.e.: ^{13}C-^{18}O-^{16}O, ^{12}C-^{18}O-^{18}O, ^{13}C-^{18}O-^{18}O, or any combination which contains more than one ^{13}C,

^{17}O, or ^{18}O), could be accurately measured in air samples. This proportion was reported as the abundance of $^{47}CO_2$ in comparison to the expected abundance of $^{47}CO_2$ in a stochastic mixture of the same isotopic composition, and was designated Δ_{47}. Additionally, Eiler and Schauble (2004) suggested that carbonate minerals may record and preserve their formation temperature, and might be analyzed through measurement of CO_2 liberated through acid digestion of those minerals. The fact than such a paleothermometer could work entirely independently of the isotopic composition of component material, means that it may be applied to carbonate minerals from past and present marine environments where the $\delta^{18}O$ of the water from which the carbonates precipitated is unknown.

Ghosh et al. (2006) demonstrated that this water-independent mineral-based thermometer does work by determining the relationship between formation temperatures and the relative abundance of ^{13}C-^{18}O bonds (best represented by Δ_{47}/T^2) in calcites grown in the laboratory at temperatures ranging from 1 to 50 °C. Measurements of three coral samples suggested that the carbonate skeletons of marine organisms may also conform to the Δ_{47}/T^2 relationship demonstrated by the inorganic calcites. Since the corals used are aragonitic in composition, the authors concluded that there is little difference in Δ_{47}/T^2 measured in aragonite and calcite. As these corals demonstrated "vital effects" in their bulk $\delta^{13}C$ and $\delta^{18}O$ values, the authors concluded that clumped-isotope thermometry is little, if at all, affected by "vital effects" that might influence the isotopic composition of biogenic carbonates.

1.3 EARLY CLUMPED-ISOTOPE PALEOTHERMOMETRY OF PALEOZOIC FOSSILS

The first application of clumped-isotope paleothermometry to ancient (Paleozoic) fossils compared clumped-isotope measurements in fossil shells from two ages (Silurian and Pennsylvanian) thought to represent very different global climate states (Came et al., 2007). Well-preserved early Silurian (Aeronian) brachiopods from the Jupiter Formation of Anticosti Island, Canada (Azmy et al., 1998), were chosen to represent the greenhouse conditions thought to dominate global climate during the early Paleozoic. Exceptionally-preserved aragonitic molluscs from the Middle Pennsylvanian (Moscovian) Boggy Formation of Oklahoma were selected to represent the icehouse conditions of the Late Paleozoic Ice Age (LPIA).

Temperatures calculated from measured Δ_{47} values indicated warmer growth temperatures for the Silurian samples (~ 35 °C) than for the Pennsylvanian samples (~ 25 °C). However, using those temperatures and the $\delta^{18}O$ values reported for the shells the authors calculated that the $\delta^{18}O$ of ocean water was approximately −1.1 ‰ SMOW during the Silurian and about −1.7 ‰ SMOW during the Pennsylvanian (Table 1 and Fig. 3 in Came et al., 2007). These results are the opposite of those expected: $\delta^{18}O$ for the ocean should be roughly −1 ‰ for an ice-free Earth and is estimated to have been about +1 ‰ during the LGM. As previously mentioned, evidence for widespread glaciation suggests that ice volumes during colder phases of the Late Paleozoic Ice Age were comparable to Pleistocene glacial maxima, so the $\delta^{18}O$ of the LPIA oceans should have been significantly heavier, not lighter than −1 ‰.

When comparing $\delta^{13}C$ and $\delta^{18}O$ in shells deemed "altered" and "suspected of alteration", Came et al. (2007) noted that measured values contradicted expectations based on studies of alteration (Land 1986; Knauth and Kennedy, 2009). In the Pennsylvanian samples, clumped-isotope temperatures increase with both $\delta^{13}C$ and $\delta^{18}O$. However, alteration through exchange of oxygen isotopes with ^{18}O-depleted meteoric water at elevated temperature should drive $\delta^{18}O_{carbonate}$ to lower values, the opposite of the observed trend. As a result, calculated values for ocean $\delta^{18}O$ also increase with degree of alteration. Although isotopic exchange with an ^{18}O-enriched brine (Clayton et al., 1966) would easily explain this sort of observation, it does not for these samples. The Pennsylvanian samples measured by Came et al. (2007) came from the Buckhorn Asphalt Quarry, where early impregnation of the surrounding sediments by hydrocarbons prevented aragonite destruction, and preserved shell microstructures and microornaments that would have been destroyed by interaction with circulating pore waters (Seuß et al., 2009). An alternative hypothesis is that these samples were buried with seawater that partially escaped very soon after burial. In this situation, the samples that had lost the greatest amount of water would have the most ^{18}O enriched residual water left to then exchange oxygen isotopes with the aragonite. However, to explain the magnitude of increase in $\delta^{18}O$ values (~2.5 ‰) of the "altered" shells would require a significant amount of residual water.

The Silurian brachiopods studied by Came et al. (2007) yielded higher clumped isotope temperatures, but no discernable trend in $\delta^{18}O$ with perceived alteration (as reflected by their Δ_{47} values). These results suggest that the Silurian samples were somehow altered without having exchanged oxygen isotopes with water of a different oxygen isotopic composition. New

mechanisms may be needed to explain alteration observed in both the Silurian and Pennsylvanian samples (Chapter 4).

Finnegan et al. (2010) measured Δ_{47} in Late Ordovician (Katian-Hirnantian) and Silurian (Rhuddanian-Aeronean) rugose corals, brachiopods, trilobites and bryozoans from Anticosti Island, Canada to assess changes in water temperature and ice volume during the Hirnantian large positive carbon isotope excursion. The results indicated, as long expected, an abrupt (~ 5 °C) drop in tropical surface water temperatures coincident with geologic indicators for glaciation at high latitudes and a global marine mass extinction. However, estimates of global ocean $\delta^{18}O$ of up to + 3 ‰ at the peak of the carbon isotope excursion are problematic. Ocean oxygen isotopic ratios as high as this imply either ice volumes far in excess of volumes estimated for the LGM (Fig. 3D in Finnegan et al., 2010), or volumes similar to those of the LGM of extraordinarily isotopically light ice ($\delta^{18}O < -60$ ‰; Fig. S11 in Finnegan et al., 2010). In addition, the results imply that the initial glaciation of Gondwana occurred with little or no cooling of the tropical oceans, that tropical sea surface temperatures exceeded those of the modern day throughout all but the peak of Gondwanan glaciation, and that the return to high (~ 35 °C) water temperatures occurred quickly and remained elevated (~34–38 °C) despite several million years with substantial ice volume on the Gondwanan supercontinent. Finnegan et al. (2010) concluded that their results should be regarded as maximum estimates of sea surface temperatures.

It is important to note that the brachiopods from Anticosti Island, which were used in both studies, are some of the best preserved from their time. Azmy et al. (1998) took great care

in screening the samples, using the methods mentioned above, for the purpose of determining the carbon and oxygen isotopic compositions of Silurian seawater. Samples in Azmy et al.'s collection demonstrating the least evidence (or no evidence) of alteration in the original study were selected for clumped-isotope analysis. Similarly, Finnegan et al. (2010) screened a "large and representative subset of samples" and concluded that most samples were well preserved based on trace element abundance and visual inspection using SEM. However, the previously mentioned tests only indicate alteration where carbonate has interacted significantly with intrastratal fluids in an open system, and will not be able to detect subtle, closed-system alteration.

1.4 ADVANCES IN Δ_{47} MEASUREMENT

At the time that this research began, other laboratories were reporting difficulties in accurately measuring Δ_{47} in CO_2 gas. The first issue to be reported was a dependence of measured Δ_{47} on sample $\delta^{47}CO_2$ ($\delta^{47}CO_2 \approx \delta^{13}C + 2\delta^{18}O$). It was found that CO_2 standards that are re-equilibrated at known temperatures and are different in isotopic composition from the reference CO_2 gas used in making the measurements, give temperatures that are either too low when the standard is heavier in $\delta^{47}CO_2$, or too high when the standard is lighter in $\delta^{47}CO_2$ (Huntington et al., 2009). This problem became known as "non-linearity" (Huntington et al., 2009), even though the relationship between Δ_{47} and $\delta^{47}CO_2$ is known to be approximately linear. The non-linearity problem was shown to be a feature of all of the mass spectrometers that

had measured clumped-isotopes in CO_2 at that point in time (all being Thermo-Finnigan 253s), and to be unstable at the scale of weeks to months.

A method was soon developed in order to define and correct for this "non-linearity", the "heated gas" (HG) correction of Huntington et al. (2009), but the process responsible for the "non-linear" behavior, and other methods to correct it, remained uncertain until 2012. Since then, several laboratories have had success in reducing or removing the non-linearity by monitoring and subtracting instrument backgrounds known to be caused by the presence of secondary electrons (Yeung et al., 2012; He et al., 2012; Bernasconi et al., 2013; this study Chapter 2).

In addition, inter-laboratory comparisons of the clumped-isotope results remain difficult despite similar measurement and data correction methods. This was at least partially due to a so-called "scale compression" effect whereby the difference in Δ_{47} measured between two samples of identical composition but equilibrated at different temperatures, was found to be laboratory-dependent (Dennis et al., 2011). These authors suggested that fragmentation and recombination reactions that occurred in the sources of mass spectrometers were responsible, and could be negated by transferring values measured in each laboratory to a "universal reference frame". This reference frame is based on the theoretical values for ^{13}C-^{18}O-^{16}O clumping of Wang et al. (2004) and measurements are transferred by means of a $\Delta_{47theoretical}/\Delta_{47measured}$ calibration line. Originally published as an "absolute reference frame", this standardization has more recently been referred to as the carbon dioxide equilibrium scale (CDES; Henkes et al., 2013). Comparisons of recent measurements of Δ_{47} in CO_2 liberated from modern biogenic carbonates

in different laboratories indicates that, despite the CDES scale, precise inter-laboratory calibration is incomplete (Chapter 3).

1.5 TEMPERATURE CALIBRATIONS FOR THE CARBONATE CLUMPED-ISOTOPE THERMOMETER

Temperatures obtained from Δ_{47} measured from fossils, must necessarily be made by comparison to an empirical calibration generated from measurements of Δ_{47} in carbonates precipitated at known temperatures. Previously mentioned studies of Δ_{47} in fossils employed the Ghosh calibration of inorganic calcite grown in the laboratory at temperatures ranging from 1 – 50 °C (Ghosh et al., 2006). Dennis et al. (2011) transferred this calibration to the CDES scale. Early studies involving modern bivalved molluscs and brachiopods (Came et al., 2007, supplementary information p. 2), foraminiferans and coccoliths (Tripati et al., 2010), and corals (Thiagarajan et al., 2011), all of which were measured in the same laboratory as the inorganic calcites grown by Ghosh et al. (2006), generally agree well with the Ghosh calibration. A second inorganic calcite-based calibration (Dennis and Schrag, 2010) indicated a less sensitive Δ_{47}/T^2 relationship (lower slope). Another study of foraminiferans (Grauel et al., 2013) also produced a line lying close to Ghosh et al.'s (2006) calibration. However, recent work suggests that living molluscs and brachiopods do not conform to this widely used Δ_{47}/T^2 relationship (Henkes et al., 2013; Dennis et al., 2013; this study Chapter 3), and are in fact more similar to the inorganic calcite-based calibration of Dennis and Schrag (2010).

1.6 CURRENT STATE OF CLUMPED-ISOTOPE PALEOTHERMOMETRY IN PALEOZOIC FOSSILS

At present, it is difficult to accept temperatures derived from measurements of Δ_{47} in CO_2 derived from ancient fossils at face value. It is likely that temperature trends are fairly well represented by measurements of clumped-isotopes in single species that are found in close stratigraphic association (e.g., Finnegan et al., 2010). However, differences in Δ_{47} values obtained from shells of a single species, but measured in different laboratories, illustrate complications with carbonate calibration efforts. It is currently not known whether this disagreement is due to laboratory-specific differences in CO_2 liberation, gas handling and purification methods, or instrument-related effects. This thesis addresses current issues concerning instrumentation, measurement and data correction methods, and interruptions to the carbonate clumped-isotope thermometer due to diagenetic processes.

1.7 REFERENCES

Azmy K., Veizer J., Bassett M.G. and Copper P. (1998). Oxygen and carbon isotopic composition of Silurian brachiopods: Implications for coeval seawater and glaciations. *GSA Bulletin* **110**, 1499–1512.

Bernasconi S.M., Hu B., Wacker U., Fiebig J., Breitenbach S.F. and Rutz T. (2013) Background effects on Faraday collectors in gas–source mass spectrometry and implications for clumped isotope measurements. *Rapid Communications in Mass Spectrom.* **27**, 603–612.

Came R.E., Eiler J.M., Veizer J., Azmy K., Brand U. and Weidman C.R. (2007) Coupling of surface temperatures and atmospheric CO_2 concentrations during the Palaeozoic Era. *Nature* **449**, 198–201.

Clayton R.N., Friedman I., Graf D.L., Mayeda T.K., Meents W.F. and Shimp N.F. (1966) The origin of saline formation waters: 1. Isotopic composition. *J. Geophys. Res.* **71**, 3869–3882.

Dennis K.J. and Schrag D.P. (2010) Clumped isotope thermometry of carbonatites as an indicator of diagenetic alteration. *Geochim. Cosmochim. Acta* **74**, 4110–4122.

Dennis K. J., Affek H. P., Passey B. H., Schrag D. P. and Eiler J. M. (2011) Defining an absolute reference frame for 'clumped' isotope studies of CO_2. *Geochim. Cosmochim. Acta* **75**, 7117–7131.

Dennis K.J., Cochran J.K., Landman N.H. and Schrag D.P. (2013) The climate of the Late Cretaceous: New insights from the application of the carbonate clumped isotope thermometer to Western Interior Seaway macrofossil. *Earth Planet. Sci. Lett.* **362**, 51–65.

Eiler J.M. and Schauble E.A. (2004) $^{18}O^{13}C^{16}O$ in Earth's atmosphere. *Geochim. Cosmochim. Acta* **68**, 4767–4777.

Finnegan S., Bergmann K., Eiler J.M., Jones D.S., Fike D.A., Eisenman I., Hughes N.C, Tripati A.K. and Fischer W.W. (2011) The magnitude and duration of late Ordovician-early Silurian glaciation. *Science* **331**, 903–906.

Gat J.R., Shemesh A., Tziperman E., Hecht A., Georgopoulos D. and Basturk O. (1996) The stable isotope composition of waters of the eastern Mediterranean Sea. *J. Geophys. Res.: Oceans* **101**, 6441–6451.

Ghosh P., Adkins J., Affek H., Balta B., Guo W., Schauble E. A., Schrag D. P. and Eiler J. M. (2006) ^{13}C–^{18}O bonds in carbonate minerals: a new kind of paleothermometer. *Geochim. Cosmochim. Acta* **70**, 1439–1456.

Grauel A.L., Schmid T.W., Hu B., Bergami C., Capotondi L., Zhou L. and Bernasconi S.M. (2013) Calibration and application of the 'clumped isotope' thermometer to foraminifera for high-resolution climate reconstructions. *Geochim. Cosmochim. Acta* **108,** 125–140.

He B., Olack G.A. and Colman A.S. (2012) Pressure baseline correction and high-precision CO_2 clumped-isotope (Δ_{47}) measurements in bellows and micro-volume modes. *Rapid Communications in Mass Spectrom*. **26**, 2837–2853.

Henkes G.A., Passey B.H., Wanamaker Jr. A.D., Grossman E.L., Ambrose Jr. W.G. and Carroll M.L. (2013) Carbonate clumped isotope compositions of modern marine mollusk and brachiopod shells. *Geochim. Cosmochim. Acta* **106**, 307–325.

Holmden C. and Muehlenbachs K. (1993) The $^{18}O/^{16}O$ ratio of 2-billion-year-old seawater inferred from ancient ocean crust. *Science* **259**, 1733–1736.

Huntington K.W., Eiler J.M., Affek H.P., Guo W., Bonifacie M., Yeung L.Y., Thiagarajan N., Passey B.H., Tripati A., Daëron M. and Came R. (2009) Methods and limitations of 'clumped' CO_2 isotope (Δ_{47}) analysis by gas-source isotope ratio mass spectrometry. *J. Mass Spectrom*. **44**, 1318–1329.

Kasting J.F., Howard M.T., Wallmann K., Veizer J., Sheilds G. and Jaffres J. (2006) Paleoclimates, ocean depth, and the oxygen isotopic composition of seawater. *Earth Planet. Sci. Lett.* **252**, 82–93.

Knauth L.P. and Kennedy M.J. (2009) The late Precambrian greening of the Earth. *Nature* **460**, 728–732.

Land L.S. (1986) Limestone diagenesis – some geochemical considerations. *US Geol. Surv. Bulletin* **1578**, 129–137.

LeGrande A. N. and Schmidt G. A. (2006) Global gridded data set of the oxygen isotopic composition in seawater. *Geophys. Res. Lett.* **33**, L12604, 5 pp.

Muehlenbachs K. and Clayton R.N. (1976) Oxygen isotope composition of the oceanic crust and its bearing on seawater. *J. Geophys. Res.* **81**, 4365–4369.

Pearson P.N. (2012) Oxygen isotopes in foraminifera: overview and historical review, in: Ivany, L.C., Huber, B.T. (Eds.), *Reconstructing Earth's Deep-Time Climate.* Yale University Printing and Publishing, pp.1–38.

Samtleben C., Munnecke A., Bickert T. and Pätzold J. (2001) Shell succession, assemblage and species dependent effects on the C/O-isotopic composition of brachiopods - examples from the Silurian of Gotland. *Chem. Geol.* **175**, 61–107.

Seuß B., Nützel A., Mapes R.H. and Yancey T.E. (2009) Facies and fauna of the Pennsylvanian Buckhorn Asphalt Quarry deposit: a review and new data on an important Palaeozoic fossil *Lagerstätte* with aragonite preservation. *Facies* **55**, 609–645.

Thiagarajan N., Adkins J. and Eiler J. (2011) Carbonate clumped isotope thermometry of deep-sea coral and implications for vital effects. *Geochim. Cosmochim. Acta* **75**, 4416–4425.

Tripati A. K., Eagle R. A., Thiagarajan N., Gagnon A.C., Bauch H., Halloran P.R. and Eiler J.M. (2010) ^{13}C–^{18}O isotope signatures and 'clumped isotope' thermometry in foraminifera and coccoliths. *Geochim. Cosmochim. Acta* **74**, 5697–5717.

Walker J.C.G. and Lohmann K.C. (1989) Why the oxygen isotopic composition of seawater changes with time, *Geophys. Res. Lett.* **16,** 323–326.

Wang Z., Schauble E.A. and Eiler J. M. (2004) Equilibrium thermodynamics of multiply substituted isotopologues of molecular gases. *Geochim. Cosmochim. Acta* **68**, 4779–4797.

Wefer G. and Berger, W. (1991) Isotope paleontology: growth and composition of extant calcareous species. *Marine Geol.* **100**, 207–248.

Urey H.C. (1947) The thermodynamic properties of isotopic substances. *Journal of the Chemical Society (Resumed)*, 562–581.

Urey H.C., Lowenstam H.A., Epstein S. and McKinney, C.R. (1951) Measurement of paleotemperatures and temperatures of the Upper Cretaceous of England, Denmark, and the southeastern United States. *GSA Bulletin **62***, 399–416.

Yeung L.Y., Young E.D. and Schauble E.A. (2012) Measurements of $^{18}O^{18}O$ and $^{17}O^{18}O$ in the atmosphere and the role of isotope-exchange reactions. *J. Geophys. Res.* **117**, DOI: 10.1029/2012JD017992.

CHAPTER 2

HIGH PRECISION DETERMINATION OF ^{13}C-^{18}O BONDS IN CO_2 USING MULTICOLLECTOR PEAK HOPPING[1]

[1] Manuscript co-authored by D.A. Petrizzo and Young E.D. prepared for submission to *Rapid Communications in Mass Spectrometry*, March 2013.

2.1 ABSTRACT

RATIONALE: Rapid development of the CO_2 'clumped-isotope' temperature proxy (Δ_{47}) has involved both resource and labor intensive analytical methods. We report strategies for measuring Δ_{47} on a conventional mass spectrometer, with the usual CO_2 set of three Faraday collectors while reducing the time devoted to standardization with temperature-equilibrated CO_2.

METHODS: We measured Δ_{47} in CO_2 on a mass spectrometer using only three Faraday cups by "multicollector peak hopping", directing $m/z = 46$ and $m/z = 47$ ion beams into the Faraday cups used for $m/z = 44$ and $m/z = 45$. We then calculated Δ_{47} from sample $\delta^{13}C$ and $\delta^{18}O$ and measured $^{47/46}CO_2^+$. We invoke a protocol for correcting ion-beam intensities for secondary electrons to address common problems with compositional non-linearity and both long and short-term measurement stability.

RESULTS: Our method removes reliance on a mass spectrometer equipped with an "isotopologue" configuration consisting of six Faraday cups. By using a correction based on removing the effects of secondary electrons, we remove Δ_{47} dependence on $\delta^{47}CO_2$. Our methods are robust against mass-spectrometer operating conditions.

CONCLUSIONS: Δ_{47} can be precisely measured on mass spectrometers currently employed for measuring $\delta^{13}C$ and $\delta^{18}O$ without significant resource investment. Accounting for ion scatter during measurements of CO_2 results in improved external precision and long-term stability, while significantly increasing machine time available for sample analysis.

2.2 INTRODUCTION

"Clumped isotope" geochemistry of carbonates, the study of multiply-substituted isotopologues of CO_2 derived from acid digestion of carbonate minerals, has been applied as a geochemical tool in many investigations in geology and paleoclimatology. Enthusiasm for this proxy is great, partly because the concentration of ^{13}C-^{18}O bonds within carbonate minerals serves as an intra-mineral thermometer; one can establish carbonate growth temperatures without a priori knowledge of the isotopic composition (i.e., $\delta^{18}O$) of the water in which the carbonate formed using only the ^{13}C-^{18}O bond ordering (Eiler and Schauble, 2004; Ghosh et al., 2006). While there has been considerable work on improving the precision and accuracy of measuring relative abundances of $^{13}C^{18}O^{16}O^{16}O^{2-}$ in carbonate via liberated $^{13}C^{18}O^{16}O$ (Huntington et al., 2009; Affek et al., 2009; Dennis et al., 2011) these measurements remain challenging. One impediment is that one requires modification to the usual carbonate Faraday cup configuration for the multiple-collector gas-source mass spectrometer. Another is the need to correct for a compositional dependency on the measurement of the excess in $^{47}CO_2$ (isotopomers of $^{18}O^{13}C^{16}O$) often referred to as a "non-linearity." These two factors contribute to a significant barrier for any laboratory intending to employ the clumped isotope proxy. Here we address both issues and demonstrate that measurement of the rare mass-47 isotopologue of CO_2 can be performed with a conventional cup configuration used for more traditional CO_2 isotope ratio measurements, and that the compositional non-linearity can be removed entirely by correcting measured rare ion beam intensities for background.

Conventional measurements of $^{13}C/^{12}C$ and $^{18}O/^{16}O$ in CO_2 (expressed as per mil deviations from a standard, $\delta^{13}C$ and $\delta^{18}O$, respectively ($\delta^{13}C$ or $\delta^{18}O = [(R_{smp} - R_{std}) / R_{std}] \times 10^3$ where $R = {}^{13}C/{}^{12}C$ or $^{18}O/^{16}O$, smp = sample, std = reference standard) require a collection system with only three Faraday cups to measure each of three ion beams $^{44}CO_2^+$, $^{45}CO_2^+$, $^{46}CO_2^+$. These signals are converted to ratios ^{45}R and ^{46}R, where ^{i}R is the ratio of isotopologue *i* relative to the most abundant isotopologue $^{44}CO_2$ ($^{16}O^{12}C^{16}O$), that in turn can be used to calculate $^{13}C/^{12}C$ and $^{18}O/^{16}O$ assuming a known relationship between $^{18}O/^{16}O$ and $^{17}O/^{16}O$ in the samples (e.g., Santrock et al., 1985). Clumped-isotope geochemistry involves measuring the abundances of rare multiply-substituted isotopologues, molecules containing more than one heavy isotope. In practice, the CO_2 isotopologue with cardinal mass 47, $^{16}O^{13}C^{18}O$, is the most accessible for measurement due to its relatively high abundance among doubly-substituted CO_2 species. The convention is to report the excess of this rare isotopologue relative to the stochastic abundance prescribed by the random distribution of the ^{13}C, ^{12}C, ^{18}O, ^{17}O, and ^{16}O isotopes among the CO_2 isotopologues (Eiler and Schauble, 2004). The latter is the high-temperature limit for the relative abundances of the isotopic species of CO_2. The excess in per mil is usually expressed as:

$$\Delta_{47} = [((^{47}R/^{47}R^*) -1) - ((^{46}R/^{46}R^*) - 1) - ((^{45}R/^{45}R^*) - 1)] \times 1000 \qquad (1)$$

where $^{i}R^*$ is the stochastic isotopologue ratio.

Equation (1) shows that a minimum of four ion beams are required rather than the usual three required for $\delta^{18}O$ and $\delta^{13}C$, the additional being $^{47}CO_2^+$. In order to measure ^{45}R, ^{46}R and ^{47}R (equation 1) it is current practice to utilize a minimum of four CO_2 collectors to measure simultaneously $^{44}CO_2^+$, $^{45}CO_2^+$, $^{46}CO_2^+$, $^{47}CO_2^+$, (these instruments usually have 6 collectors for

CO_2 with the additional two cups used to measure $^{48}CO_2^+$ and $^{49}CO_2^+$ for diagnostic purposes). Most instruments in the world today are not set up for such a measurement, as only three collectors are normally dedicated to CO_2, the remainder being spaced for other gases (e.g. N_2, O_2, etc.). This is an issue because it is common for the spacing between Faraday collectors on a gas-source instrument to be fixed, requiring the user to specify in advance the gases and ion beams to be analyzed. Additionally, measurements made on current instruments (virtually all being Thermo-Finnigan MAT 253 instruments, cf. Yoshida et al. 2013), exhibit a spuriously high measured Δ_{47} when the combined $\delta^{13}C$ and $\delta^{18}O$, or $\delta^{47}CO_2$ ($\delta^{47}CO_2 \approx \delta^{13}C + 2\delta^{18}O$), of sample CO_2 is greater than the composition of the working standard gas, and spuriously low Δ_{47} when sample CO_2 is isotopically lighter than the working gas (Huntington et al., 2009; Dennis et al., 2011). This compositional non-linearity varies from instrument to instrument and has been observed to change over time for the same machine on the scale of weeks to months. Huntington et al. (2009) present a method to correct for this effect by defining the non-linearity for any given mass spectrometer. This is done by comparing a suite of CO_2 gases of different composition (over a range of ~ 50‰ in $\delta^{47}CO_2$) that have been heated to high temperatures sufficient to impart a stochastic distribution of isotopes among all possible isotopologues ($\Delta_{47} \approx 0$‰) to the reference gas in the mass spectrometer (i.e. "heated gas" correction). Building on this approach, Dennis et al. (2011) developed an "absolute reference frame" (more recently referred to as carbon-dioxide equilibration scale or CDES in Henkes et al., 2013) to facilitate inter-laboratory comparison. The "absolute reference frame", or calibration, corrects for machine-specific shifts in scale (so called scale compression) by comparing CO_2 samples with reference gas isotopic

composition (i.e. $\delta^{47}CO_2 = 0$) re-equilibrated over a wide temperature range, ideally from ~0 to ~1000 °C. Both compositional non-linearity and scale compression have been attributed to ion fragmentation and recombination (scrambling) in the source (Huntington et al., 2009; Dennis et al., 2011). Utilizing these two methods is labor-intensive, and introduces additional assumptions and uncertainties into clumped-isotope measurements.

Here we demonstrate that accurate measurements of Δ_{47} can be obtained using only the three Faraday cups normally dedicated to conventional CO_2 isotope ratio measurements, with precision comparable to that of previous studies (Δ_{47} standard error ~0.020 ‰). In addition, we show that the compositional non-linearity described by Huntington et al. (2009) is largely, if not entirely, attributable to non-zero backgrounds resulting from secondary electron scatter near the Faraday collectors, as previously shown for clumped-isotope measurements of O_2 (Yeung et al., 2012). In this regard, our findings are similar to those of He et al. (2012), though arrived at by different sets of experiments. We apply a simple background correction that reduces Δ_{47} dependence on $\delta^{47}CO_2$ below detection, while producing a $\Delta_{47measured}/\Delta_{47theoretical}$ calibration line from temperature equilibrated gases that is very similar to those reported in other laboratories. We note that a major advantage of removing the compositional non-linearity is that it is possible to compare any CO_2 sample to a heated (approximately stochastic) aliquot of the same gas, permitting a more direct measurement of Δ_{47} for the sample, since this removes the shift in measured Δ_{47} arising from minor shifts in $\delta^{47}CO_2$ that occur when heating CO_2 in a quartz ampule. The methods documented here should be transferable to most mass spectrometers using conventional Faraday collector sets intended to measure only $\delta^{13}C$ and $\delta^{18}O$ in CO_2, replacing an

amplifier resistor being the only modification required. The effort required to obtain analyses is minimized by removing the non-linearity effects. Both advances should make the clumped-isotope proxy available to many more laboratories than it is currently.

2.3 EXPERIMENTAL

2.3.1 Instrumentation for Δ_{47} measurements

The mass spectrometer used in this study is fitted with a collection system consisting of 9 Faraday cups (Fig. 2.1) to monitor several rare isotopologues of CO_2 and O_2 (*m/z* = 32 through *m/z* = 36). For reasons described below, the Faraday cup intended to measure *m/z* = 47 in this configuration performed erratically, forcing us to utilize only three Faraday cups, those monitoring *m/z* = 44 through *m/z* = 46, with normally $3x10^8$, $1x10^{10}$ and $1x10^{11}$ Ω resistors, respectively. We used these three Faraday cups to first measure $^{13}C/^{12}C$ and $^{18}O/^{16}O$, then two of those cups to measure *m/z* = 46 and *m/z* = 47 with $1x10^{10}$ Ω and $1x10^{12}$ Ω resistors, yielding $^{47}CO_2/^{46}CO_2$. Carbon dioxide gas was introduced to the mass spectrometer through a dual inlet system. Variable-volume bellows were adjusted to provide ~ 14 V for *m/z* = 44 ($3x10^8$ Ω resistor) during the first measurements, and ~ 6 V for *m/z* = 46 ($1x10^{10}$ Ω resistor) for the second set of measurements for 47/46.

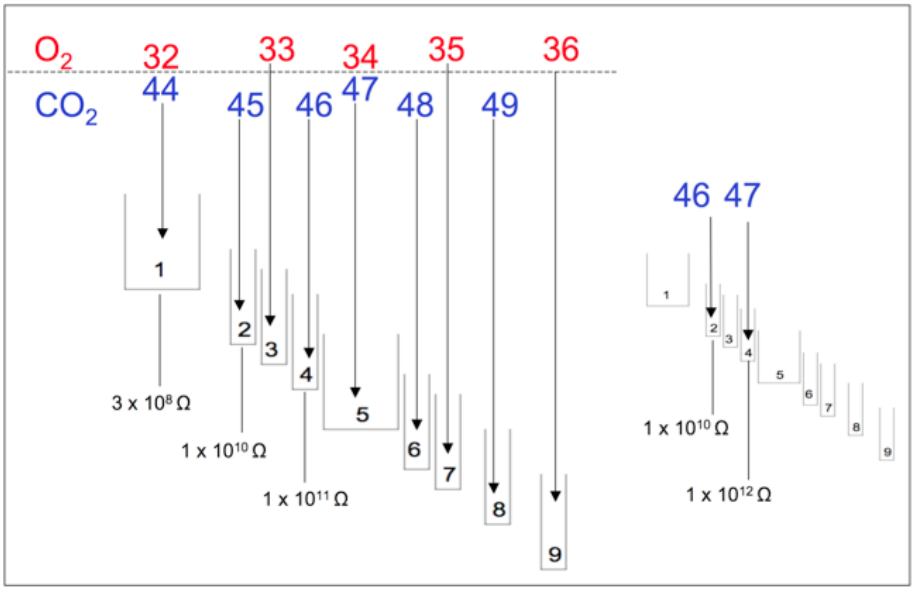

Fig. 2.1. Schematic of O_2/CO_2 collector set used in this study showing approximate spacing and cup width for nine Faraday cups intended to measure ion beams for either $^{32}O_2$, $^{33}O_2$, $^{34}O_2$, $^{35}O_2$, $^{36}O_2$, or $^{44}CO_2$, $^{45}CO_2$, $^{46}CO_2$, $^{47}CO_2$, $^{48}CO_2$, $^{49}CO_2$. Inset shows cups used to measure $^{46/47}CO_2^+$ using cups normally used for $^{45}CO_2$ and $^{46}CO_2$. The beams are repositioned by shifting the magnetic field and accelerating voltage.

For convenience of presentation, our study is divided into four periods, P1 (December 2010 to May 2011), P2 (January 15th to April 10th, 2012), P3 (April 13th to May 9th), and P4 (May 10th to July 14th). For the elapsed time between P1 and P2 the mass spectrometer was used to measure O_2 exclusively. In order to switch from O_2 to CO_2, the mass spectrometer required no major maintenance or alterations other then changing from stainless steel capillaries used for O_2 to more highly polished nickel capillaries for CO_2. P2, P3 and P4 were separated by major machine maintenance, necessitating breaking vacuum.

We constructed a small volume (~ 200 ml) glass vacuum line backed by a turbomolecular pump for CO_2 handling and purification of all gases used in this study. Samples were passed through glass traps chilled to −78° C by dry ice/ethanol baths to remove water, and then were entrained in helium carrier gas at a flow rate of 15 ml/min for purification through a two-meter GC column packed with Porapak Q chilled to −28 to −30 °C. Sample gas effluent from the GC was isolated in a metal trap at liquid nitrogen temperature (approximately −196 °C). Carrier He was pumped away before moving sample CO_2 into a vessel for introduction to the mass spectrometer. Multiple passes through this system result in no changes in $\delta^{13}C$, $\delta^{18}O$ or Δ_{47} values, suggesting that contaminants are effectively removed, and that the distributions of isotopologues in low temperature samples are not affected.

2.3.2 Multicollector peak hopping (MPH)

The physical distance *d* between any two beams at the approximate focal plane of the magnetic sector mass spectrometer can be estimated from the relation:

$$d_{2/1} = D \ \Delta M / (½ (m_1/m_2)) \quad (2)$$

where *D* is the dispersion of the instrument, ΔM is the mass difference, and m_1 and m_2 are the masses of the ions that compose the beams. For the mass spectrometer used in this study *D* = 460mm (~2 times the radius), so that $d_{46/45}$ = 10.1 mm and $d_{47/46}$ = 9.9 mm. These distances are sufficiently similar (differing by ~0.2 mm) in comparison to the cup widths that one can use the same cups at their fixed spacing to measure $^{45/46}R$ and $^{47/46}R$ with small adjustments to the

accelerating voltage and magnet current. As a result, two separate measurements can be used to obtain the required ion current ratios for a complete analysis of CO_2.

2.3.3 Calculating Δ_{47} from $^{47/46}R$ and $\delta^{13}C$ and $\delta^{18}O$

We wrote a Fortran program that calculates Δ_{47} from input ion currents (voltages) based on our MPH method (*see Appendix for code and additional detail*). In this scheme, measured ^{46}R and ^{45}R from the first set of measurements yield $\delta^{18}O$ (SMOW) and $\delta^{13}C$ (PDB) assuming stochastic distributions of the isotopes across isotopologues (the conventional assumption with negligible loss in accuracy, e.g., Santrock et al.,1985) and then $^{47/46}R$ measured separately is combined with ^{46}R of the sample to yield ^{47}R (i.e., $(^{46}CO_2/^{44}CO_2)(^{47}CO_2/^{46}CO_2) = (^{47}CO_2/^{44}CO_2)$. While measured ratios from non-synchronous measurements are not comparable, we overcome this by converting all ion voltage ratios to absolute ratios via the usual comparison with the working reference gas. The Δ_{47} of the reference gas is known. Correction for negative backgrounds produced by secondary electrons in the $m/z = 46$ and $m/z = 47$ cups is obtained by subtracting backgrounds measured off-peak with the accelerating voltage deflected to lower values. Subtractions are made for both sample and standard gases, and are obtained from the mean of measurements taken before and after on-peak analyses of sample and standard. We found no significant difference in measured Δ_{47} when we modeled background voltage as a non-linear time dependant function rather than simple averages (i.e.: we assume linear drifts in background in time with no obvious penalty in accuracy, similar to the He et al. (2012) "47 interpolation method").

The code applies two versions of data reduction calculations. One is based on the slope of plots of Δ_{47} vs. $\delta^{47}CO_2$ without subtracting background voltages, and is equivalent to the "heated gas line" (hereafter HGL) or "temperature equilibrated" correction schemes of Huntington et al. (2009) and Dennis et al. (2011) respectively. The other is based on correcting for the $\Delta_{47}/\delta^{47}CO_2$ non-linearity by subtracting the off-peak background voltages measured in Faraday cups used for $m/z = 47$ and $m/z = 46$. The slopes of temperature equilibrated gas lines created after applying this background correction are in most cases indistinguishable from zero.

The program corrects for potential instrument-dependent inaccuracies in absolute Δ_{47} values by applying a calibration line depicting measured Δ_{47} at various temperatures vs. theoretical Δ_{47} values for CO_2 following the recommendation of Dennis et al. (2011)

Algorithms for normal CO_2 ion corrections are based on Santrock et al. (1985) with modifications to the input parameters. Rare isotopologue corrections are similar to Dennis et al. (2011) with the exception of the background corrections.

Uncertainties in the final Δ_{47} are calculated using a Monte Carlo approach to account for uncertainties among the blocks of unequal numbers of cycles in the acquisitions (e.g., fewer cycles are used to measure backgrounds). Sources of uncertainty considered include the inter-cycle internal precision of each measurement block, both on- and off-peak, and uncertainties in calibration slopes of temperature-equilibrated gas lines ($\Delta_{47}/\delta^{47}CO_2$ non-linearity) where such gas lines are used in the data reduction.

2.3.4 Background measurements

It has been customary in gas-source isotope ratio mass spectrometry to apply corrections for backgrounds with no gas entering the instrument. These "dark" backgrounds are measured on peak. However, this method is unable to account for any change in the background signal during sample gas measurement. Work in our laboratory demonstrated that secondary electron scatter is a critical source of background voltage that must be accounted for when measuring rare isotopologues of O_2 (Yeung et al., 2012). As these electrons are generated when ion beams are present, measurements of these backgrounds must be made with gas flowing. By examining off-peak positions while sample gas is present, we observed a similar negative signal in Faraday cups used to measure $m/z = 46$ and $m/z = 47$ surrounding the analyte mass peaks. This effect has been reported in at least one other laboratory (He et al., 2012) and was also attributed to secondary electrons, perhaps sputtered off the metal ceiling of the flight tube. We found that background voltage is strongly affected by a hand-held magnet placed strategically near the collector array, verifying that the effect is due to electrons. Though impossible to observe directly, it is likely that the background signal is also depressed at on-peak positions during measurement, influencing the on-peak signals measured by Faraday cups. The magnitude of the negative bias is greater in more sensitive amplifiers, requiring corrections for the $1x10^{12}$ Ω and in some cases $1x10^{10}$ Ω amplifiers. Correcting for these non-zero background voltages effectively removes Δ_{47} dependence on $\delta^{47}CO_2$.

We found that three cycles of background measurements of $m/z = 46$ and $m/z = 47$ before and after a ten-cycle analysis was sufficient to assess the effect of electron scatter during an

analysis. Measurements were made with a 20 V decrease in accelerating voltage relative to the peak value. We found that the magnitude of the negative backgrounds changed significantly over a fifty-five-day period, from –0.75 mV to –1.00 mV and from –24.5 mV to –29.5 mV for *m/z* = 46 and *m/z* = 47 respectively (Fig. 2.2a and 2.2b). Background voltage drifted at different rates during these measurements, 0.03 mV/cycle in April and 0.065 mV/cycle in May for *m/z* = 47. For both *m/z* = 46 and *m/z* = 47, the increase was nearly linear, suggesting that linear interpolation from measured values is sufficient to obtain on-peak backgrounds. The procedure we use is represented diagrammatically in Fig. 2.3. We use two blocks composed of ten measurement cycles for sample and standard to determine $\delta^{13}C$ and $\delta^{18}O$, followed by the peak hop (shift in magnet settings) to measure *m/z* = 46, *m/z* = 47 and adjacent backgrounds. For these measurements we use an analysis block composed of ten on-peak cycles, bracketed by three off-peak cycles to measure backgrounds both before and after the ten cycles. We repeat the analysis block five to ten times for each sample. All cycles are 8 s integrations throughout this sequence.

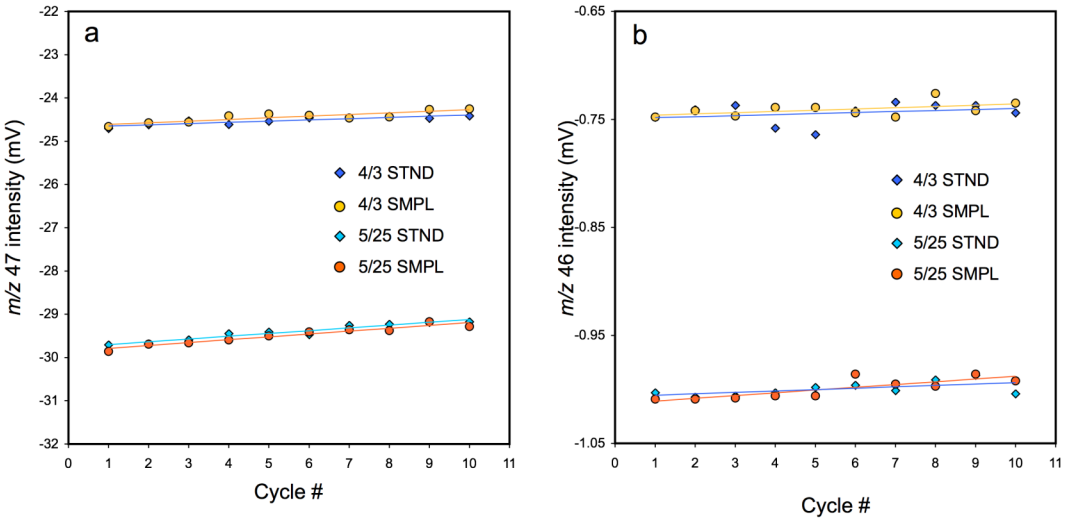

Fig. 2.2. Off-peak voltages measured in Faraday cups used for (a) m/z = 47 and (b) m/z = 46 collected with 10 cycles of 8 s duration with CO2 present on two different days. Background voltage is noticeably lower on May, 25th, but the rate of increase (~ 0.02 to 0.07 mV/cycle for *m/z* = 47; 0.001 to 0.003 mV/cycle for *m/z* = 46) is similar between sample and standard measurements and adequately described by a linear function over the course of an analysis.

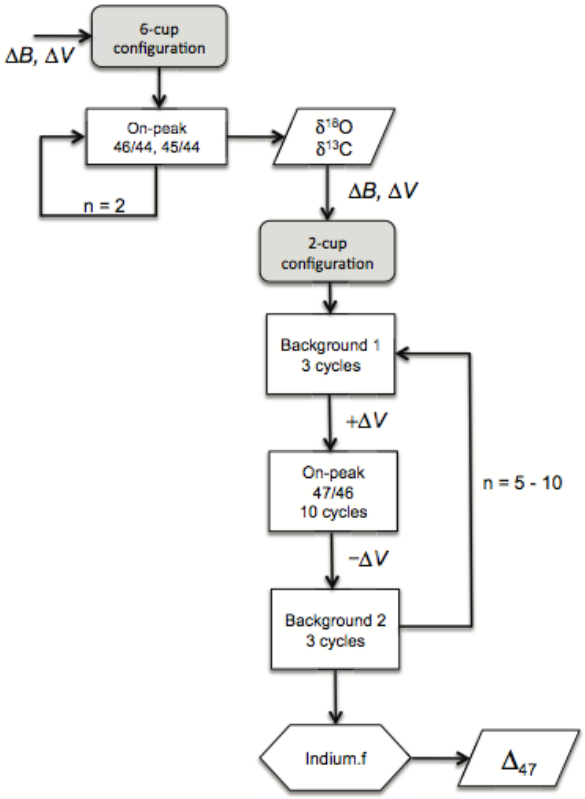

Fig. 2.3. Schematic illustrating sample analysis procedure used in this study. After normal procedures to pressure balance, peak center, and scan dark backgrounds, we measure m/z = 44, 45 and 46 by running 2 sets of 10 cycles per gas in the 6-cup configuration to determine $\delta^{13}C$ and $\delta^{18}O$. Next we reposition the magnet (ΔB) and accelerating voltage (ΔV) to measure *m/z* = 46 and *m/z* = 47 using Faraday cups previously used for *m/z* = 45 and *m/z* = 46 (2-cup configuration). Backgrounds are measured both before and after the on-peak sample analysis. Since background voltage typically does not stabilize until after the first introduction of sample gas, we discard the first reference gas measurement in the 10-cycle analysis and in both 3-cycle sets used to determine background voltage for the correction.

2.3.5 Standard gases

Two canisters of CO_2 reference gas were purchased from OzTech (Dallas, TX, USA) for use in this study. One canister was employed exclusively as a working gas in each calendar year. The compositions of references gases used are: $\delta^{13}C = -47.52$ ‰ PDB, $\delta^{18}O = +2.75$ ‰ SMOW (WG1) and $\delta^{13}C = -3.58$ ‰ PDB, $\delta^{18}O = +24.96$ SMOW ‰ (WG2) used during P1, and P2 through P4, respectively. Both canisters have Δ_{47} values reflective of near room-temperature equilibration.

Standards approximating stochastic distributions of isotopes were created using methods similar to those of Huntington et al. (2009). Carbon dioxide gases from several different sources were mixed to produce aliquots with bulk composition ranging from approximately –60 ‰ to + 28 ‰ in $\delta^{47}CO_2$. Aliquots were isolated in flame-sealed quartz ampules, and heated in a muffle furnace to 1000 °C for at least three hours. While we could not confirm a nearly stochastic distribution of isotopologues commensurate with perfect equilibrium and quenching at 1000 °C, we sought to minimize potential back-equilibration at lower temperature by immediately quenching ampules in cold water. Stochastic gases were passed through our purification system within two hours of quenching with very few exceptions.

Additional standards were equilibrated at lower temperatures of 2 °C and 25 °C by allowing CO_2 to exchange oxygen isotopes with water at controlled temperature in one of several stopcock-sealed vessels. Gases equilibrated at 25° C were held in a temperature-controlled water bath for 72 to 192 hours. Gases equilibrated at 2 °C were partially submerged in a beaker of water held in a laboratory refrigerator for approximately one month.

2.4 RESULTS AND DISCUSSION

2.4.1 Initial multicollector peak hopping experiments

During P1, we found greater than expected instability (std err. frequently > 0.045 ‰, occasionally > 0.080 ‰) when measuring Δ_{47} using the nine-Faraday cup collection system. We suspect this is a byproduct of the Faraday cup used to measure *m/z* = 47. This cup is approximately three times the width of those of the standard cups, and this geometry makes it vulnerable to even the slightest contamination of non-analyte ions, which may be introduced with any CO_2 sample. We confirmed this by passing contaminated stochastic CO_2 samples through an imperfect purification system multiple times. We observed a decrease in Δ_{47} measured on the wide cup with each purification pass, and a significantly smaller such decrease using the narrow cup. Since our stochastic gases have a minimum Δ_{47}, decreases in Δ_{47} with incomplete purification must be spurious due to a decrease in stray ions impacting the 47 Faraday cup. In addition, the amplifier card for this cup is designed to accommodate output from two separate cups via a switch, and this switch likely adds some instability.

We compared Δ_{47} measured using the nine-Faraday cup collection system to Δ_{47} measured with MPH using a suite of purified CO_2 samples of similar composition equilibrated with water at different temperatures. The results are plotted in Fig. 2.4. They demonstrate that measurements using the wide cup in the nine-cup configuration result in less precise and less accurate measurements than those derived by using the narrower cup with MPH.

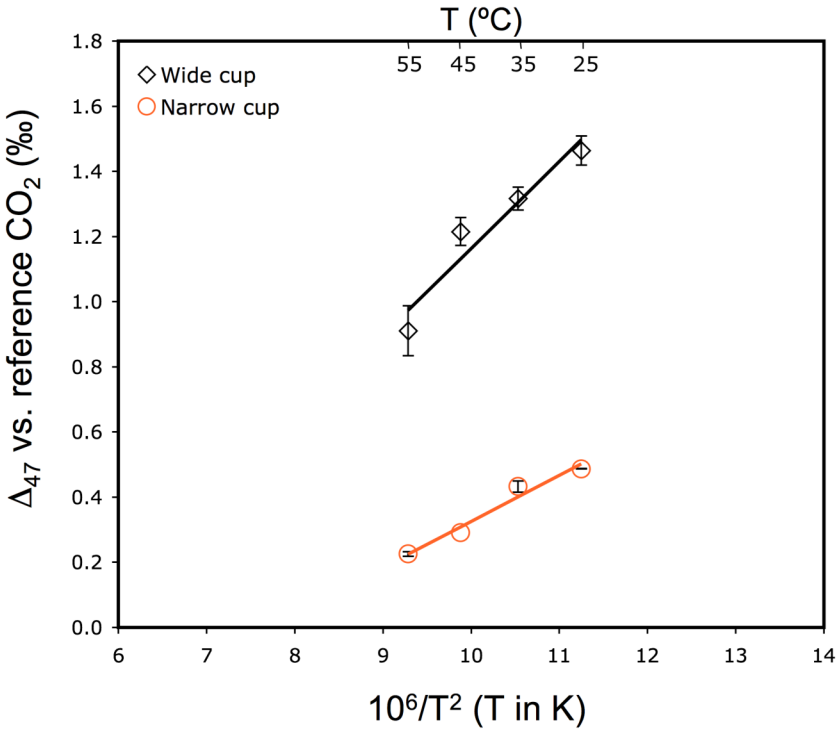

Fig. 2.4. Comparison of 6-cup configuration (black diamonds, wide cup) and 2-cup configuration (MPH method, orange circles, narrow cup) Δ_{47} measurements of temperature equilibrated CO_2 samples against reference CO_2. Error bars represent one external standard error for each measurement composed of multiple blocks.

Initially, in P1, we attempted to reduce the time necessary to "define the non-linearity" of our mass spectrometer. We hoped to do this by comparing each sample to its stochastic counterpart (we have referred to this as the "Direct method" for determining departures from stochastic distributions of isotopes) instead of preparing and running heated gases daily as suggested by Huntington et al. (2009). We made stochastic counterparts by recollecting the sample gas and heating it to 1000 °C in sealed quartz ampules (as for the stochastic standards described above). The accuracy of this approach was hindered by the fact that all samples shifted

in $\delta^{18}O$ by variable amounts of between 2 and 7 ‰ during heating, presumably through exchange with the quartz ampule. This strategy is therefore limited by the ability to prevent isotopic exchange between CO_2 and SiO_2 at 1000 °C or to correct for the effect of 2 to 7 ‰ difference in $\delta^{47}CO_2$ on Δ_{47}.We solved this problem by eliminating the latter, and believe this is a sound strategy which may prove useful in circumstances where measuring the sufficient number of standards to "define the non-linearity" and calibrate mass spectrometer "scale compression" against theoretical values is impractical.

2.4.2 Exploring $\Delta_{47}/\delta^{47}CO_2$ relationship and electron scatter

The non-linearity observed when using the MPH method is similar in scale to those reported in other laboratories using six-Faraday cup collector systems. We observed $\Delta_{47}/\delta^{47}CO_2$ slopes ranging from 0.0170 ± 0.0004 (2σ) to 0.0114 ± 0.0006 (Fig. 2.5) as compared to 0.0064 to 0.0128 at the California Institute of Technology (Huntington et al., 2009), 0.0081 at Harvard University, 0.0059 at Johns Hopkins University and 0.0055 at Yale University (Dennis et al., 2011). Previously published studies report instability in the Δ_{47}-δ^{47} relationship, particularly as a consequence of mass spectrometer service. We observed one major shift in our Δ_{47}-$\delta^{47}CO_2$ relationship. The shift occurred some time between March 1st, and April 17th, where the slope of our stochastic standard line changed from 0.0170 ± 0.0004 to 0.0114 ± 0.0006, where it remained for P3 and P4 (Fig. 2.5). We suggest this event was related to machine maintenance that began on April 10th.

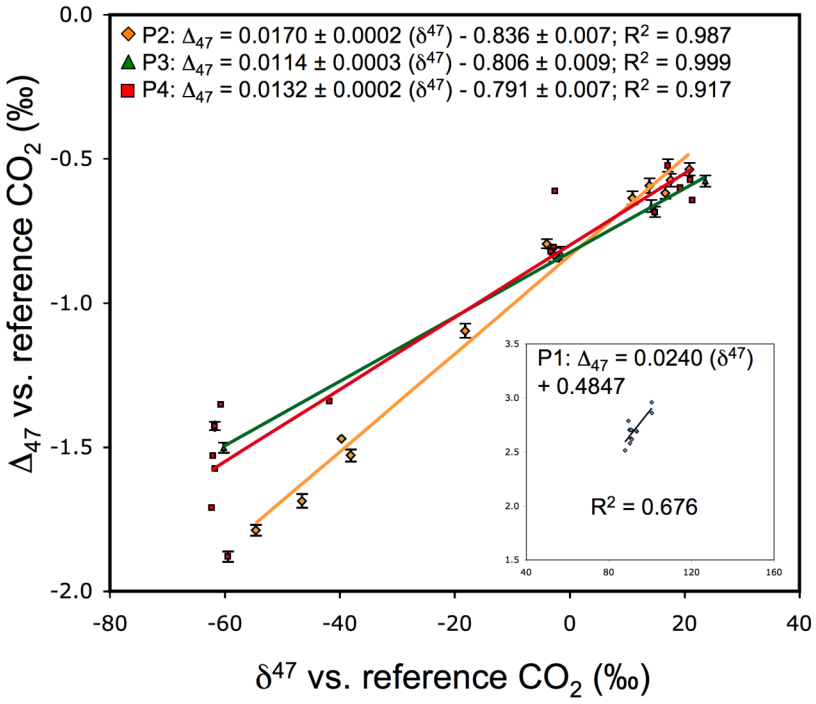

Fig. 2.5. Variation in measured Δ_{47} with $\delta^{47}CO_2$ relative to reference gas for CO_2 samples equilibrated at 1000 °C. Abscissa indicates difference in sample bulk composition from reference CO_2. Slope changed significantly from P1 to P2 for reference gases of different composition. Smaller changes occurred with the same reference CO_2 over time (represented by intervals P2-P4). Uncertainties in best fit lines are 1σ.

Before the start of P2 we employed corrections for secondary electron scatter to effectively remove Δ_{47} dependence on $\delta^{47}CO_2$. Comparing measurements of temperature equilibrated samples with (Fig. 2.6b) and without (Fig. 2.6a) electron scatter correction demonstrates this approach is as effective for MPH as it is for machines equipped with six-Faraday cup collection systems (e.g., He et al., 2012). This method also remained robust despite machine maintenance activities that changed the Δ_{47}-$\delta^{47}CO_2$ relationship. During the transition

from P2 to P3, the slope of the line representing stochastic gas Δ_{47} vs. $\delta^{47}CO_2$ shifted as described above, while correcting these same measurements for background voltage eliminated the slope in both periods P2 and P3. While Δ_{47} measurements became much more scattered during P4, the slope of the line approximating stochastic gas measurements accumulated from May 10th to July 14th remained very near zero (–0.0006 ± 0.0001) when corrected for background voltage. This supports suggestions that background voltage contributed by secondary electron scatter is most responsible for the Δ_{47}-$\delta^{47}CO_2$ non-linearity, and that changing the amount of electron scatter measured by Faraday cups likely results in the observed changes to the slopes of temperature equilibrated gas lines.

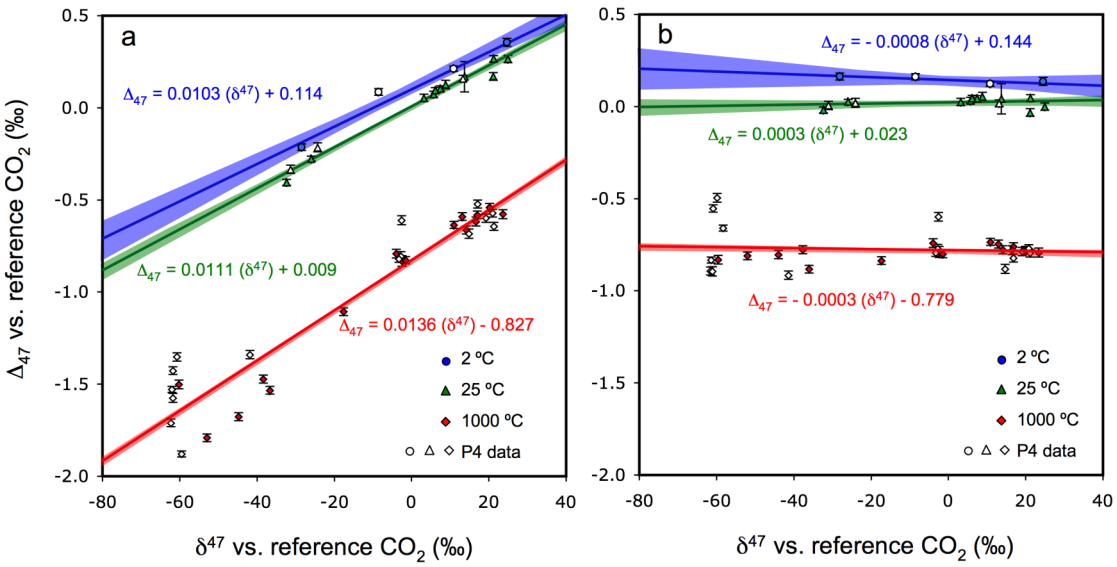

Fig. 2.6. Plots of Δ_{47} versus $\delta^{47}CO_2$ relative to reference gas for CO_2 samples equilibrated at different temperatures during P2, P3 and P4. 1000 °C = red diamonds, 25° C = green triangles, 2°C = blue circles. a) Measurements without background correction demonstrate slopes similar to previous studies, and slightly non-parallel lines. b) Measurements corrected for background demonstrate no discernible non-linearity and more closely approximate parallelism as expected. Shaded envelopes indicate 95% confidence interval.

Dennis et al. (2011) describe a scheme to port all Δ_{47} measurements into an "absolute reference frame" by means of a calibration line between measured Δ_{47} values and theoretical Δ_{47} values (for further discussion of additional uncertainties introduced see He et al. (2012). We found the MPH method produces similar calibration lines to those of other laboratories, and that accounting for background voltage reduces uncertainty. Incorporating all data from temperature equilibrated standards measured during P2, P3 and P4 produces a calibration line of $\Delta_{47theoretical} = 1.119 \pm 0.016\ (2\sigma)\Delta_{47measured} + 0.899 \pm 0.010$ ($R^2 = 1.000$) with background correction or $\Delta_{47theoretical} = 1.082 \pm 0.018\Delta_{47measured} + 0.921 \pm 0.008$ ($R^2 = 0.9998$) without correction. A comparison of several previously published calibrations is found in Table 2.1 and Fig. 2.7.

Table 2.1

	Slope[a]	T (ºC)	Intercept	R^2	Calibration line[b]	R^2
California Institute of Technology	0.0065	8	0.0788	0.9859	$\Delta_{47t} = 1.1548\Delta_{47m} + 0.9343$	0.9986
		25	-0.0271	0.9417		
		50	-0.0957	0.9133		
		1000	-0.7869	0.9386		
Harvard University	0.0081	10	0.048	0.9916	$\Delta_{47t} = 1.0105\Delta_{47m} + 0.9539$	0.9999
		25	-0.0216	0.9367		
		50	-0.1473	0.9375		
		1000	-0.9182	0.9167		
Johns Hopkins University	0.0059	0	0.1412		$\Delta_{47t} = 1.0303\Delta_{47m} + 0.9194$	0.9997
		27	-0.0077	0.8316		
		50	-0.1002			
		1000	-0.8686	0.9988		
Yale University	0.0055	10	0.0812	0.8086	$\Delta_{47t} = 1.0630\Delta_{47m} + 0.9227$	0.9999
		25	0.0013	0.8886		
		50	-0.1094	0.4155		
		1000	-0.8431	0.9206		
University of Chicago		3.8				
(PBL correction)	-0.0019	21.5			$\Delta_{47t} = 1.1121\Delta_{47m} + 0.9271$	1.0000
		60				
(without PBL correction)	0.0144	1000			$\Delta_{47t} = 1.1151\Delta_{47m} + 0.9377$	0.9992
This study		2	0.144	0.144	$\Delta_{47t} = 1.119\Delta_{47m} + 0.899$	1.0000
(with background correction)	-0.0003	25	0.023	0.023		
		1000	-0.779	-0.779		
(without correction)	0.0133	2	0.113	0.113	$\Delta_{47t} = 1.082\Delta_{47m} + 0.921$	0.9998
		25	0.009	0.009		
		1000	-0.827	-0.827		

[a] Slopes of temperature equilibrated gas lines are assumed to be parallel and are calculated by collapsing all temperature equilibrated sample data into a single set by removing respective means to derive a common slope.

[b] Calibration line of theoretical values from Wang et al. (2004) against measured values (equivalent to the "ETF" of Dennis et al., 2011).

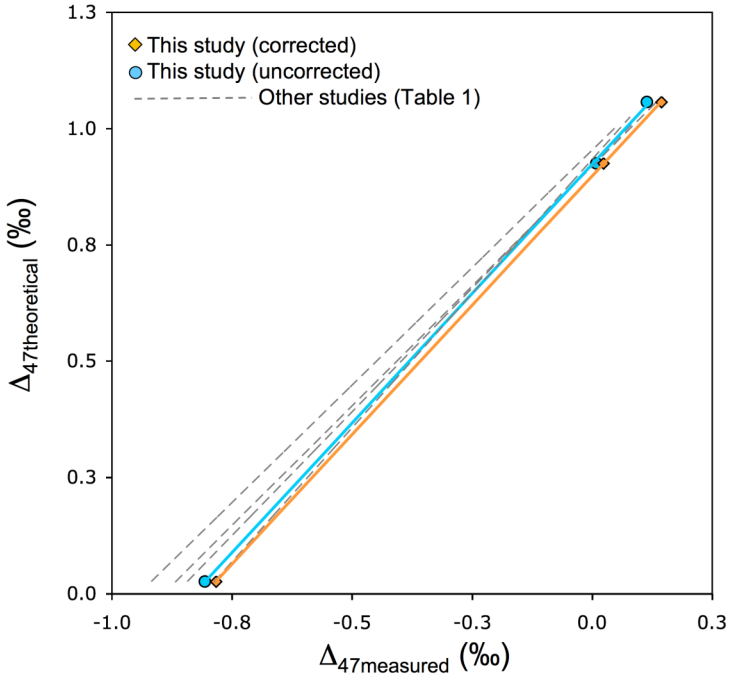

Fig. 2.7. Comparison of $\Delta_{47theoretical}/\Delta_{47measured}$ calibration lines (Dennis et al., 2011). Temperatures used in this study are 2 °C, 25 °C and 1000 °C. The MPH method results are similar to those from other laboratories. Correcting temperature equilibrated standard gases for measured background voltage changes the slope and y-intercept of the calibration line slightly. Slopes and intercepts of these lines and those reported in other laboratories are listed in Table 2.1.

2.4.3 Electron scatter response to instrument maintenance

We found that backgrounds evolved over time. This is demonstrated by tracking the first *m/z* = 46 and 47 background cycles taken each day over the course of six months (Fig. 2.8). In general, we found background signals became gradually less negative during the course of the study, opposite to observations by He et al. (2013, their Fig. S3).

In January 2012, the mass spectrometer was baked and sat idle under high vacuum for approximately 2 weeks. The *m/z* = 47 backgrounds were approximately –47 mV and climbed

slowly (and asymptotically) through April 10th to –23 mV. The day to day variability appears to correspond to idle time, as the largest increases (less negative) in background voltage follow short idle times (< 8 hours) and the decreases (more negative) in background levels occur after longer idle periods (12 – 48 hours).

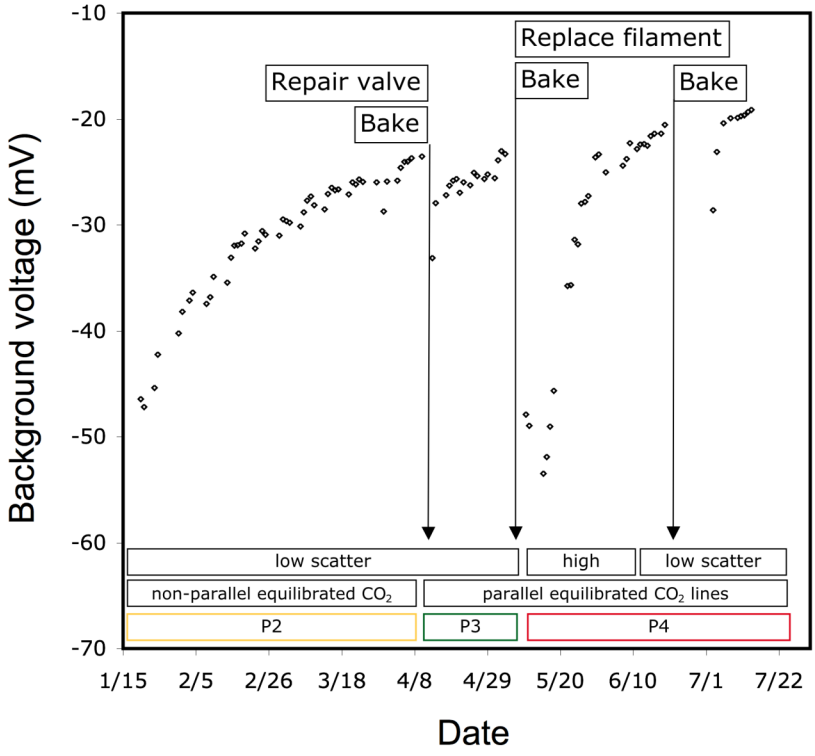

Fig. 2.8. Evolution of background signals during the six-month study period. Ordinate is the first m/z = 47 background for reference gas for each operating day. Short idle times (< 24 hours) usually result in less negative backgrounds. Long idle times (> 48 hours) usually result in more negative backgrounds. Cleaning (by baking) results in significantly lower backgrounds. During six months of study, backgrounds never fully stabilized at a maximum value. Corresponding measurements *m/z* = 46 demonstrate almost identical patterns, although compressed to a range of ~ 1 mV.

On April 10th, the sample-side inlet valve failed and had to be rebuilt. To minimize the possibility of contamination, we vented the instrument to nitrogen. Following the repair, we cleaned the mass spectrometer by baking for 24 hours. Upon resuming operation on April 13th, the background voltage had dropped approximately 10 mV to −33 mV, but resumed the P2 rate of increase within two days. Repairing the valve and baking the instrument resulted in a time (P3) during which we observed the lowest measurement scatter of the study. Measuring stochastic standards at four different bulk compositions (+23.6 ‰, +14.2 ‰, −1.5 ‰ and −60.3 ‰ $\delta^{47}CO_2$) produced a heated gas line of slope 0.0114 ± 0.0006 (R^2 = 0.9999). The change in slope brought the heated gas line closer to parallel with temperature-equilibrated lines at 25 °C and 2 °C with slopes of 0.0111 ± 0.0004 and 0.0103 ± 0.0010, respectively, than during P2.

The transition from P3 to P4 is defined by failure of the source filament. Replacing the filament necessitates venting the machine and exposing the source to laboratory air. After replacing the source filament, we cleaned the interior by baking for 48 hours. While backgrounds again began at their lowest point during this study (−50 mV), changing the filament appeared to cause a severe disruption to measurement stability. It took two weeks for background signal to stabilize near previous levels, and it was difficult to find either a stable peak center or stable off-peak positions to measure ion beams.

It is clear that the magnitude of negative background signals are very sensitive to mass spectrometer baking. We suggest two possible explanations, 1) baking removes contamination (oxides or water) from metal surfaces in the ion source. These contaminants are a constant source of positive ions, counteracting the negative current from secondary electrons, or 2) baking

removes oxides which shield metal surfaces, and cleaner metal surfaces are more easily able to contribute secondary electrons to be scattered during measurement. The latter is less likely in that we do not normally bake the detector end of the flight tube where secondary electrons are generated. While secondary electron production is proportional to ion beam intensities, the long-term observations suggests that other internal conditions also influence electron production and scatter.

2.5 CONCLUSIONS

We have demonstrated that clumped-isotope measurements of CO_2 can be made using a conventional three-Faraday cup array, by multicollector peak hopping (MPH), where Δ_{47} is obtained from measurements of $\delta^{13}C$ and $\delta^{18}O$, and $^{47}CO_2^+$ / $^{46}CO_2^+$ measured by steering these ion beams conventional cup locations by slightly altering the magnet field and accelerating voltage of the instrument. We have shown that measurements of temperature equilibrated standards, and calibration lines created from them, are very similar to those reported from other laboratories using six-Faraday cup collection systems. The precision of measurements made with MPH is similar to those made with the collection system commonly used for clumped-isotope measurements and thus sufficient to be useful for all applications of the proxy. Additionally, we show that the Δ_{47}-$\delta^{47}CO_2$ non-linearity reported in clumped-isotope studies employing Thermo-Finnigan 253 mass spectrometers is indeed predominantly caused by secondary electron scatter, and that correction for this effect eliminates $\Delta_{47}/\delta^{47}CO_2$ non-linearity. We describe the long-term

evolution of electron scatter within our mass spectrometer, which implies that short idle times between measurements and the frequency of cleaning procedures can affect the Δ_{47}-$\delta^{47}CO_2$ relationship and therefore effect measurements and correction schemes.

2.6 REFERENCES

Affek H.P., Zaarur S. and Douglas P. M. J. (2009) Mass spectrometric effects on 'clumped isotopes' calibration. *Geochim. Cosmochim. Acta* **73**, A15.

Dennis K. J., Affek H. P., Passey B. H., Schrag D. P. and Eiler J. M. (2011) Defining an absolute reference frame for 'clumped' isotope studies of CO_2. *Geochim. Cosmochim. Acta* **75**, 7117–7131.

Eiler J.M. and Schauble E.A. (2004) $^{18}O^{13}C^{16}O$ in Earth's atmosphere. *Geochim. Cosmochim. Acta* **68**, 4767–4777.

Eiler J. M. (2007) Clumped-isotope geochemistry — The study of naturally-occurring multiply-substituted isotopologues. *Earth Planet. Sci. Lett.* **262**, 309–327.

Ghosh P., Adkins J., Affek H., Balta B., Guo W., Schauble E. A., Schrag D. P. and Eiler J. M. (2006) ^{13}C–^{18}O bonds in carbonate minerals: a new kind of paleothermometer. *Geochim. Cosmochim. Acta* **70**, 1439–1456.

Grauel A. L., Schmid T. W., Hu B., Bergami C., Capotondi L., Zhou L., and Bernasconi S. M. (2013) Calibration and application of the 'clumped isotope' thermometer to foraminifera for high-resolution climate reconstructions. *Geochim. Cosmochim. Acta* **108,** 125 - 140.

Guo W., Mosenfelder J. L., Goddard, III, W. A. and Eiler J. M. (2009) Isotopic fractionations associated with phosphoric acid digestion of carbonate minerals: insight from first-principles theoretical modeling and clumped isotope measurements. *Geochim. Cosmochim. Acta* **73**, 7203–7225.

He B., Olack G.A. and Colman A.S. (2012) Pressure baseline correction and high-precision CO_2 clumped-isotope (Δ_{47}) measurements in bellows and micro-volume modes. *Rapid Communications in Mass Spectrom*. **26**, 2837 - 2853.

Huntington K.W., Eiler J.M., Affek H.P., Guo W., Bonifacie M., Yeung L.Y., Thiagarajan N., Passey B.H., Tripati A., Daëron M. and Came R. (2009) Methods and limitations of 'clumped' CO_2 isotope (Δ_{47}) analysis by gas-source isotope ratio mass spectrometry. *J. Mass Spectrom*. **44**, 1318–1329.

Santrock J., Studley S. A. and Hayes J. M.(1985) Isotopic analyses based on the mass spectrum of carbon dioxide. *Anal. Chem.* **57**, 1444–1448.

Wang Z., Schauble E.A. and Eiler J. M. (2004) Equilibrium thermodynamics of multiply substituted isotopologues of molecular gases. *Geochim. Cosmochim. Acta* **68**, 4779–4797.

Yeung L.Y., Young E.D. and Schauble E.A. (2012) Measurements of $^{18}O^{18}O$ and $^{17}O^{18}O$ in the atmosphere and the role of isotope-exchange reactions. *J. Geophys. Res.* **117**, DOI: 10.1029/2012JD017992.

Yoshida N., Vasilev M., Ghosh P., Abe O., Yamada K., and Morimoto M. (2013) Precision and long-term stability of clumped-isotope analysis of CO_2 using a small-sector isotope ratio mass spectrometer. *Rapid Communications in Mass Spectrom.* DOI: 10.1002/rcm.6431.

CHAPTER 3

HIGH-PRECISION MEASUREMENTS OF ^{13}C-^{18}O BONDS IN CO_2 AND EFFECTS ON CARBONATE CLUMPED-ISOTOPE THERMOMETRY IN MODERN BIVALVED MOLLUSC SHELLS[2]

[2] Manuscript co-authored by D.A. Petrizzo, B.N. Runnegar and E.D. Young prepared for submission to *Geochemica et Cosmochemica Acta*, April 2013.

3.1 ABSTRACT

We report a temperature calibration for Δ_{47} for bivalves that lies within error of theoretical prediction (Guo et al., 2009). The temperature sensitivity of this calibration is lower than for calibrations based on inorganic calcite, corals, foraminiferans and coccoliths, and one that used brachiopods and bivalved molluscs, but it agrees with the Δ_{47}/T^2 relationship reported recently in one study of clumped-isotopes in mollusc and brachiopod shells. While it is possible that temperature-Δ_{47} variability is attributable to phylum-specific vital effects, we demonstrate that mollusc shell temperature calibrations originating from separate laboratories which have not been corrected for backgrounds may differ by as much as 0.05‰ in Δ_{47} over the range of marine temperatures investigated (~ 0 - 30 °C). This variation is similar in magnitude to the difference between calibrations obtained from mollusc shells and inorganic calcite, indicating that Δ_{47} measured in natural materials may be more significantly influenced by instrument-specific effects, as well as sample preparation, and handling and purification of CO_2 than current techniques are able to correct for.

3.2 INTRODUCTION

The considerable investment in time and resources devoted to the application of clumped-isotope thermometry to naturally occurring carbonates is testament to the potential of this proxy as a wholly independent mineral-based paleothermometer. However, following the first

published calibration of the clumped-isotope thermometer (Ghosh et al., 2006), inconsistencies in measurements of Δ_{47} in natural materials have been reported. In all cases the same kind of mass spectrometer, the Thermo-Finnigan 253 (cf. Yoshida, 2013) has been employed, suggesting inaccuracies arise because of two effects: 1) the dependency of Δ_{47} on $\delta^{47}CO_2$, (referred to as a "non-linearity") where measured Δ_{47} exhibits a positive correlation with $\delta^{47}CO_2$ relative to the reference gas ($\delta^{47}CO_2 \approx \delta^{13}C + 2\ \delta^{18}O$, where $\delta^{13}C$ or $\delta^{18}O = [(R_{smp} - R_{std}) / R_{std}] \times 10^3$ and where $R = {}^{13}C/{}^{12}C$ or ${}^{18}O/{}^{16}O$, smp = sample, std = reference standard), and 2) inter-laboratory discrepancies in the differences in Δ_{47} measured between CO_2 samples representing two different temperatures (referred to as "scale compression"). For example, the difference in Δ_{47} between CO_2 samples of identical isotopic composition equilibrated at 1000 ºC and 25º C may be determined to be 0.90 ‰ in one laboratory and 0.76 ‰ in another (Table 1 in Dennis et al., 2011). Initial efforts to resolve these discrepancies have employed a strategy of quantifying these effects for each instrument during the experimental phase. This approach necessarily incurs additional sources of error.

Although originally attributed to scrambling of analyte ions in the source of the mass spectrometers (Affek et al., 2009; Huntington et al., 2009), recent work suggests that the $\Delta_{47}/\delta^{47}CO_2$ non-linearity results from an apparent reduction in positive ion beam voltage that is caused by the inclusion of negative background voltage in the total measured by the Faraday cups during sample analysis (Yeung et al., 2012; He et al., 2012; Chapter 2). Experiments demonstrate that this negative voltage is due to secondary electrons sputtered from metallic surfaces inside the mass spectrometer. As expected, the effect is more pronounced for Faraday

cups with higher amplification (e.g., resistance ~ 1 x 10^{12} Ω). The method commonly used to overcome $\Delta_{47}/\delta^{47}CO_2$ non-linearity is to perform a heated gas line (HGL) correction where CO_2 samples of different isotopic composition are re-equilibrated at 1000 °C to impart a stochastic distribution of isotopologues on the samples (i.e., $\Delta_{47} = 0$), and then measured to define the non-linearity for the mass spectrometer during the period of study in order to correct for it. However, this non-linear relationship can be more easily eliminated by subtracting backgrounds that have been measured immediately before and immediately after each sample is measured (Yeung et al., 2012; He et al., 2012; Chapter 2). Furthermore, Yoshida et al. (2013) have shown that secondary electrons may not be a problem on some kinds of mass spectrometers, as they observed no non-linearity using a Thermo Delta XP.

Currently, inter-laboratory discrepancies of scale compression are nullified by correcting measured Δ_{47} values to values expected from theory. This calibration is referred to variously as the "absolute reference frame" or carbon dioxide equilibrium scale (CDES) of Dennis et al. (2011). The calibration curve relating measured Δ_{47} to theoretical Δ_{47} invokes the theoretically calculated relationship between Δ_{47} and temperature obtained by Wang et al. (2004). Similar to the HGL, the calibration line necessary for moving data to the CDES scale must be determined in each laboratory during the period of study.

Despite these efforts, questions remain. For example, are there clear differences in Δ_{47} between inorganic carbonate and biologically deposited carbonate, and if so, why? A first step toward a better understanding of Δ_{47}/T^2 in natural carbonates is to achieve inter-laboratory agreement for measurements of various species. Here we report measurements of Δ_{47} in bivalved

mollusc shells, which have been corrected by subtraction of simultaneously measured background voltage, and compare those results to the uncorrected measurements. It is shown that intra- and inter-laboratory problems in clumped-isotope thermometry are at least partly attributable to lack of attention to backgrounds that are variable in time on the scale of weeks.

3.3 MATERIALS AND METHODS

3.3.1 Modern shell samples

The calibration lines shown in Fig. 3.1 come from the carbonate shells of six modern bivalve species, which together represent a wide range of marine environments and water temperatures. Shells of deep-water species were alive when dredged; those from near-shore environments were disarticulated valves collected from intertidal settings. Shells used in this study come from cold, deep-water sites in the Caribbean and Hawaii and from warmer, shallower sites in Australia and Maine (Table 3.1). Four of the species have aragonitic shells, one is predominantly calcitic, and one has a calcitic outer shell layer and an aragonitic inner layer. Samples were obtained by scraping selected regions of the valves with a scalpel or—in the case of delicate shells—small pieces were broken off and ground to a powder in an agate mortar and pestle.

3.3.2 Bivalve growth temperatures

The temperature calibration for clumped-isotope thermometry requires estimates of water temperatures at the locations where the sampled bivalves grew. In the case of the two deep-water species, *Euciroa pacifica* from Hawaii and *Propeamussium dalli* from Panama, the sub-thermocline water temperatures in which they lived are thought to have been nearly constant during the lifetimes of the animals. We therefore allocate small error estimates (± 1°C) to their growth temperatures. Shallow-water temperatures are more seasonably variable than temperatures beneath the thermocline, but we were able to estimate average annual growth temperature for the shallow-water species using data from nearby meteorological stations or, in one case, an archival record from associated reef corals. Locality information and evidence for the growth temperature of each species studied is summarized briefly below:

CIS 004 *Propeamussium dalli* Smith 1885. Uncataloged specimens from the U.S. Fish and Wildlife Service MV. Collected (trawled) on May 31, 1962 at *Oregon* station 3600 (west of Colon, Panama; 9°03'N, 81°18'W) from a depth of, 300 fm (550 m). For the calibration we used water temperature (7 ± 1 °C) reported at nearby Smithsonian Institution MV *Hannibal* station 241 (9°19'N, 81°22'W) at depth of 576 m, and 7.04 °C by Wüst (1964, Table IV, p. 164). Large-scale hydrodynamic circulation of the Caribbean Sea indicated little variability in temperature (approximately ±1 °C) at that depth (Gordon, 1962; Morrison and Nolan, 1982). We measured clumped-isotopes in CO_2 liberated from foliated calcite taken from the commissural areas of two left valves.

CIS 006 *Euciroa pacifica* Dall 1895. USNM 335528, U.S. Fish Commission Steamer *Albatross* station 3865, 256–283 fm (469–518 m), N of Nakalele Point, Maui, within the Pailolo Channel, Hawaii (21°09'20"N, 156°35'10"W); collected (dredged) on April 10, 1902. For the calibration, we used the water temperature reported (44.9 °F = 7.2 °C) at station 3865 when collected (U.S. Fish Commission Report for 1902, p. 407). Temperatures at that depth are reported to be ~6 ± 1°C regionally and annually during the 1980s (Sansone et al., 1988), suggesting that variability is low. We measured samples of nacreous aragonite from the left valve.

CIS 025 *Mya arenaria* Linneaus 1758. Salisbury Cove, ~6 km NW of Bar Harbor, Mount Desert Island, Maine (44.433°N, 68.283°W). These shells were collected from the intertidal zone at low tide on July 23, 2003. Average water temperatures for the period July 1, 2002 to June 30, 2003 based on hourly records from NOAA/NOS/CO-OPS meteorological station 8413320 in Bar Harbor (44.392°N, 68.205°W) are 7.2 ± 5.6°C. However, in eastern Maine most shell growth in *M. arenaria* occurs between early April and the beginning of September (Beal et al., 2001; Beal, 2002), so we used that constraint and the earliest available tabulated records for station 8413320 (2010) to obtain a calibration temperature of 11 ± 2.7°C. We measured samples of crossed-lamellar aragonite from the commissural areas of two valves.

M. arenaria occurs in intertidal mudflats along the western Atlantic coast from the southern United States to Canada, as a Holocene immigrant to the United Kingdom, Ireland and nations bordering the North Sea, and as an invasive species along the U.S. Pacific northwest and adjacent coasts of Canada and Alaska (Petersen et al., 1992; Powers et al., 2006; Strasser 1999; Crocetta and Turolla, 2011). Its abundance and wide geographic distribution may make it a

useful inter-laboratory reference standard for future clumped-isotope paleoenvironmental studies. As a first step in this direction, we compare our results with clumped-isotope data obtained from *M. arenaria* by Henkes et al. (2012) (Fig. 3.4).

CIS 023 *Perna canaliculus* (Gmelin) 1791. Wellington Harbour, Wellington, New Zealand (41° 18'S, 174° 47'E). These shells were collected from the shoreline on February 15, 1980. For the calibration, we used average sea surface temperatures (14.5 ± 3 °C) from high-resolution satellite (Uddstrom and Oien, 1999). Hickman (1979) reports a mean average annual temperature of 14.5 °C, based on measurements made in Wellington Harbour during the years 1971–1973. This temperature also agrees well with measurements given by Booth (1972) for the years 1970–1972 (14.3 ± 2.6 °C). Larger shells, such as the one sampled (190 mm in length) grow at approximately the same rate throughout the year (Fig. 5 in Hickman, 1979). We measured clumped-isotopes in samples of both calcitic outer prismatic layer and aragonitic inner nacreous layer from commissural edge of valves.

CIS 022 *Cleidothaerus albidus* (Lamarck) 1819. Depot Beach, north of Batemans Bay, New South Wales, Australia (35° 37.8'S, 150° 19.7'E). These shells were collected from the intertidal zone on October 27, 2011. *C. albidus* is an anomalodesmatid "oyster" that is cemented by its right valve to hard substrates in subtidal water depths of 10–35 m (Allan, 1950). For the calibration we used the average of monthly water temperatures (18.8 ± 5.5 °C) at ~70 m water depth from nearby Directional Waverider buoy (35°42.4'S, 150°20.6'E) during the period 09/21/1999–12/31/2011 (Manly Hydraulics Laboratory, N.S.W. Office of Environment and Heritage). We measured samples of the aragonitic nacreous layer of the left valve.

CIS 020 *Pharaonella pharaonis* (Hanley) 1844. Mission Beach, S of Innisfail, Queensland, Australia (17.89°S, 146.10°E). These shells were collected from the beach on August 28, 1978. For the calibration we used water temperature (25 ± 3 °C) reported at nearby Pandora Reef (18.81°S, 146.43°E) in McClulloch et al. (1994) for 1978–1983, and based on high-resolution Sr/Ca and $\delta^{18}O$ sclerochronological records from the coral *Porites lutea*. We measured samples of crossed-lamellar aragonite from one pulverized valve.

3.3.3 Clumped-isotope measurements

All measurements were made at the University of California, Los Angeles in the Department of Earth and Space Sciences on a Thermo-Finnigan 253 gas-source mass spectrometer during February to May of 2012. Due to the unusual arrangement of Faraday cups in this instrument, permitting measurements of either O_2 or CO_2, we used the multicollector peak hopping (MPH) method of analysis described in Chapter 2. MPH uses sample $\delta^{13}C$, $\delta^{18}O$ and $^{46}CO_2/^{47}CO_2$ to calculate Δ_{47} (the abundance of ^{13}C-^{18}O-^{16}O, ^{13}C-^{16}O-^{18}O and symmetrical variants). Prior to this study, we found that the $\Delta_{47}/\delta^{47}CO_2$ non-linearity, described by Huntington et al. (2009) could be eliminated by measuring and subtracting the background signal created by secondary electrons. Our strategy is similar to the "pressure baseline" (PBL) method of He et al. (2012), but is simpler in that we only need to use the two minor beams for *m/z* 46 and *m/z* 47 to make the correction. Internal precision using MPH is similar to that reported in other clumped-isotope studies (~ 0.022 ‰ standard error). Further details of the multicollector peak hopping (MPH) method are given in Chapter 2.

3.3.3.1 Temperature-equilibrated CO_2 standards

Stochastic CO_2 standards were created using methods similar to those of Huntington et al. (2009). Initial gas came from several different sources of CO_2, ranging in bulk composition from -55 ‰ to +28 ‰ in $\delta^{47}CO_2$. Aliquots were isolated in quartz ampules, flame-sealed, and then heated in a muffle furnace to 1000 °C for at least three hours. While it is impossible to confirm a truly stochastic distribution of CO_2 isotopologues following cooling, we sought to minimize potential back-equilibration at intermediate temperature by immediately quenching the ampules in cold water.

Additional temperature-equilibrated standards were prepared by allowing CO_2 to exchange oxygen with water at two controlled temperatures (2 °C and 25 °C) in stopcock-sealed vessels. These vessels may be fitted directly to the extraction line, minimizing handling time and likelihood of back-equilibration during extraction. Standards equilibrated at 25 °C were held in a water bath for 72 to 192 hours. Standards equilibrated at 2 °C were immersed in a beaker of water held at temperature for approximately one month.

3.3.3.2 Phosphoric acid digestion of carbonates

Approximately 10 mg of powdered sample is loaded into one leg of a two-leg reaction vessel opposite ~ 2 ml of high-density phosphoric acid (specific gravity = 1.92 mg/ml), and then evacuated on the extraction line for 6-10 hours (typically overnight). The vessels are sealed off with a baseline pressure of $< 1 \times 10^{-5}$ mb then moved into a water bath held at 25 °C and allowed to equilibrate for > 30 min. Next, sample vessels were tipped to introduce acid to the carbonate,

and then returned to the water bath to react at constant temperature for at least 16 hours. Although most reactions were complete by visual inspection after 16 hours, inspection under a binocular microscope revealed a few cases where microscopic bubbles were still being produced after CO_2 extraction, indicating less than 100% reaction. However, we do not expect the trivial quantity of CO_2 retained in residual carbonate to have a noticeable effect on the measured isotope ratios.

3.3.3.3 CO_2 purification

We use a glass vacuum extraction line with on-line gas chromatograph to remove contaminants from CO_2 samples prior to analysis. The CO_2 liberated from carbonate by reaction with H_3PO_4 at 25 °C, is separated from H_2O cryogenically, and then entrained in ~ 12-15 ml/min helium flow through a ~2 m porapak Q column chilled to -30 °C. After passing through the column, CO_2 samples are recaptured by freezing in a metal u-trap and helium is pumped away. Finally, the CO_2 is transferred to stopcock-sealed borosilicate sample vessels for analysis. Each standard and sample is analyzed within five hours of passing through this system in order to minimize the possibility of re-equilibration of CO_2 at room temperature.

3.3.3.4 Mass spectrometric analysis

Each sample is introduced to the mass spectrometer through a dual-inlet system using nickel capillaries that were evacuated and then cleaned by heating until red-hot between samples. Bellows pressure is adjusted to produce a mass 44 signal of ~14 volts (amplifier resistor = 10^8 Ω)

for determining $\delta^{13}C$ and $\delta^{18}O$, and then is re-adjusted to produce a mass 46 signal of ~6 volts (amplifier resistor = 10^{10} Ω) in order to measure $^{47}CO_2/^{46}CO_2$. The measurement sequence consists of: 1) two ten-cycle blocks measuring *m/z* 44, 45 and 46, 2) reducing the accelerating voltage to direct mass 46 and 47 beams into the Faraday cups normally used for masses 45 and 46, 3) running a three-cycle pre-analysis background measurement, 4) running the ten-cycle sample analysis, and 5) running another three-cycle background analysis after the sample analysis.

3.3.3.5 Reference gas

All measurements in this study were made against the same reference gas purchased from OzTech (Dallas, TX, USA). The composition of this reference gas is $\delta^{13}C = -3.58$ ‰ PDB, $\delta^{18}O = +24.96$ SMOW ‰. The reference gas has Δ_{47} values reflective of near room-temperature equilibration.

3.3.3.6 Data reduction and analysis

In order to provide both a clear comparison of the effects of different measurement procedures and to produce a temperature calibration comparable to calibrations reported in other laboratories, we wrote a Fortran program to reduce the data using the "heated gas line" (HGL) method of Huntington et al. (2009) and our own background correction method (Fortran code and further description are provided in Appendix). Additionally, we report data in the CDES scale, for both HGL-only corrected and background corrected data, using a $\Delta_{47theoretical}/\Delta_{47measured}$

calibration line as described by Dennis et al. (2011). This results in four different Δ_{47} values for each sample (Table 3.1): 1) HGL correction only [$\Delta_{47,HGL}$], 2) HGL correction after measured background correction [$\Delta_{47,BG}$], 3) HGL correction, and conversion to CDES [$\Delta_{47,CDES}$], and 4) HGL correction after background correction, followed by conversion to CDES [$\Delta_{47,BG,CDES}$].

3.4 RESULTS

Table 3.1 reports isotopic compositions ($\delta^{13}C$, $\delta^{18}O$, $\delta^{47}CO_2$ and Δ_{47}) and growth temperatures inferred or measured (sec. 3.3.2) for all bivalves sampled. Bulk composition ($\delta^{47}CO_2$) is needed for heated gas lines with and without background correction, necessitating the reporting of $\delta^{47}CO_2$ values with and without background corrections in Table 3.1. Fig. 3.1 is a plot of the two distinct calibrations resulting from CDES-normalized data with (blue) and without (red) background corrections.

Internal precision using standard error for twenty-three of twenty-five analyses of Δ_{47} comprising the temperature calibration in this study are < ± 0.02 ‰ (1 std. error), similar to that reported in previous studies of methods employed in measuring Δ_{47} by gas-source mass spectrometry (Huntington et al., 2009). The two exceptions are one analysis of *Mya arenaria* and one analysis of *Pharaonella pharaonis* (internal standard error = ± 0.027 ‰, and ± 0.024 ‰, respectively). External standard error in the mean is typically ± 0.01 based on 2 to 7 replicates, and varied only slightly with measurement/data reduction method.

Table 3.1. Isotopic composition ($\delta^{13}C$, $\delta^{18}O$, $\delta^{47}CO_2$, Δ_{47}) and known growth temperatures of marine bivalves.

Species	Growth Temp. (°C)	$\delta^{18}O$ (PDB)	$\delta^{13}C$ (PDB)	$\delta^{47}CO_2$ (‰, ref)	$\delta^{47}CO_{2,BG}$ (‰, ref)[a]	$\Delta_{47,HGL}$ (‰, ref)[b]	$\Delta_{47,BG}$ (‰, ref)[c]	$\Delta_{47,CDES}$ (‰, sto)[d]	$\Delta_{47,BGCDES}$ (‰, sto)[e]
Propeamussium dalli	7.0 ±1.0	2.75	2.10	24.95	24.73	-0.195	-0.151	0.707	0.731
Propeamussium dalli	7.0 ±1.0	2.68	2.03	24.80	24.59	-0.199	-0.137	0.702	0.746
Propeamussium dalli	7.0 ±1.0	2.74	2.01	24.83	24.62	-0.211	-0.150	0.689	0.731
Propeamussium dalli	7.0 ±1.0	2.87	2.00	24.97	24.74	-0.196	-0.155	0.705	0.726
Propeamussium dalli	7.0 ±1.0	2.79	1.98	24.95	24.63	-0.206	-0.162	0.695	0.718
Euciroa pacifica	7.2 ± 1.0	3.00	0.07	23.18	22.98	-0.195	-0.142	0.707	0.740
Euciroa pacifica	7.2 ± 1.0	2.81	-0.34	22.60	22.41	-0.168	-0.117	0.736	0.768
Euciroa pacifica	7.2 ± 1.0	2.88	-0.16	22.82	22.63	-0.199	-0.134	0.703	0.749
Euciroa pacifica	7.2 ± 1.0	2.82	-0.39	22.49	22.30	-0.234	-0.184	0.663	0.693
Euciroa pacifica	7.2 ± 1.0	2.81	-0.36	22.54	22.33	-0.200	-0.173	0.701	0.707
Euciroa pacifica	7.2 ± 1.0	2.86	-0.45	22.52	22.27	-0.200	-0.198	0.701	0.678
Euciroa pacifica	7.2 ± 1.0	2.88	-0.16	22.85	22.61	-0.168	-0.164	0.737	0.716
*Mya arenaria**	11.0 ±2.7	1.09	1.57	22.64	22.45	-0.231	-0.168	0.666	0.712
Mya arenaria	11.0 ±2.7	1.09	1.57	22.66	22.45	-0.212	-0.169	0.688	0.710
Perna canaliculis	14.5 ±3.0	1.42	1.06	22.48	22.29	-0.222	-0.171	0.676	0.708
Perna canaliculis	14.5 ±3.0	1.44	1.01	22.46	22.26	-0.214	-0.171	0.685	0.709
Cleidothaerus albidus	18.8 ±5.0	1.08	0.01	22.08	21.87	-0.218	-0.181	0.681	0.697
Cleidothaerus albidus	18.8 ±5.0	0.94	0.93	21.86	21.68	-0.210	-0.161	0.690	0.720
Pharaonella pharaonis	25.0 ±3.0	-0.37	-0.45	19.07	18.92	-0.274	-0.168	0.632	0.683
*Pharaonella pharaonis**	25.0 ±3.0	-0.38	-0.51	19.00	18.82	-0.243	-0.219	0.653	0.655
Pharaonella pharaonis	25.0 ±3.0	-0.32	-0.52	19.06	18.89	-0.247	-0.207	0.649	0.668
Pharaonella pharaonis	25.0 ±3.0	-0.34	-0.48	19.07	18.91	-0.254	-0.206	0.641	0.669

Note: Each measurement represents a single acid digestion of shell material analyzed with 5-10 off-peak background/on-peak analysis/off-peak background blocks. Standard errors of the means ($1\sigma/\sqrt{n}$ where 1σ is the standard deviation of n analyses) for all measurements are < 0.01 for $\delta^{18}O$ and $\delta^{13}C$, < 0.02 for $\delta^{47}CO_2$ and $\delta^{47}CO_{2BG}$, < 0.02 for all types of Δ_{47} except for two samples marked with * where standard error of the mean < 0.03.

[a] $\delta^{47}CO_2$ is reported against reference gas and is slightly different with background correction.

[b] Δ_{47HGL} = corrected with HGL of Huntington et al. (2009) only.

[c] Δ_{47BG} = corrected for backgrounds then HGL method.

[d] Δ_{47CDES} = corrected with HGL and transferred to CDES scale of Dennis et al. (2011).

[e] $\Delta_{47BGCDES}$ = corrected for backgrounds then HGL and transferred to CDES scale.

ref = reference gas

sto = stochastic

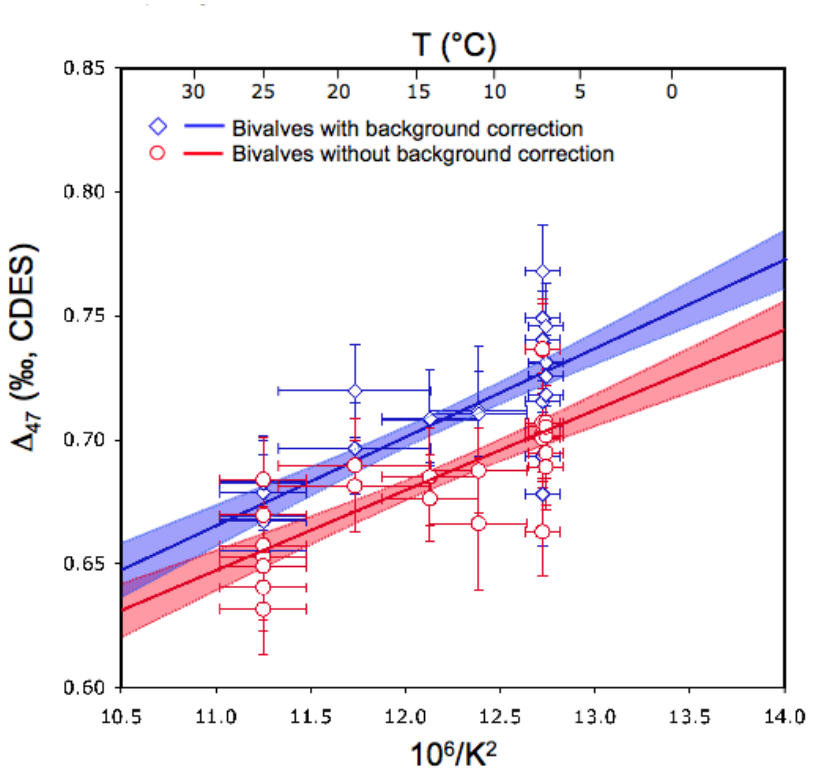

Fig. 3.1. All measurements of Δ_{47} in CO_2 liberated from bivalve shells grown at known temperature. Measurements corrected for backgrounds (blue diamonds) appear to be ~ 0.025‰ enriched in Δ_{47} against uncorrected measurements (red circles) of the same CO_2 samples. Each data point represents a separate phosphoric acid digestion at 25 °C, analyzed using 5-10 off-peak background/on-peak sample/off-peak background blocks (exact details in Chapter 2). Error bars represent standard error of the mean ($=1\sigma/\sqrt{n}$). Error envelopes are 95% confidence level. Standard error in the mean for each measurement is generally unaffected when backgrounds are included, although Δ_{47} for one sample in this study moved relative to its calibration line by as much as 0.03‰.

Bivalves believed to have grown in the coldest waters (*Euciroa pacifica* and *Propeamussium dalli*) are the most enriched in Δ_{47}, with mean values of 0.722 ‰ ± 0.012 and 0.730 ‰ ± 0.005(with background correction) or 0.707 ‰ ± 0.009 and 0.700 ‰ ± 0.003 (without background correction), while the tropical bivalve species (*Pharaonella pharaonis*) is

the least enriched in Δ_{47}, with mean values of 0.672 ‰ ± 0.004 (with background correction) or 0.655 ‰ ± 0.007 (without background corrected). We find no significant outlier in Δ_{47} as it relates to temperature among the species we examined. Least squares linear regression of the Δ_{47} data versus $1/T^2$ results in two distinct calibration lines. For background-corrected data we obtain

$$\Delta_{47} = 0.0358\ (\pm\ 0.0060)\ \text{x}\ 10^6/T^2 + 0.2717\ (\pm\ 0.0734).$$

Without background correction we obtain

$$\Delta_{47} = 0.0323\ (\pm\ 0.0060)\ [10^6/K^2] + 0.2918\ (\pm\ 0.0729).$$

The R^2 values for these equations are 0.856 and 0.722 respectively.

Although calcite shells are predicted to be ~ 0.02 ‰ depleted in Δ_{47} as compared to aragonite shells (Guo et al., 2009), we are unable to discern a difference in Δ_{47} related to the $CaCO_3$ phase of the shells. Mean values for both the sample of *Propeamussium dalli*, composed solely of calcite and *Perna canaliculis,* composed of both calcite and aragonite are < 0.01 ‰ from the calibration line.

3.5 DISCUSSION

The clumped-isotope temperature calibrations reported here result from employing different methods to analyze individuals of several different species of bivalved molluscs that grew in a wide range of water temperatures (7 to 25 °C). Here, in section 3.5 we seek to explain the differences we observed between measurements made with and without background correction, and their potential effects on clumped-isotope thermometry. In section 3.5.2 we

explore differences between our calibrations and previous calibrations from measurements of shells from other marine organisms and laboratory-grown inorganic calcite. We do not compare our findings to Δ_{47} data from non-marine environments (soil carbonate nodules and speleothems) as they introduce additional uncertainties in the form of kinetic effects that affect measured Δ_{47} (Affek et al., 2008).

3.5.1 Effects of background correction

3.5.1.1 Absolute value of Δ_{47}

Correcting measurements for measured backgrounds significantly changes Δ_{47} values measured in CO_2 derived from the acid digestion of carbonates (Fig. 3.1). As we are dealing with the same gas sample in each case, the difference is not attributable to variability in gas handling during extraction and purification. It also cannot be due to the small differences in $\Delta_{47theoretical}/\Delta_{47measured}$ calibration lines used for conversion to the CDES scale, as differences in Δ_{47} (~0.45 ‰) between background-corrected and non-background-corrected data are apparent prior to correction (Table 3.1). Negative background voltages registered by Faraday cups during measurements reduce the apparent intensities of the ion beams measured in the cups. Since the Faraday cup that measures mass 47 typically has a higher resistor, it is more sensitive to secondary electrons and therefore displays a more negative background voltage. Therefore, removing the background voltages should increase the measured 47 beam intensity more than the 46 or 44 beam intensities, resulting in larger measured Δ_{47}. Incomplete nulling of these effects when background corrections are omitted by comparison to the reference gas (e.g., background

difference between sample and reference gases) could be an explanation for the relative positions of our background corrected and uncorrected calibration lines.

3.5.1.2 Magnitude of effect on thermometry

When comparing background-corrected data with the background corrected calibration and non-background data to the non-background corrected calibration the difference in derived growth temperature is typically small (± 2.0 °C). However, the most affected species in this study *Mya arenaria*, yields Δ_{47} = 0.712 ‰ ± 0.027 and 0.710 ‰ ± 0.017 in two separate analyses when background corrected and Δ_{47} = 0.666 ‰ ± 0.027 and 0.688 ‰ ± 0.017 when not corrected for background. If the growth temperature for this shell (11.0 ± 2.7 °C) were not known, the background correction method would suggest an average temperature of 12.3 °C, while omitting the background correction would indicate in average temperature of 16.5 °C. In other words, correcting for backgrounds shifted the sample 4.2 °C closer to the calibration line.

3.5.2 Comparisons to previous calibrations

Figs. 3.2 and 3.3 include lines representing previous clumped-isotope temperature calibrations generated from acid-digestion of modern shells and inorganic carbonates, as well as theoretical slopes for Δ_{47}/T^2, all of which are reported in the CDES scale and should therefore be directly comparable.

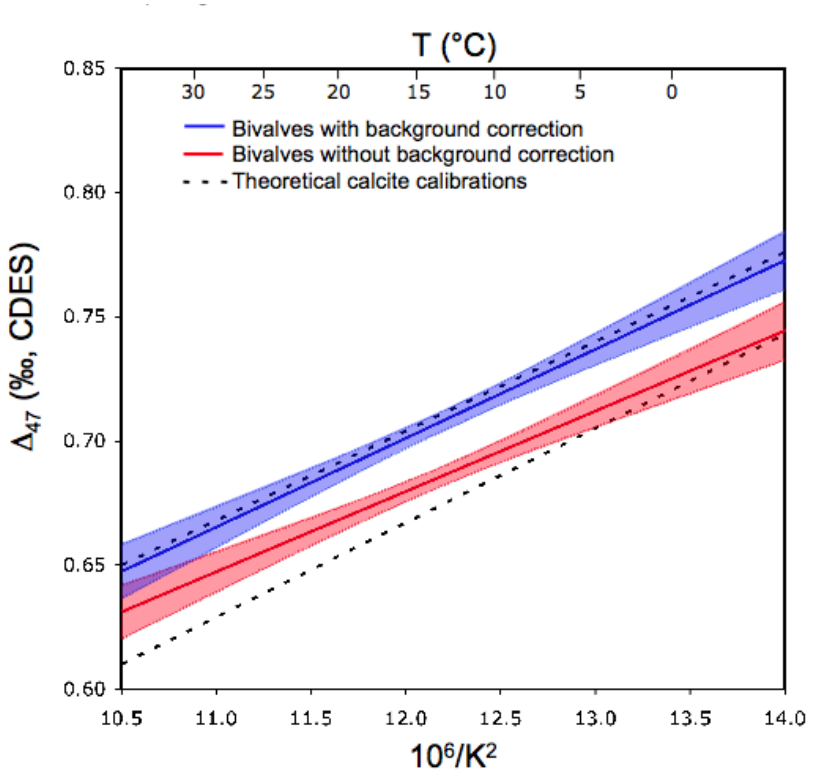

Fig. 3.2. Calibration of mollusc shells (background corrected = blue line, without background correction = red line) and theoretical calibrations for calcite (short-dashed lines: lower = ab initio, upper = recalculated by Henkes et al. (2013) using experimentally determined acid fractionation factor).

3.5.2.1 Clumped-isotopes in mollusc shells

Both background-corrected and non-background-corrected temperature calibrations are in reasonable agreement with the calibration of Henkes et al. (2013; Fig. 3.3). This study and Henkes et al. together include 17 extant species of molluscs, one species of *Nautilus* (Henkes et al., 2013), and one species of gastropod (Henkes et al., 2013). This suggests that biomineralization of either calcite or aragonite by molluscs consistently produces shell carbonate

with clumped-isotope signatures reflective of the precipitation temperature. However, our calibration lines differ from the previously mentioned calibration in the absolute magnitude of clumped-isotope enrichment (Δ_{47}) for mollusc shells that grew at any given temperature. The difference in Δ_{47} between this study and that of Henkes et al. is ~ 0.02 ‰ with background correction and ~ 0.05 ‰ without background correction. Oddly, the Δ_{47}/T^2 slopes in both this study and that of Henkes et al. (2013) differ significantly from the original slope reported by Came et al. (2007). The latter found three species of mollusc (and three species of brachiopod) conforming to the inorganic calcite Δ_{47}/T^2 calibration of Ghosh et al. (2006; described further in section 4.2.3). Additionally, the Δ_{47}/T^2 obtained here and by Henkes et al. from mollusc shells are within error of the theoretical Δ_{47}/T^2 for phosphoric acid digestion of carbonate minerals (Schauble et al., 2006; Guo et al., 2009).

Dennis et al. (2013), found the temperature range inhabited by *Nautilus* to be too narrow to define a viable calibration, but noted that measured Δ_{47} was much lower than expected based on the inorganic calcite calibration of Ghosh et al. (2006), and concluded therefore, that there must be unidentified vital effects specific to cephalopods that led to real depletions (~0.05‰, and in some cases as much as 0.1‰) of Δ_{47} in sampled shell material. Regression of the Dennis et al. (2013) data provides little clarity, as the slope of the calibration line (0.0463 ± 0.0135) is very uncertain, and falls between those of Ghosh et al. (2006) and Henkes et al. (2013). Accordingly, it is possible that the mollusc calibration given here, which agrees with theoretical Δ_{47}/T^2, may apply to other species of molluscs as well, including *Nautilus* (Fig. 3.4).

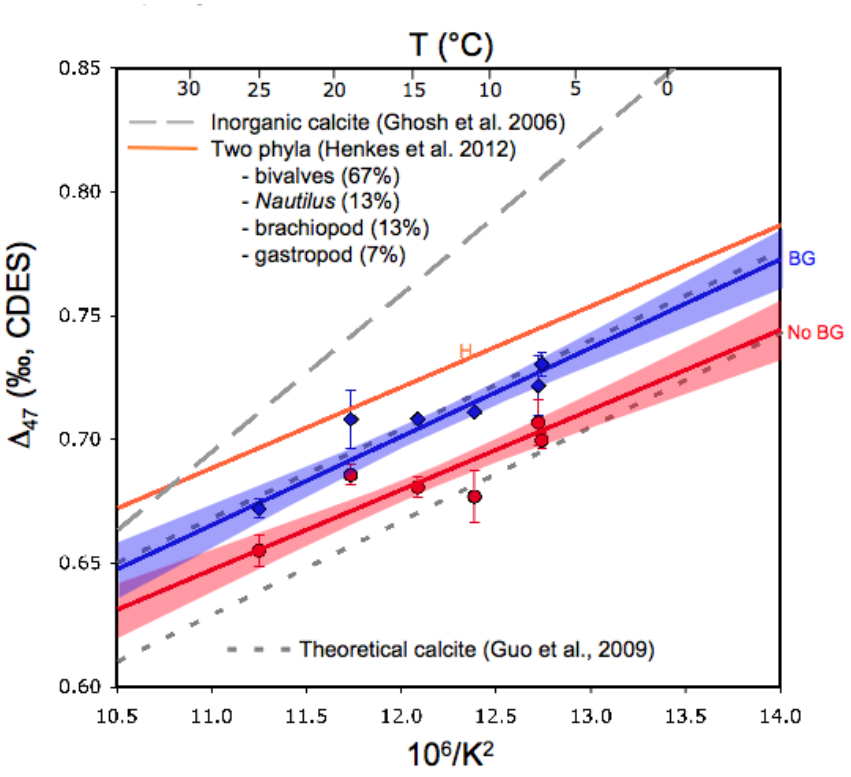

Fig. 3.3. Comparison of clumped-isotope temperature calibrations. Empirical calibrations derived from acid digestion of: inorganic laboratory-grown calcite (long-dashed line; Ghosh et al., 2006; recalculated by Dennis et al., 2011), molluscs and brachiopods (orange line marked with "H"; Henkes et al., 2013), bivalves with background correction (blue line marked with "BG" and blue diamonds; this study), bivalves without background correction (red line marked with "No BG" and red diamonds; this study), and theoretically calculated calibrations for calcite (short-dashed lines: lower = ab initio calculations of Guo et al., (2009); upper = recalculated by Henkes et al. (2013) using experimentally determined acid fractionation factor). All slopes depicted here are in the common reference frame (CDES of Dennis et al., 2011) and should be directly comparable. Calibrations derived from mollusc shells (this study) or almost completely from mollusc shells (Henkes et al., 2013) demonstrate general agreement with the relationship between Δ_{47} of liberated CO_2 and known shell growth temperatures. This occurs despite differences in acid digestion temperature, sample preparation methods, and gas handling equipment. Calibrations using corals and foraminifera generally conform to the inorganic calcite calibration (section 3.5.2.3). Diamonds and circles represent means for each sample. Error bars represent standard errors ($1\sigma/\sqrt{n}$). Error envelopes are 95% confidence level.

3.5.2.2 Direct comparison of species in common

Henkes et al. (2013) included six individuals of *Nautilus pompilius* and three individuals of *Mya arenaria* in their calibration, allowing a direct comparison to be made with *Nautilus pompilius* measured by Dennis et al., (2013) and *Mya arenaria* used in this study. Fig. 3.4 shows Δ_{47} values measured in these mollusc shells, demonstrating the current state of inter-laboratory calibration. In addition, Henkes et al. (2013; J) report an inter-laboratory comparison of Δ_{47} values measured in the same *Hiatella arctica* shell, by distributing aliquots of shell to laboratories at Yale University (Y) and California Institute of Technology (C). These are plotted in Fig. 3.4 as squares labeled with a single letter to identify their sources.

Measurements of *Hiatella arctica* demonstrate minor pre-CDES inter-laboratory differences. Measurements of Δ_{47} in the same shell distributed to Yale University, Johns Hopkins University and California Institute of Technology differ by as much as 0.02‰. The CDES scale is intended to nullify the effects of instrument-specific source fragmentation or recombination (scrambling) reactions during analysis as well as "scale compression" of Δ_{47} in order to bring all laboratories into a "common reference frame". The objective of a common reference frame is to produce statistically indistinguishable Δ_{47} values from shells of the same species grown at the same temperature, independent of laboratory. However this was not achieved in two measurements of *Nautilus pompilius*, as after CDES scaling, the inter-laboratory differences in Δ_{47} remain (Fig. 3.4). Six individuals used in the Henkes et al. (2013) calibration appear to be enriched by approximately 0.025‰ in Δ_{47} compared with the twelve specimens sampled by Dennis et al. (2013). Since this difference is similar in magnitude to the difference between our

background-corrected and uncorrected calibration lines, we speculate that inter-laboratory differences in backgrounds are responsible for the different values of Δ_{47} measured in *Nautilus pompilius* shells of similar temperature.

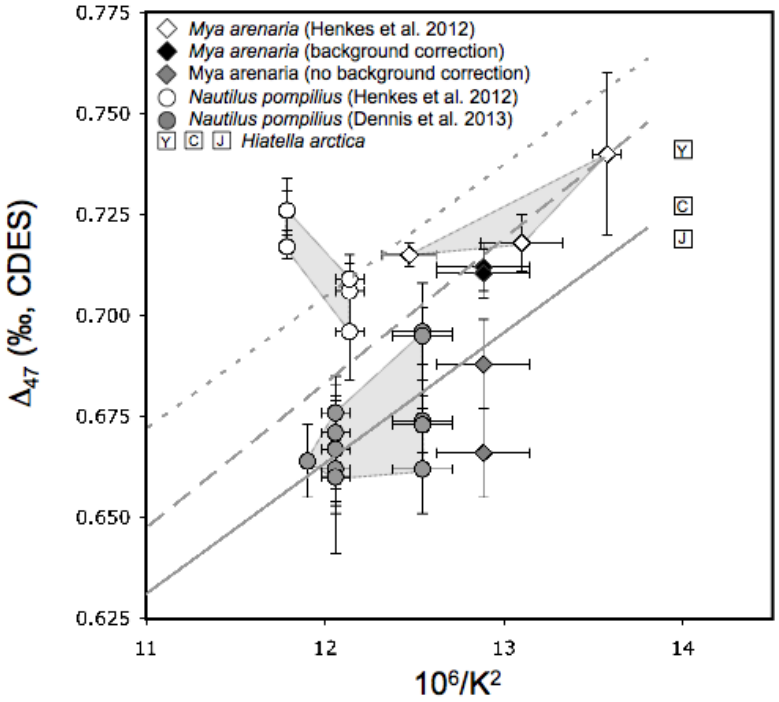

Fig. 3.4. Comparison of mollusc species common to multiple published empirical calibrations (all measurements reported in CDES). *Mya arenaria* appears in both Henkes et al. (2013; open diamonds) and this study (background corrected = filled diamonds, without background correction = gray diamonds). *N. pompilius* is common to both Henkes et al. (2013; open circles) and Dennis et al. (2013; filled circles). Gray polygons emphasize range of measured Δ_{47}/T^2. Square symbols represent measurements of the same *Hiatella arctica* shell measured in three different laboratories (Y = Yale University, C = California Institute of Technology, J = Johns Hopkins University) and corrected by comparison to stochastic gas standards, but not converted to the universal reference frame (Henkes et al., 2013). Although these measurements are not directly comparable to the calibrations pictured here, the scale of difference in these measurements is similar to that of CDES data, indicating that inter-laboratory bias remains significant. Calibrations: short-dashed = Henkes et al. (2013), long-dashed = with background correction, solid = without background correction.

However, *Mya arenaria* shells measured by Henkes et al. (2013) demonstrate a similar range of Δ_{47} values to the background corrected measurements of *Mya arenaria* presented in this study (Fig 3.4). Uncorrected measurements of *Mya arenaria* from this study are lower in Δ_{47} by ~ 0.05‰ relative to the background corrected measurements, as expected from Fig. 3.2. One difference between our measurements *Mya arenaria* and those of Henkes et al. (2013) is the bulk oxygen isotope ratio. It is conceivable, but to us seems unlikely, that a small difference in $\delta^{18}O$ influences measurements of Δ_{47} at the same temperature at the 0.01 ‰ level.

3.5.2.3 Laboratory-grown calcite, corals, foraminiferans

Both versions of the calibration reported in this study differ significantly in slope from the Δ_{47}-temperature relationships determined in studies using inorganically precipitated carbonates (Ghosh et al., 2006), foraminiferans and coccoliths (Tripati et al., 2010; Grauel et al., 2013), and corals (Thiagarajan et al., 2011), and the earliest measurement of clumped-isotopes in bivalved molluscs and brachiopods (Came et al., 2007, supplementary information) all of which found greater temperature sensitivity (slopes of ~ 0.060 in CDES; Table 3.2). Our calibration lines with and without background correction intersect the inorganic calcite calibration line of Ghosh et al. (2006) [as recalculated by Dennis et al. (2011)], at 44°C and 51°C, respectively. Similarly, Henkes et al. (2013), found lower Δ_{47}-temperature relationship in a multi-phyletic study of mostly molluscs (slope = 0.0327).

Table 3.2. Comparison of several carbonate clumped-isotope thermometer calibrations.

	Temp. Range (°C)	Slope	Intercept
Ghosh et al. (2006 and 2011*)	2 to 50	0.0636 ± 0.0049	–0.0047 ± 0.0520
Henkes et al. (2013)	-1 to 29	0.0327 ± 0.0022	0.3286 ± 0.0278
Dennis et al. (2013)**	15 to 23	0.0463 ± 0.0153	0.1345 ± 0.1570
This study (background correction)	7 to 25	0.0358 ± 0.0060	0.2717 ± 0.0734
This study (no background correction)	7 to 25	0.0323 ± 0.0060	0.2918 ± 0.0729

* Original empirical calibration of clumped-isotope thermometer using laboratory-grown calcite ($\Delta_{47} = 0.05927 \times 10^6/T^2$) was converted to CDES by Dennis et al. (2011). This calibration fits several others derived from corals, foraminiferans and coccoliths, and bivalves and molluscs (section 4.2).
** Data regressed for comparison purposes in this study only.

3.5.3 Comparing Δ_{47}/T^2 among molluscs, theory, and other phyla

We find it telling that our mollusc calibration and that of Henkes et al. (2013) agrees with theory, suggesting an absence of vital effects in these samples. They explored possible explanations for the differences in Δ_{47}/T^2 between molluscs and laboratory-grown calcites, corals and foraminifera, including: 1) differences in acid digestion temperature among laboratories, 2) mixing isotopically diverse regions of sample shell for analysis, 3) the inclusion of amorphous calcium carbonate that is a component of some shell samples, 4) differences in the proportion of dissolved inorganic carbon involved in precipitation (laboratory-grown calcite) or shell formation, 5) differences in dissolved inorganic carbon species in precipitation (laboratory-grown calcite) or shell formation, 6) possible inheritance of ^{13}C-^{18}O bonds from original CO_2 gas without equilibration as CO_3^{2-} used to form carbonate. Some of these possibilities were demonstrated to be implausible with additional experiments, and several of the other possibilities would produce an effect opposite to that observed in measured Δ_{47}. If theory is correct, "vital

effects" compromising the true Δ_{47}/T^2 relationship occur in corals, foraminiferans, and inorganic calcite. We have considered the possibility that inter-laboratory variability in backgrounds is responsible for significant differences in Δ_{47}/T^2 measured in natural materials, but the effects of backgrounds in this study do not seem large enough to explain the large difference in slope.

3.6 CONCLUSIONS

The results presented here confirm that Δ_{47} values obtained by methods that correct for measured background voltage can be appreciably different from Δ_{47} values derived from by heated gas line (HGL) corrections alone. For our dataset, the average offset between these two ways of measuring Δ_{47} is 0.025 ‰, similar in magnitude to discrepancies between laboratories measuring the same material. However, the slopes of the temperature calibration lines produced by applying either of these measurement methods to bivalved mollusc shells are similar.

Our calibration agrees with one recent mollusc-based calibration of the clumped-isotope thermometer, but significantly different from those made from measurements of laboratory-grown calcite, corals, foraminiferans and coccoliths and bivalves (Came et al., 2007). It appears that the temperature-dependence of clumped-isotopes in mollusc shells is established, but agreement on the absolute magnitude of Δ_{47} for any specific temperature of shell formation is not yet clear. If that is the case, then clumped-isotope temperatures of unknown shells obtained from machine-specific and time-specific calibration curves should be widely applicable, even though

the absolute magnitude of Δ_{47}, which is not important for carbonate thermometry, may remain uncertain.

Measurements of CO_2 liberated from natural carbonates in this study approximate the theoretically calculated Δ_{47}-temperature relationship for carbonate minerals better than others to date, but this means that temperatures standardized by comparison to theoretical or empirical calibrations from other laboratories may be susceptible to significant error. However, by using background corrections, and therefore proper measures of ion beam intensities, the need for in-house temperature calibrations might be lessened.

3.7 REFERENCES

Affek H.P., Bar-Matthews M., Ayalon A., Matthews A. and Eiler J.M. (2008) Glacial/interglacial temperature variations in Soreq cave speleothems as recorded by 'clumped isotope' thermometry. *Geochim. Cosmochim. Acta* **72**, 5351–5360.

Allan J. (1950) *Australian Shells*. Georgian House, Melbourne.

Beal B.F., Parker M.R. and Vencile K.W. (2001) Seasonal effects of intraspecific density and predator exclusion along a shore-level gradient on survival and growth of juveniles of the soft-shell clam, *Mya arenaria* L., in Maine, USA. *J. Exp. Marine Bio. and Ecol.* **264**, 133–169.

Beal B.F., 2002. Adding value to live, commercial size soft-shell clams (*Mya arenaria* L.) in Maine, USA: results from repeated, small-scale, field impoundment trials. *Aquaculture* **210**, 119–135.

Booth J.D. (1972) Studies on New Zealand bivalve larvae, with observations on the adults and on the hydrology of bay islands and Wellington Harbour. Unpublished Ph. D. thesis in Biology, University of Wellington.

Crocetta F. and Turolla E. (2011) *Mya arenaria* Linné, 1758 (Mollusca: Bivalvia) in the Mediterranean Sea: its distribution revisited. *J. Bio. Res. - Thessaloniki* **16**, 188 – 193.

Dennis K.J., Affek H.P., Passey B.H., Schrag D.P. and Eiler J.M. (2011) Defining an absolute reference frame for 'clumped' isotope studies of CO_2. *Geochim. Cosmochim. Acta* **75**, 7117–7131.

Dennis K.J., Cochran J.K., Landman N.H. and Schrag D.P. (2013) The climate of the Late Cretaceous: New insights from the application of the carbonate clumped isotope thermometer to Western Interior Seaway macrofossil. *Earth Planet. Sci. Lett.* **362**, 51–65.

Ghosh P., Adkins J., Affek H., Balta B., Guo W., Schauble E.A., Schrag D.P. and Eiler J.M. (2006) ^{13}C–^{18}O bond in carbonate minerals: a new kind of paleothermometer. *Geochim. Cosmochim. Acta* **70**, 1439–1456.

Gordon A. L. (1967) Circulation in the Caribbean Sea. *J. Geophys. Res.* **72**, 6207–6222.

Grauel A.L., Schmid T.W., Hu B., Bergami C., Capotondi L., Zhou L. and Bernasconi S.M. (2013) Calibration and application of the 'clumped isotope' thermometer to foraminifera for high-resolution climate reconstructions. *Geochim. Cosmochim. Acta* **108,** 125–140.

Guo W., Mosenfelder J. L., Goddard, III, W.A. and Eiler J.M. (2009) Isotopic fractionations associated with phosphoric acid digestion of carbonate minerals: insight from first-principles theoretical modeling and clumped isotope measurements. *Geochim. Cosmochim. Acta* **73**, 7203–7225.

Henkes G.A., Passey B.H., Wanamaker Jr. A.D., Grossman E.L., Ambrose Jr. W.G. and Carroll M.L. (2013) Carbonate clumped isotope compositions of modern marine mollusk and brachiopod shells. *Geochim. Cosmochim. Acta* **106**, 307–325.

Hickman R.W. (1979) Allometry and growth of the green-lipped mussel *Perna canaliculus* in New Zealand. *Mar. Bio.* **51**, 311–327.

McCulloch M.T., Gagan M.K., Mortimer G.E., Chivas A.R. and Isdale P.J. (1994) A high-resolution Sr/Ca and $\delta^{18}O$ coral record from the Great Barrier Reef, Australia, and the 1982–1983 El Niño. *Geochim. Cosmochim. Acta* **58**, 2747–2754.

Morrison J.M. and Nowlin W.D. (1982) General distribution of water masses within the eastern Caribbean Sea during the Winter of 1972 and Fall of 1973. *J. Geophys. Res.* **87**, 4207–4229.

Powers S.P., Bishop M.A., Grabowski J.H. and Peterson C.H. (2006) Distribution of the invasive bivalve *Mya arenaria* L. on intertidal flats of southcentral Alaska. *J. Sea Res.* **55,** 207–216.

Sansone F.J., Smith S.V., Price J.M., Walsh T.W., Daniel T.H. and Andrews C.T. (1988) Long-term variation in seawater composition at the base of the thermocline. *Lett. Nature* **332**, 714–717.

Strasser M. (1999), *Mya arenaria*- an ancient invader of the North Sea coast. *Helgoländer Meeresuntersuchungen* **52**, 309–324.

Thiagarajan N., Adkins J. and Eiler J. (2011) Carbonate clumped isotope thermometry of deep-sea coral and implications for vital effects. *Geochim. Cosmochim. Acta* **75**, 4416–4425.

Tripati A.K., Eagle R.A., Thiagarajan N., Gagnon A.C., Bauch H., Halloran P.R. and Eiler J.M. (2010) ^{13}C–^{18}O isotope signatures and 'clumped isotope' thermometry in foraminifera and coccoliths. *Geochim. Cosmochim. Acta* **74**, 5697–5717.

Uddstrom M.J. and Oien N.A. (1999) On the use of high-resolution satellite data to describe the spatial and temporal variability of sea surface temperatures in the New Zealand region. *J. Geophys. Res.* **104**, 20,729–20,751.

Wang Z., Schauble E.A. and Eiler J.M. (2004) Equilibrium thermodynamics of multiply substituted isotopologues of molecular gases. *Geochim. Cosmochim. Acta* **68**, 4779–4797.

Wüst G. (1964) *Stratification and circulation in the Antillean-Caribbean basins. Part one. Spreading and mixing of the water types with an oceanographic atlas.* Columbia University Press, New York and London, 201 pp.

Yeung L.Y., Young E.D. and Schauble E.A. (2012) Measurements of $^{18}O^{18}O$ and $^{17}O^{18}O$ in the atmosphere and the role of isotope-exchange reactions. *J. Geophys. Res.* **117**, DOI:

10.1029/2012JD017992.

CHAPTER 4

CLUMPED-ISOTOPES IN PERMIAN BIVALVES DEMONSTRATE "SOLID-STATE" ALTERATION IN A CLOSED SYSTEM[3]

[3] Draft manuscript co-authored by D.A. Petrizzo, B.N. Runnegar and E.D. Young.

4.1 ABSTRACT

We measured clumped-isotopes in two valves of the Permian bivalve *Eurydesma cordatum* in order to obtain an independent indication of carbonate growth temperatures. A previous study found evidence of cyclicity in shell $\delta^{18}O$ that is in-phase with growth banding, indicating that these shells had probably avoided oxygen isotopic exchange following burial. Despite apparent $\delta^{13}C$ and $\delta^{18}O$ fidelity, temperatures derived from Δ_{47} are too high (40 to 65 °C) to represent water temperatures during growth, but are also significantly lower than maximum burial temperatures estimated for the northern edge of the Sydney Basin. The results suggest a subtle form of alteration occurs that allows re-ordering of ^{13}C-^{18}O bonds, without shifting the bulk $\delta^{13}C$ and $\delta^{18}O$ values. We hypothesize that these shells preserved a closed (or nearly closed) system, but retained trace amounts of ocean water so that a process similar to Ostwald ripening could facilitate reordering of ^{13}C-^{18}O bonds over long periods of time.

In addition, we examined shells of the modern veneroid bivalve *Microfragum erugatum* as a "blind test" of our carbonate clumped-isotope calibration. Although *Microfragum erugatum* precipitates its shell rapidly, derives the bulk of its nutrition from zooxanthellae, lives in a high-salinity environment (Hamelin Pool, Western Australia), and has unusually heavy shell $\delta^{13}C$ and $\delta^{18}O$ compositions, measurements of Δ_{47} in *Microfragum erugatum* give growth temperatures that are very close to those obtained from records of Hamelin Pool water temperatures. We conclude *M. erugatum* demonstrates no significant vital effects that might invalidate temperatures obtained from Δ_{47} measured in its shell.

4.2 INTRODUCTION

The proportion of cations containing two or more multiple heavy isotopes of carbon (^{13}C) and oxygen (^{18}O) in carbonate minerals ("clumped-isotopes", expressed as Δ_{47} and measured in CO_2 gas liberated through acid digestion of minerals) is determined by growth temperature and is independent of the isotopic composition of the solution from which the carbonate forms. Properly applied, a wholly mineral-based paleothermometer has the capacity to provide past water temperatures, critical information for research in paleobiology, paleoecology and paleoclimatology. However, application of the clumped-isotope paleothermometer to ancient natural materials formed at Earth-surface temperatures has been less straightforward than originally hoped. Many published results require acceptance of either surprisingly warm low-latitude ocean water temperatures during periods of continental glaciation (Came et al., 2007), a very different ocean oxygen isotopic composition (Finnegan et al., 2010), unrealistic estimates of former ice volumes, or ice sheets that were exceptionally depleted in ^{18}O (Finnegan et al., 2010). Measurements of clumped-isotopes in some fossil shells suggest that Paleozoic water temperatures were warmer than the maximum temperatures tolerated by their extant relatives. To date, no set of samples from deep time (> 250 Ma) has recorded the presence of cool to cold water (< 20 °C) during shell growth. As a result, confidence in the capacity of clumped-isotope paleothermometry to provide realistic water temperatures remains uncertain. This situation will prevail until cool environmental temperatures are recovered (~ 0–5 °C) or alternatively, mechanisms that may alter Δ_{47} in fossils and ancient carbonates are better understood.

Several processes may be responsible for smaller Δ_{47} values (and hence higher temperatures) measured in fossils that are presumed to have grown at low temperatures. First, it is possible that clumped-isotope values measured in ancient fossils are original, but are representative of a very different (greenhouse) conditions. Second, ancient Earth may have been populated by animals that regularly grew shell out of equilibrium with their environment, either normally or due to environmental stress factors such as abnormal salinity, pH or the content of dissolved inorganic carbon. However, it is also possible that the Δ_{47} values measured in most ancient fossils are not original, having been altered by diagenetic processes during the time between death and recovery. Such alteration is known to occur rapidly through exchange of oxygen atoms with seawater near the sediment-water interface or during early burial (Pearson, 2012), but it has also been suggested to occur very slowly over long periods of time without the involvement of fluids (Dennis and Schrag, 2010).

We examined a species whose growth environment and geologic history has been constrained in previous studies, *Eurydesma cordatum*, from the Permian Sydney Basin of Australia. Ivany and Runnegar (2010) reported isotopic fidelity, as judged by the preservation of annual cycles in $\delta^{18}O$ in one of the samples used here, while Beard et al. (2012) showed that isotopic fidelity is widespread in *Eurydesma* shells from southeastern Australia. Close stratigraphic association with glacial dropstones and glendonites (calcite psuedomorphs after ikaite, $CaCO_3 \bullet 6H_2O$; Frank et al., 2008) indicate that *Eurydesma* was a cool to cold-water (<~ 7 °C) clam living around a glaciated supercontinent.

4.3 MATERIALS AND METHODS

4.3.1 Mass spectrometric measurements of Δ_{47}

Methods for measuring Δ_{47} by subtracting machine backgrounds and reducing and transferring data to the carbon dioxide equilibrium scale (CDES) of Dennis et al. (2011) are the same as described previously (Chapter 2). Methods and equipment used for acid digestion, extraction and purification of liberated CO_2 were identical to those used for modern shell samples composing the calibration presented in Chapter 3. All fossil and modern shells were measured using the same OzTech reference canister (composition: $\delta^{13}C = -3.58$ ‰ PDB, $\delta^{18}O =$ +24.96 SMOW ‰). Since we report our measurements in the carbon dioxide reference frame (CDES) of Dennis et al. (2011) our measurements should be directly comparable to those made in other laboratories that have also been converted to the CDES scale.

4.3.2 Temperature determination from Δ_{47} measurements

The lack of inter-laboratory agreement among calibrations using CO_2 derived from natural materials has been disappointing. Although differences still exist concerning the absolute magnitude of Δ_{47} measured in samples grown at any known temperature, at least two laboratories have found a relationship between Δ_{47} and T^2 (the calibration slope) in modern mollusc shells that agrees with theoretical clumped-isotope values for CO_2 liberated from carbonates by acid-digestion (Guo et al., 2009; Henkes et al., 2013, this study Chapter 3). We obtained all clumped-isotope temperatures using one of these equations, the calibration presented earlier in Chapter 3:

$$\Delta_{47} = 0.0358 (\pm 0.0060) \times 10^6/T^2 + 0.2717 (\pm 0.0734) \quad (1)$$

It is possible that ancient molluscs precipitated carbonate differently than their modern relatives, and that this difference in behavior produced shells reflecting different a different relationship between Δ_{47} and temperature. However we think that this is unlikely, and that temperatures determined by comparison to extant members of the same phylum, and measured on the same mass spectrometer, should be less uncertain than those obtained by comparison with calibrations based on unrelated taxa or inorganic materials.

4.3.3 Shell samples

4.3.3.1 Eurydesma cordatum

CIS 007 *Eurydesma cordatum* Morris 1845 UNE L1113A (Bimbadeen), section 5 of McClung (1975) 7.2 km SW of Cessnock, Hunter Valley, New South Wales, Australia. These shells were collected by G.A. Short, G. McClung and B. Runnegar, 1972; L. Ivany, D. Petrizzo and B. Runnegar, 2010. Samples come from an umbonal piece cut from matrix that was collected in the 1970s. It was crushed by D. Petrizzo to obtain an "annually averaged" sample of the shell.

CIS 008 *Eurydesma cordatum* Morris 1845. Same locality. This is the disarticulated left valve studied by Ivany and Runnegar (2010) and re-sampled for clumped isotope analysis by Andrew Beard in 2011.

Eurydesma is an abundant fossil in many locations in eastern Australia and other former parts of Gondwana (Fig. 1 in Runnegar, 1979). The prominent umbones of *Eurydesma* are

massively calcified, similar to the modern tridacnid *Hippopus*, and are presumed to have stabilized the bivalves in an umbone down orientation, consistent with a benthic, sessile, epifaunal, and suspension feeding mode of life (Runnegar, 1979). In the northern and southern Sydney Basin, *Eurydesma* occurs stratigraphically close to glendonites, indicating water temperatures of $< \sim 7°$ C near the time of their growth. Paleogeographic reconstructions suggest that *Eurydesma* had a circum-polar distribution during the early Permian (Cisuralian; Runnegar, 1979).

4.3.3.2 Thermal history of the Sydney Basin

Previous studies have attempted to assess the thermal history of the Sydney Basin through vitrinite reflectance measurements of coals or coalified phytoclasts from petroleum exploration boreholes (Diessel, 1975; Mallett and Russell, 1992; Ward et al., 2007), preservation and overprinting of remnant magnetism (Middleton and Schmidt, 1982) and thermochronological methods (Persano et al., 2005). Coals lying stratigraphically above *Eurydesma* localities in the northern (Hunter River Valley) section of the Sydney Basin have vitrinite reflectances of <0.7 % (Ward et al., 2007), suggesting that they have experienced maximum temperatures <120-140°C.

4.3.3.3 Microfragum erugatum

CIS 021 *Microfragum erugatum* Tate 1889 (= *Fragum hamelini* Iredale 1949) Hamelin Pool, Shark Bay, Western Australia (26.4°S, 114.2°E). Average of monthly water temperatures for 1989–1995 is 23.5°C (Edmonds et al., 1999).

Microfragum erugatum is a small (< 14 mm) cardioid clam that ranges along the coast of Western Australia and is particularly abundant in Shark Bay. Living just below the water/sediment interface, it subsists partly on filterable material, but derives most of its nutrition from photosymbiotic zooxanthellae (Morton, 2000). *M. erugatum* has a lifespan of only a single year, yet dominates one of the oddest modern marine environments, the hypersaline, oligotrophic waters of Hamelin Pool of Shark Bay, with population densities of about 4000 per m^2. Hamelin Pool is a highly evaporative body of water that has only limited communication with the open ocean, resulting in twice-normal ocean salinity and very heavy oxygen isotopic composition.

4.4 RESULTS

4.4.1 Measurements of $\delta^{13}C$, $\delta^{18}O$ and Δ_{47} in *Eurydesma cordatum*

Four separate acid digestions of *Eurydesma* shell samples yielded mean bulk $\delta^{13}C$ and $\delta^{18}O$ compositions as follows: $\delta^{13}C$ = +5.44 ‰ ±0.002 to +5.94 ‰ ± 0.002, $\delta^{18}O$ = – 1.14 ‰ ± 0.006 to –0.66 ‰ ± 0.008 (Table 4.1). These are near the mean values ($\delta^{13}C$ = +5.9‰, $\delta^{18}O$ = – 0.8‰) measured by Ivany and Runnegar (2010; Fig. 4.1). However, Δ_{47} values of

0.628 ± 0.024, 0.582 ± 0.018, 0.620 ± 0.019, and 0.605 ± 0.017, imply temperatures from 44 °C to 66 °C. Furthermore, two measurements of shell calcite, each believed to represent one summer and one winter growth interval, are statistically indistinguishable. With the limited data so far available, we cannot discern any seasonality as expressed by Δ_{47} in the shell.

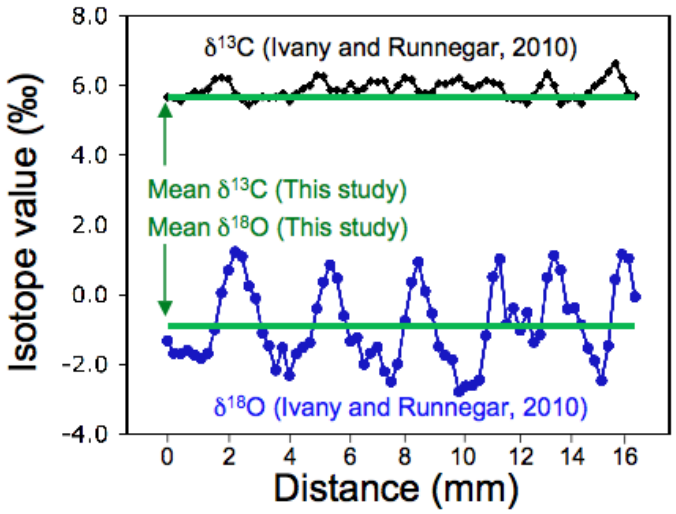

Fig. 4.1 Comparison of mean $\delta^{13}C$ and $\delta^{18}O$ values measured in *Eurydesma* in this study (green horizontal lines) to measurements of $\delta^{13}C$ (black diamonds) and $\delta^{18}O$ (blue circles) in shell microsamples representing a portion of its ontogeny (~ 6 years) by Ivany and Runnegar (2010).

4.4.2 Measurements of $\delta^{13}C$, $\delta^{18}O$ and Δ_{47} in *Microfragum erugatum*

Four separate acid digestions of *Microfragum erugatum* shells yielded heavy $\delta^{18}O$ (4.02 ‰ ± 0.004), and $\delta^{13}C$ (4.39 ‰ ± 0.032; Table 4.1) values. These shells also have Δ_{47} values (0.688 ‰ ± 0.006) that are close to expectations (0.678 ‰) based on the inferred annual

growth temperature (23.5 °C ± 3.0) and the calibration based on modern mollusc shells. Calculating the oxygen isotopic composition of Hamelin Pool water from this temperature yields $\delta^{18}O_{water}$ ~ 5.9 ‰, 2‰ higher than the measured value assuming isotopic equilibrium between water and shell carbonate.

Table 4.1. Isotopic compositions of modern and fossil bivalved mollusc shells

Species[a]	Growth T (ºC)[b]	$\delta^{13}C$ (‰ PDB)[c]	$\delta^{18}O$ (‰ PDB)[d]	Δ_{47} (‰ CDES)[e]	Δ_{47} T (ºC)[f]	$\delta^{18}O_{water}$ (‰ SMOW)[g]
Microfragum erugatum	23.5 ± 3	4.34	4.03	0.701 (±0.018)	15.6	4.4
Microfragum erugatum	23.5 ± 3	4.48	4.03	0.693 (±0.021)	18.3	5.0
Microfragum erugatum	23.5 ± 3	4.38	4.02	0.682 (±0.018)	22.2	5.9
Microfragum erugatum	23.5 ± 3	4.36	4.02	0.676 (±0.019)	24.3	6.3
Mean		4.39	4.02	0.688 (±0.006)	20.0	
Eurydesma cordatum	0 - 12	5.44	- 1.14	0.628 (±0.024)	44.1	4.9
Eurydesma cordatum	0 - 12	5.50	- 0.92	0.582 (±0.018)	66.4	8.9
Eurydesma cordatum (s)	0 - 12	5.80	- 0.80	0.620 (±0.019)	47.5	5.8
Eurydesma cordatum (w)	0 - 12	5.94	- 0.66	0.605 (±0.017)	54.4	7.2
Mean		5.67	- 0.88	0.609 (±0.010)	53.1	

[a] Each row represents a separate acid digestion analyzed using 5-10 blocks as described in Chapter 2. *Eurydesma cordatum* samples marked with (s) and (w) represent summer and winter intervals sampled from sample CIS 008, used by Ivany and Runnegar (2010). Other measurements of *Eurydesma cordatum* come from sample CIS 007 from the same locality.

[b] *Microfragum erugatum* lives only ~1 year; estimated growth temperature is the 1989-1995 average sea surface temperature for Hamelin Pool (Edmonds et al., 1999). Estimated temperatures for *Eurydesma cordatum* are inferred from geological evidence (Ivany and Runnegar, 2010).

[c] Standard errors of the means ($1\sigma/\sqrt{n}$ where 1σ is the standard deviation of n analyses) for all $\delta^{13}C$ measurements < 0.004 ‰.

[d] Standard errors of the means ($1\sigma/\sqrt{n}$ where 1σ is the standard deviation of n analyses) for all $\delta^{18}O$ measurements ≤ 0.008 ‰.

[e] Errors listed are internal standard errors for each separate acid digestion, external standard errors for sample means.

[f] Temperatures estimated by comparison to modern bivalved mollusc calibration in Chapter 3.

[g] $\delta^{18}O_{water}$ calculated using equation of Kim and O'Neil (1997).

4.5 DISCUSSION

4.5.1 Alteration of Δ_{47} in *Eurydesma*

Temperatures suggested by clumped-isotopes in the *Eurydesma cordatum* valves we examined seem impossibly high for the Permian circum-polar waters that the shells grew in, and are in conflict with geologic evidence for near-freezing winter water temperatures in the early Permian of eastern Australia. At the same time, other methods used to study the thermal history of the Sydney basin suggest that the basin experienced temperatures in excess of 100 °C at outcrop depths along the northern (Hunter River Valley) margin. The fact that clumped-isotope temperatures (44 °C to 66 °C) are lower than temperatures thought to have been experienced by these fossils suggests incomplete alteration of the clumped-isotope composition of the calcitic shells.

The similarity of Δ_{47} measured in winter and summer growth bands could be a coincidence arising from the minimal number of measurements we made (one measurement for each of two bands) or time-averaging sufficient shell to produce enough sample. The latter explanation is supported by similar $\delta^{18}O$ values measured in the two samples, – 0.80 ‰ ± 0.007 for summer and – 0.66 ‰ ± 0.008 for winter, approximately the means of previously measured summer and winter extremes (+ 1.2‰ and – 2.5‰) for $\delta^{18}O$ of 70 micromilled samples of shell (Ivany and Runnegar, 2010). Advances in methods for measuring clumped-isotopes in small CO_2 samples (He et al., 2013) should allow for a more accurate determination of temperatures from individual growth bands in any future study.

4.5.1.1 "Normal" alteration and clumped-isotopes

"Normal" post-depositional alteration of clumped-isotopes was identified by Finnegan et al., (2011) through measuring Δ_{47} in micrite samples taken from < 1m, ~ 5m, and ~13.5m distance from a cross-cutting dike of Jurassic age. Although heated for only a brief interval of geologic time, samples nearest the dike were significantly affected, yielding clumped-isotope temperatures greater than 200 °C, while the samples furthest from the dike gave Δ_{47} values that are indicative of only ~39 °C. Also, samples nearest the dike were ~ 4 ‰ lower in $\delta^{18}O$ than the ones furthest away, suggesting that alteration occurred in the presence of meteoric water. These results imply that a blocking temperature of approximately 200 °C exists, even in the presence of meteoric water, for short duration heating.

We can be confident that the $\delta^{18}O$ values of these *Eurydesma* shells are original, as they display variations of ~ 3.5 ‰ in phase with growth banding, which is indicative of seasonal changes in water temperature of ~ 14 ºC (Ivany and Runnegar, 2010). In addition, several other *Eurydesma* fossils from different areas of the Sydney Basin show similar seasonality in $\delta^{18}O$ (Beard et al., 2012). If large amounts of oxygen had been exchanged with fluids at elevated temperature, the cyclic variation in $\delta^{18}O$ should have been modified or obliterated. Therefore, the original $\delta^{18}O$ of the water the shell grew in is still largely represented by the measured $\delta^{18}O$ values although, for reasons not discussed here, the shell either grew at temperatures beyond accepted biological limits, out of equilibrium with seawater of ~ 0 ‰, or in equilibrium with isotopically light seawater (~ – 4‰; Ivany and Runnegar, 2010). Clearly Δ_{47} may be affected by

"normal" alteration (Finnegan et al., 2010), but this process does not easily explain the observations of Δ_{47} in the valves of *Eurydesma* that we studied.

4.5.1.2 "Solid-state" alteration of clumped-isotopes

Dennis and Schrag (2010) suggested that solid-state re-ordering of ^{13}C-^{18}O bonds occurs in carbonatites by diffusion of carbon and oxygen atoms through the carbonate lattice without bulk recrystallization. They estimated that diffusion is slow enough to affect clumped-isotope ratios very little on the scale of 10^8 years. In addition, they suggested that a blocking temperature (~100 °C) exists for carbonates, below which re-ordering of ^{13}C-^{18}O bonds should not occur. We cannot discount this type of alteration based on the observed Δ_{47} values in *Eurydesma* shells, but the scale of re-ordering observed in *Eurydesma,* presuming near freezing growth temperatures, requires that this shell spent a significant proportion of its total history at or beyond its presumed maximum burial temperature, and then also experienced either a "blocking temperature" significantly lower than 100 °C, or a significant volume of shell continued to be re-ordered well below the blocking temperature.

4.5.1.3 A new mechanism for alteration of clumped-isotopes

If neither normal (re-equilibration with circulating oxygen-rich fluids) or solid state (diffusion of carbon and oxygen atoms through the carbonate lattice) alteration explains the isotopic composition of the studied valves of *Eurydesma*, then two questions remain: 1) what

mechanism is responsible for reordering ^{13}C-^{18}O bonds? and 2) if Δ_{47} measured in fossil shells does not represent formation temperature, what does it represent?

Ostwald ripening is a thermodynamic phenomenon that affects crystalline solids immersed in a solution. Since atoms at the surface of a crystal are less stably bound then interior atoms, small crystals with a high surface area to volume ratio are less stable and are more likely to experience mass loss by diffusion into the solution. Conversely, larger crystals are more likely to gain ions by condensation from the solution. This process is expected to modify isotopic compositions by facilitating exchange of carbon and oxygen atoms between dissolved carbonate ions and pore waters. We suggest that this mechanism is not sufficient to explain the elevated clumped-isotope temperatures found in *Eurydesma*, because water was not present in sufficient amount to shift the bulk $\delta^{13}C$ and $\delta^{18}O$ values. However, it may be that a trace amount of water was present in the tiny volume of intercrystalline spaces within the shells, and this water facilitated slow partial re-ordering of ^{13}C-^{18}O bonds.

If this mechanism is responsible, then the clumped-isotope results obtained from *Eurydesma* may represent the temperature when re-ordering effectively ceased because the shell became sufficiently dehydrated. However, since this mechanism works at the micro-scale, it is more likely that our samples contain both unaltered calcite (with original clumped-isotopes) and re-ordered calcite together, and that clumped-isotope measurements represent the contributions of both. We plan to acquire more clumped-isotope data from *Eurydesma* shells known to have experienced different thermal histories to explore these possibilities.

4.5.2 Measured $\delta^{13}C$, $\delta^{18}O$ and Δ_{47} in *Microfragum erugatum*

The heavy oxygen isotope ratios we measured in *Microfragum erugatum* are a reflection of the highly evaporative environment of Hamelin Pool, where the hypersaline seawater is enriched in ^{18}O. The heavy carbon isotope ratios may be due to a depletion of ^{12}C as a result of exceptionally high primary productivity, either within the water column of Shark Bay (Bastow et al., 2002) or within the bivalve's tissues from photosymbiont activity (Morton, 2000). As the clumped isotope temperatures are very near the average water temperature for Shark Bay, there is no evidence for unusual clumped-isotope effects resulting from the specialized lifestyle of *Microfragum erugatum*.

4.6 CONCLUSIONS

Despite apparent oxygen and carbon isotope fidelity in many specimens of *Eurydesma* from the Permian of eastern Australia, our few clumped-isotope measurements give temperatures that are too warm to be growth temperatures, and so the shells must have been altered in some way. The "normal" type of alteration, due to oxygen isotopic exchange with water in an open system, is unlikely to be responsible for somewhat elevated clumped-isotope temperatures. An alternative mechanism, solid-state diffusion is expected to operate as a closed system, but there may not have been enough time for the observed amount of alteration to occur by diffusion of carbon and oxygen atoms through the carbonate lattice. We suggest that these shells have undergone a subtle kind of alteration, with only trace amounts of water present, enough to

facilitate ^{13}C-^{18}O bond reordering through an Ostwald ripening-like process, but an insufficient amount to alter the oxygen isotope compositions of the shells. This process, if it occurs, could be especially problematic for clumped-isotope paleothermometry in Paleozoic fossils, as methods currently used to screen fossils for diagenetic alteration generally track processes that involve water in an open, circulating system.

4.7 REFERENCES

Beard J.A., Ivany, L.C. and Runnegar B.N. (2011). Seasonal variation of carbon and oxygen isotopes from the Permian of southeastern Australia, as recorded by a circumpolar Gondwanan bivalve (*Eurydesma* Morris, 1845). GSA Northeastern Section meeting Hartford, Conn., March 18-20, Paper no. 45–6.

Came R.E., Eiler J.M., Veizer J., Azmy K., Brand U. and Weidman C.R. (2007) Coupling of surface temperatures and atmospheric CO_2 concentrations during the Palaeozoic era. *Nature* **449**, 198–201.

Dennis K.J. and Schrag D.P. (2010) Clumped isotope thermometry of carbonatites as an indicator of diagenetic alteration. *Geochim. Cosmochim. Acta* **74**, 4110–4122.

Dennis K.J., Affek H.P., Passey B.H., Schrag, D.P. and Eiler J.M. (2011) Defining an absolute reference frame for 'clumped' isotope studies of CO_2. *Geochim. Cosmochim. Acta* **75**, 7117–7131.

Diessel C.F.K. (1975) The Carboniferous coals of New South Wales. *Economic Geology of Australia and Papua New Guinea–2. Coal, Monograph Series* **6**, 58–63.

Faiz M., Saghafi A., Sherwood N. and Wang I. (2007) The influence of petrological properties and burial history on coal seam methane reservoir characterisation, Sydney Basin, Australia. *International Journal of Coal Geology **70***, 193–208.

Finnegan S., Bergmann K., Eiler J.M., Jones D.S., Fike D.A., Eisenman I., Hughes N.C, Tripati A.K., Fischer W.W. (2011) The magnitude and duration of late Ordovician-early Silurian glaciation. *Science* **331**, 903–906.

Frank T.D., Thomas S.G. and Fielding C.R. (2008) On using carbon and oxygen isotope data from glendonites as paleoenvironmental proxies: a case study from the Permian system of eastern Australia. *J. Sediment. Res.* **78**, 713–723.

Ghosh P., Adkins J., Affek H., Balta B., Guo W., Schauble E.A., Schrag D.P. and Eiler J.M. (2006) ^{13}C–^{18}O bond in carbonate minerals: a new kind of paleothermometer. *Geochim. Cosmochim. Acta* **70**, 1439–1456.

Guo W., Mosenfelder J.L., Goddard III W.A. and Eiler J.M. (2009) Isotopic fractionations associated with phosphoric acid digestion of carbonate minerals: insight from first-principles theoretical modeling and clumped isotope measurements. *Geochim. Cosmochim. Acta* **73**, 7203–7225.

He B., Olack G.A., Colman A.S. (2012) Pressure baseline correction and high-precision CO_2 clumped-isotope (Δ_{47}) measurements in bellows and micro-volume modes. *Rapid Communications in Mass Spectrom.* **26**, 2837–2853.

Henkes G.A., Passey B.H., Wanamaker Jr. A.D., Grossman E.L., Ambrose Jr. W.G., and Carroll M. L. (2013) Carbonate clumped isotope compositions of modern marine mollusk and brachiopod shells. *Geochim. Cosmochim. Acta* **106**, 307–325.

Ivany L.C. and Runnegar B.N. (2010) Early Permian seasonality from bivalve $\delta^{18}O$ and implications for the oxygen isotopic composition of seawater. *Geology* **38** (11), 1027–1030.

Kim S.T. and O'Neil J.R. (1997) Eqilibrium and nonequilibrium oxygen isotope effects in synthetic carbonates. *Geochim. Cosmochim. Acta* **61**, 3461–3475.

Mallett C.W. and Russell N.J. (1992) The thermal history of the Bowen-Gunnedah-Sydney basins. *Coalbed Methane Symposium*. Townsville, Queensland, pp. 75–79.

McClung, G. (1975) Late Paleozoic biostratigraphy of the northern Sydney Basin. Unpublished Ph.D. thesis, University of New England, Armidale, Australia.

Middleton M.F. and Schmidt P.W. (1982) Paleothermometry of the Sydney Basin. *J. Geophys. Res.* **87**, 5351–5359.

Morton B. (2000) The biology and functional morphology of *Fragum erugatum* (Bivalvia: Cardiidae) from Shark Bay, Western Australia: the significance of its relationship with entrained zooxanthellae. *J. Zoology* **251**, 39–52.

Pearson P.N. (2012) Oxygen isotopes in foraminifera: overview and historical review, in: Ivany L.C., Huber B.T. (Eds.), *Reconstructing Earth's Deep-Time Climate*. Yale University Printing and Publishing, pp.1–38.

Persano C., Stuart F.M., Bishop P. and Dempster T.J. (2005) Deciphering continental breakup in eastern Australia using low-temperature thermochronometers. *J. Geophys. Res.* **110**, DOI

Runnegar B.N. (1979) Ecology of *Eurydesma* and the *Eurydesma* fauna, Permian of eastern Australia. *Alcheringa* **3**, 261–285.

Thiagarajan N., Adkins J. and Eiler J.M. (2011) Carbonate clumped isotope thermometry of deep-sea coral and implications for vital effects. *Geochim. Cosmochim. Acta* **75**, 4416–4425.

Tripati A.K., Eagle R.A., Thiagarajan N., Gagnon A.C., Bauch H., Halloran P.R. and Eiler J.M. (2010) ^{13}C–^{18}O isotope signatures and 'clumped isotope' thermometry in foraminifera and coccoliths. *Geochim. Cosmochim. Acta* **74**, 5697–5717.

Ward C.R., Li Z. and Gurba L.W. (2007) Variations in elemental composition of macerals with vitrinite reflectance and organic sulphur in the Greta Coal Measures, New South Wales, Australia. *Internat. J.Coal Geology* ***69***, 205–219.

CHAPTER 5

SUMMARY, OUTLOOK AND FUTURE WORK

5.1 THESIS SUMMARY

The main objective of this thesis was to develop the capability to make clumped-isotope measurements (Δ_{47}) in carbonates at UCLA and to apply the technique to problems involving Paleozoic marine fossils. Prior to the initiation of this work, all published measurements of Δ_{47} were made using a very specific and expensive arrangement of Faraday cups, and published methods required a substantial amount of effort to track and correct for poorly understood instrument-specific conditions that negatively affected measurement accuracy (Huntington et al., 2009; Dennis et al., 2011). In addition, the pioneering calibrations to determine the relationship between Δ_{47} and temperature in several types of modern carbonates, all measured at the California Institute of Technology (Ghosh et al., 2006; Tripati et al., 2010; Thiagarajan et al., 2011), could not be reproduced in other laboratories (Dennis and Schrag, 2010; Henkes et al., 2013), and differed appreciably from theoretical predictions for the temperature dependence of clumped-isotopes in CO_2 (Schauble et al., 2006; Guo et al., 2009). These shortcomings of the clumped-isotope method are addressed in Chapters 2 and 3, where the following points are made:

- Methods are presented for measuring Δ_{47} by multicollector peak hopping (MPH) on a conventional mass spectrometer, using the usual CO_2 set of three Faraday collectors. These eliminate the need for a special "isotopologue" collection system that is expensive and requires a mass spectrometer be dedicated only to CO_2.

- It is shown that monitoring instrument backgrounds during measurement, and subtracting them from measured ion beam intensities eliminates the problematic $\Delta_{47}/\delta^{47}CO_2$ "non-linearity" observed on all Thermo-Finnigan 253 mass spectrometers. This greatly reduces the time previously required to standardize measurements using temperature-equilibrated CO_2.
- It is demonstrated that measurements of Δ_{47} in bivalved mollusc shells that have been corrected for measured background voltage are different from non-background corrected measurements. This difference is not attributable to variability in fractionation during acid digestion, gas handling and purification procedures, or recombination in the source.
- The background corrected temperature calibration of modern bivalved mollusc shells yields a Δ_{47}/T^2 relationship that can be described by:

$$\Delta_{47} = 0.0358\ (\pm\ 0.0060)\ \text{x}\ 10^6/T^2 + 0.2717\ (\pm\ 0.0734).$$

Without background correction we obtain:

$$\Delta_{47} = 0.0323\ (\pm\ 0.0060)\ [10^6/K^2] + 0.2918\ (\pm\ 0.0729).$$

The slopes of these equations are very similar to another recent calibration of bivalved molluscs and brachiopods and a theoretical calibration for CO_2 liberated from calcite through phosphoric acid digestion (Henkes et al., 2013). The difference in absolute values of Δ_{47} between background corrected and non-background corrected calibrations is similar in scale to documented inter-laboratory differences.

Early studies of clumped isotopes in Paleozoic marine fossils (Came et al., 2007; Finnegan et al., 2010) produced some results that conflict with our understanding of either the Paleozoic climate and ocean isotopic composition and/or geologic processes that promote isotopic alteration. This problem was very briefly addressed in Chapter 4 where:

- Measurements of Δ_{47} in a bivalved mollusc fossil that does not appear to have undergone "normal" burial alteration, provided evidence for closed-system or "solid state" alteration of ^{13}C-^{18}O bonds and therefore Δ_{47}.
- It is suggested that re-ordering of ^{13}C-^{18}O bonds can occur without shifting $\delta^{13}C$ and $\delta^{18}O$, and that this is facilitated through Ostwald ripening-like process in the presence of only trace amounts of water.

5.2 OUTLOOK

Despite difficulties in making and interpreting clumped-isotope measurements in ancient fossils, accurate representations of ancient temperatures (and $\delta^{18}O_{ocean}$) from a properly applied, wholly mineral based paleothermometer would be extremely valuable for paleobiological and paleoclimatological investigations. Improved instruments and continued development of methods for measuring Δ_{47}, will certainly help further inter-laboratory calibration. A better understanding of subtle diagenetic processes that affect clumped-isotopes appears to be necessary in order to realize its full potential in application to fossils.

5.3 FUTURE PALEOTHERMOMETRY INVOLVING PALEOZOIC FOSSILS

Since previously mentioned screening methods (SEM inspection, trace element concentration) may not indicate subtle alteration (^{13}C-^{18}O bond re-ordering), reliance on those methods alone is likely insufficient. An effective approach to gauge the quality of ^{13}C-^{18}O bond preservation may be to compare samples from a single (or minimal number of closely related) thoroughly studied species demonstrating a wide geographic or temporal distribution in order to have multiple burial histories to compare. Additionally, measurements of micro-sampled material within a single shell may demonstrate varying amounts of micro-scale alteration to compare. Further advances in mass spectrometry may make such analysis possible.

5.3.1 Continued study of Δ_{47} in Eurydesma

Preliminary data have not recovered clumped-isotope signatures indicating near-freezing water temperatures in *Eurydesma cordatum* shells from the Sydney Basin, however, *Eurydesma* should be useful in assessing diagenetic effects on clumped-isotopes. The following may be valuable courses of study:

1) Geopetal calcite is not uncommon to *Eurydesma* shells. Comparing measurements of Δ_{47} and $\delta^{18}O$ in geopetal calcite and enclosing shell carbonate may help assess early diagenetic effects.

2) $\delta^{18}O$ values measured in *Eurydesma* from other areas (Namibia and Western Australia) are heavier than those from eastern Australia, and this may be a result of better preservation. Measurements of Δ_{47} in these shells may indicate colder temperatures.

3) Build on the work of Finnegan et al., (2010) and Huntington et al. (2011) by exploring how intense short- to long-term heating due to proximity to igneous intrusions affects clumped isotopes. It has been suggested that there is a time component to solid-state alteration (Dennis and Schrag, 2010), and this can be assessed by estimating cooling rates for igneous intrusions in Tasmania and the southern end of the Sydney Basin where *Eurydesma* are abundant.

5.3.2 Silurian brachiopods

Silurian brachiopods remain an excellent prospect for clumped-isotope paleothermometry. The relatively cosmopolitan nature of Silurian marine fauna has led to the widespread adoption of global chronostratigraphic terms instead of regional ones (Cramer et al., 2010). Periods of major advancement in and integration of graptolite zonation in the 1990's, conodont biostratigraphy in the late 1990s, and carbon isotope stratigraphy in the 2000s allow for global correlation of some Silurian intervals with precision better than stage level (Cramer et al., 2010).

The Silurian appears to have been a volatile period in Earth's history, hypothesized to be a high temperature greenhouse punctuated with many (~6) significant (> + 3 ‰ PDB) and very

sudden positive $\delta^{13}C$ excursions (Cramer et al., 2010), including the Lau event, which at + 7 - 8 ‰ PDB is one of the largest of the Phanerozoic. Several of the early Silurian positive excursions are coincident with geologic evidence indicating glaciation on the South American part of Gondwana (Loydell, 2007), and significant extinctions of graptolites, conodonts and acanthodian fish (Eriksson et al., 2009).

Jeppsson (1990) hypothesized that the profound cyclic lithological and correlated faunal changes of the Silurian resulted from global climate fluctuations between two extreme states, "primo" (P) and "secundo" (S) episodes (slightly modified and renamed as "humid" and "arid" states by Bickert, 1997 and Cramer and Saltzman, 2005). P-states exist during times when high latitude waters are cold (< 5 °C) and low latitudes are humid. This situation results in high nutrient supply and therefore, increased primary productivity in tropical surface waters, coinciding with low $\delta^{13}C$ in carbonates. Cool high latitude water temperatures (> 5 °C) and arid low latitudes characterize the alternative S-states, restricting primary productivity in tropical surface waters to low levels, and coinciding with high $\delta^{13}C$ in carbonates. Carbon isotope curves from correlated sections in Sweden (Bickert et al., 1997), Australia (Jeppsson et al., 2007), North America, (Cramer and Saltzman, 2005) and many other locations (Cramer et al., 2010) demonstrate good agreement in the timing and magnitude of positive $\delta^{13}C$ excursions and so, support this hypothesis.

Oxygen isotope curves however, show more regional variability, presumably a product of alteration resulting from different thermal histories, and different amounts of interaction with meteoric water. For example, carbon isotope ratios from the Coral Gardens Formation

demonstrate excellent agreement at high resolution with those of Gotland, Sweden during the Ludfordian Lau Event, but oxygen isotopes do not (Jeppsson et al., 2007). Conodont apatite is known to darken in color in proportion to how much it has been heated, allowing a rough estimate of maximum temperature experienced by comparing the color of a sample to the Conodont Alteration Index (Epstein et al., 1976). Conodont elements from Coral Gardens are dark in appearance (> 5 CAI) indicating temperatures > 300 °C. However, Coral Gardens $\delta^{18}O$ does demonstrate a similar trend to $\delta^{13}C$ as they both increase throughout the Hoburgen Secondo Episode that immediately follows the Lau Event. This implies that despite having experienced significant heating, some temperature information may be preserved in oxygen isotope ratios.

Most measurements of Silurian $\delta^{18}O$ come from analyses of brachiopod calcite deemed to be well-preserved based on visual inspection by SEM, CL and trace element composition (see Chapter 1). A smaller amount of data was produced from measurements of $\delta^{18}O$ in conodont phosphate, which is a more difficult measurement to make, but has been long considered to be more resistant to alteration than brachiopod calcite, evidenced by the fact that it indicated lower paleotemperatures than most of the best preserved coeval brachiopod calcite (Wentzel et al., 2000). However, calculating paleotemperatures from $\delta^{18}O_{phosphate}$ by using Pucèat et al.'s (2010) revised phosphate-water fractionation equation rather than Kolodny et al.'s (1983) equation results in values that are very similar to those from brachiopods for much of the Silurian.

A few brachiopods from the late Silurian of Götland have been borrowed for this purpose. Preliminary examination of $\delta^{13}C$ (> 7 ‰ PDB) and $\delta^{18}O$ (> –4 ‰ PDB) imply that these shells grew during or near the peak of the Klonk event. With many more samples, a high-

resolution clumped-isotope temperature curve for the Silurian might be possible. Shells deposited closely in time, but with the same thermal history might be directly comparable, making high-resolution studies more valuable than those comparing samples separated by long periods of time.

5.4 REFERENCES

Azmy K., Veizer J., Bassett M.G. and Copper P. (1998) Oxygen and carbon isotopic composition of Silurian brachiopods: Implications for coeval seawater and glaciations. *GSA Bulletin* **110**, 1499–1512.

Came R.E., Eiler J.M., Veizer J., Azmy K., Brand U. and Weidman C.R. (2007) Coupling of surface temperatures and atmospheric CO_2 concentrations during the Palaeozoic Era. *Nature* **449**, 198–201.

Cramer B.D., Brett C.E., Melchin M.J., Männik P., Kleffner M.A., McLaughlin P.I., Loydell D.K., Munnecke A., Jeppsson L., Corradini C., Brunton F.R. and Saltzman M.R. (2011) Revised correlation of Silurian Provincial Series of North America with global and regional chronostratigraphic units and $\delta^{13}C_{carb}$ chemostratigraphy. *Lethaia* **44**, 185–202.

Dennis K.J. and Schrag D.P. (2010) Clumped isotope thermometry of carbonatites as an indicator of diagenetic alteration. *Geochim. Cosmochim.. Acta* **74**, 4110–4122.

Dennis K.J., Affek H.P., Passey B.H., Schrag D.P. and Eiler J.M. (2011) Defining an absolute reference frame for 'clumped' isotope studies of CO_2. *Geochim. Cosmochim. Acta* **75**, 7117–7131.

Eriksson M.E., Nilsson E.K., and Jeppsson L. (2009) Vertebrate extinctions and reorganizations during the Late Silurian Lau Event. *Geology* **37**, 739–742.

Finnegan S., Bergmann K., Eiler J.M., Jones D.S., Fike D.A., Eisenman I., Hughes N.C, Tripati A.K. and Fischer W.W. (2011) The magnitude and duration of late Ordovician-early Silurian glaciation. *Science* **331**, 903–906.

Ghosh P., Adkins J., Affek H., Balta B., Guo W., Schauble E.A., Schrag D.P. and Eiler J.M. (2006) ^{13}C–^{18}O bonds in carbonate minerals: a new kind of paleothermometer. *Geochim. Cosmochim. Acta* **70**, 1439–1456.

Guo W., Mosenfelder J.L., Goddard III W.A. and Eiler J.M. (2009) Isotopic fractionations associated with phosphoric acid digestion of carbonate minerals: insight from first-

principles theoretical modeling and clumped isotope measurements. *Geochim. Cosmochim. Acta* **73**, 7203–7225.

Henkes G.A., Passey B.H., Wanamaker Jr. A.D., Grossman E.L., Ambrose Jr. W.G., and Carroll M.L. (2013) Carbonate clumped isotope compositions of modern marine mollusk and brachiopod shells. *Geochim. Cosmochim. Acta* **106**, 307–325.

Huntington K.W., Eiler J.M., Affek H.P., Guo W., Bonifacie M., Yeung L.Y., Thiagarajan N., Passey B.H., Tripati A., Daëron M. and Came R. (2009) Methods and limitations of 'clumped' CO_2 isotope (Δ_{47}) analysis by gas-source isotope ratio mass spectrometry. *J. Mass Spectrom*. **44**, 1318–1329.

Huntington K.W., Budd D.A., Wernicke B.P. and Eiler J.M. (2011) Use of clumped-isotope thermometry to constrain the crystallization temperature of diagenetic calcite. *J. Sed. Res.* **81**, 656–669.

Jeppsson L., Talent J.A., Mawson R., Simpson A.J., Andrew A.S., Calner M., and Caldon H.J. (2007) High-resolution Late Silurian correlations between Gotland, Sweden, and the Broken River region, NE Australia: lithologies, conodonts and isotopes. *Palaeogeogr. Palaeoclimatol. Palaeoecol*. **245**, 115–137.

Loydell D.K. (2007). Early Silurian positive $\delta^{13}C$ excursions and their relationship to glaciations, sea–level changes and extinction events. *Geological Journal* **42,** 531–546.

Pucéat E., Joachimski M.M., Bouilloux A., Monna F., Bonin A., Motreuil S. and Quesne D. (2010) Revised phosphate–water fractionation equation reassessing paleotemperatures derived from biogenic apatite. *Earth Planet. Sci. Lett*. **298,** 135–142.

Samtleben C., Munnecke A., Bickert T. and Pätzold J. (1996) The Silurian of Gotland (Sweden): facies interpretation based on stable isotopes in brachiopod shells. *Geologische Rundschau* **85**, 278–292.

Schauble E.A., Ghosh P. and Eiler J. M. (2006) Preferential formation of $^{13}C–^{18}O$ bonds in carbonate minerals, estimated using first-principles lattice dynamics. *Geochim. Cosmochim. Acta* **70**, 2510–2529.

Thiagarajan N., Adkins J. and Eiler J.M. (2011) Carbonate clumped isotope thermometry of deep-sea coral and implications for vital effects. *Geochim. Cosmochim. Acta* **75**, 4416–4425.

Tripati A.K., Eagle R.A., Thiagarajan N., Gagnon A.C., Bauch H., Halloran P.R. and Eiler J.M. (2010) $^{13}C–^{18}O$ isotope signatures and 'clumped isotope' thermometry in foraminifera and coccoliths. *Geochim. Cosmochim. Acta* **74**, 5697–5717.

Wenzel B. and Joachimski M.M. (1996) Carbon and oxygen isotopic composition of Silurian brachiopods (Gotland/Sweden): palaeoceanographic implications. *Palaeogeogr. Palaeoclimatol. Palaeoecol.* **122**, 143–166.

Wenzel B., Lécuyer C. and Joachimski M.M. (2000) Comparing oxygen isotope records of Silurian calcite and phosphate - $\delta^{18}O$ compositions of brachiopods and conodonts. *Geochim. Cosmochim. Acta* **64**, 1859–1872.

APPENDIX

FORTRAN PROGRAM FOR CALCULATING Δ_{47} IN CO_2 FROM ION BEAM INTENSITIES MEASURED USING MULTICOLLECTOR PEAK HOPPING (MPH)[4]

[4] Fortran program written by E.D. Young specifically for this research.

A-1

Below is the Fortran program we use to calculate Δ_{47} from input ion currents (voltages) based on our multicollector peak hopping (MPH) method.

```
      Program CO2_indium
!
! Program to calculate big delta 47CO2/44CO2 from input ion currents (voltages)
! based on the peak-hopping method for measuring CO2 44,45,46,and 47 (+48).  In
! this scheme, 44, 45, and 46 are measured to obtain d18O_SMOW and d13C_PDB, then
! a 47/46 ratio is measured separately and the results are combined.
!
! Absolute D47 values are obtained from measurements against an in-house
! standard. Backgrounds are subtracted from ion currents (voltages) for
! mass 47 and mass 46 for both sample and standard gases.
!
! Two versions of calculations are applied.  One is based on the slope
! of plots of D47 vs. d47CO2 without background subtractions, equivalent
! to the Caltech "heated gas line" correction scheme (Huntington et al., 2009). The other is based
! on correcting for the d47CO2 effect using the heated gas line slope
! with background subtraction for masses 47 and 46.  The slopes of the
! heated gas lines with background correction are in most cases indistinguishible
```

```
! from zero.
!
! Finally, correction is made for inherent inaccuracies in absolute D47
! values by correcting for a line depicting measured D47 at various
! temperatures vs. the theoretical CO2 values.  Here we follow the
! recommendation of Dennis et al. (2011, GCA)placing the reported D47
! values on what they call a universal reference frame.  We report values
! with and without this correction.
!
! Algorithms for normal CO2 ion corrections are based on Santrock et al.
! (1985, Anal. Chem. 57, 1444) with modifications to the input parameters.
! Rare isotopologue corrections are similar to Dennis et al. (2011) with
! the exception of the background corrections.
!
! There are two input files:
!
!          1. CO2_parameters.in, contains fundamental constants for the data
!             reduction, including ratios for SMOW and PDB and exponent relating
!       17R to 18R, as well as the isotopic composition of the reference gas.
!
!          2. file_name.dat, contains required ion currents (voltages) for blocks
```

```
!       of acquisitions for d18O and d13C and for 47/46. Ion currents are
!       listed for both sample and reference gases in both cases.  The header
!       of this file contains the number of blocks of data taken for each
!       cup configuration (i.e., for the d18O and d13C configuration and for
!       the 47/46 configuration. Note that this file maybe exported from
!       Excel, and if so, the following unix command will provide the right
!       line terminations:
!
!           tr '\r\n' '\n' <file_name.dat> newfile_name.dat.
!
!       This translation removes CR-LF and replaces it with just LF.
!       Also, if the input file contains tab separations between columns,
!       the tabs can be stripped and replaced by three space on the unix
!       command line with:
!
!         cat file_name.dat | expand -t 3 >newfile_name.dat
!
! Uncertainties in the final D_47 are calculated using a monte carlo approach
! to account for uncertainties among the blocks of unequal number in the
! acquisitions. Sources of uncertainty considered include the measurements
! themselves and the uncertainties in the reference heated gas lines as
```

```
! expressed by standard deviations in slopes.  Transformation to a universal
! CO2 clumping reference frame is also included (Dennis et al. 2011). This
! transformation is afforded by a calibration line that has a slope and
! intercept that also have associated uncertainties that are propagated to
! the final number for D_47.  This extra source of error can be circumvented
! by setting the uncertainties in the calibration line to zero.
!
! Abbreviations:
!
!         acid = acid digested sample, i.e. not scrambled
!         smpl = sample
!         std  = reference gas
!    cl   = clumping cup configuration, i.e. 2-cup configuration for
!           47CO2+ and 46CO2+.  Where there is no cl subscript the
!           indicated voltages are from the 6-cup configuration.
!
! The structure of the data input file is as follows (no blank lines):
!
!         sample id                       !text identifying the sample
!         hgl_slope hgl_int       !slope and intercept of heated gas line
!         hgl_s_err hgl_i_err     !errors in slope and intercept above
```

```
!       bgl_slope bgl_int       !slope and intercept of background-corrected
!                       heated gas line
!    bgl_s_err bgl_i_err     !errors in above
!    calib_slope calib_int   !Slope and intercept of line relating measured to
!                       actual big delta 47 values for CO2
!    calib_s_err calib_i_err !Errors in above
!    n_6_acid  !number of 6-cup acquisitions for carbonate CO2
!    n_2_acid  !number of 2-cup acquisitions for carbonate CO2
!    ncycles   !number of cycles comprising a block of data
!    smpl44 smpl45 smpl46 smpl47 smpl48 stnd44 stnd45 stnd46 stnd47 stnd48
!    smpl44 smpl45 smpl46 smpl47 smpl48 stnd44 stnd45 stnd46 stnd47 stnd48
!       smpl46_bg1 smpl47_bg1 stnd46_bg1 stnd47_bg1
!    smpl46 smpl47 stnd46 stnd47
!       smpl46_bg2 smpl47_bg2 stnd46_bg2 stnd47_bg2
!       smpl46_bg1 smpl47_bg1 stnd46_bg1 stnd47_bg1
!    smpl46 smpl47 stnd46 stnd47
!       smpl46_bg2 smpl47_bg2 stnd46_bg2 stnd47_bg2
!    ...
!
! Here each line shown above is actually ncycles number of lines of data
! representing a block of cycles.
```

```
!
! The data lines with 10 values are for 6-cup data and the shorter
! data lines with 4 values are for the 2-cup data. Backgrounds before and
! after each 2-cup measurement are to be subtracted from the 2-cup
! measurements. In many cases the 2nd background serves as the 1st background
! for the next block of 2-cup data, but the code is not locked into this
! structure - rather, it is handled on the input file side.
!
! The integers in the header lines tell the program how many lines of
! data exsit for each type of collection for this sample. Data are therefore
! read in the order data_acid(), data_acid(), data_acid_cl(), data_acid_cl(),
! data_acid_cl(), etc. where cl signifies the 2-cup configuration (cl
! stands for clumping). In the above example there are two 6-cup measurements
! and 2 2-cup measurements.
!
! Use of "acid" in many array and variable names is a legacy from the
! previous version of the code which distinguished acid-digestion CO2
! from heated-gas CO2. The term has been retained where convenient for
! reusing code.
!
! Some terminology:  hgl = heated gas line corrected, no backgrounds;
```

```
!                bgl = heated gas line correctd with background
!                     corrections;
!                cl = 2-cup data;
!                block = one analysis;
!                acid = sample, usually an acid-digested carbonate
!                ran = random draws from parent population
!
! NOTE REGARDING UNIVERSAL REFERENCE FRAME: This program makes use of the
! Dennis et al. (2011) suggestion of placing CO2 D47 values on a universal
! reference frame.  The proposed calibration line is between samples
! RELATIVE TO THE LABORATORY WORKING GAS vs. Wang et al. (2004) theoretical
! values for gases equilibrated at various temperatures.  Therefore, for
! this program the D47 of the working gas should be zero in the
! CO2_parameters.in file.
!
! EDY, UCLA, July 9, 2012
!
!
      implicit double precision (a-h,o-z)
      parameter (num=30)  !number of samples maximum
      parameter (nmax=500)  !numer of Monte Carlo draws maximum
```

```
!
      double precision hgl_slope, hgl_int
          double precision hgl_s_err, hgl_i_err
      double precision bgl_slope, bgl_int
      double precision bgl_s_err, bgl_i_err
      double precision calib_slope, calib_int
      double precision calib_s_err, calib_i_err
          double precision data_acid(num,10)
      double precision data_acid_cl(num,5)
      double precision data_cl_bg1(num,5),data_cl_bg2(num,5)
      double precision data_cl_bgcorr(num,5)
      double precision d18O_ran(nmax),d13C_ran(nmax)
      double precision random1(nmax),random2(nmax)
      double precision d18O(num),d17O(num),d13C(num),D48(num)
      double precision d18O_block(num),d17O_block(num),d13C_block(num)
      double precision D48_block(num)
      double precision d18O_block_err(num),d17O_block_err(num)
      double precision d13C_block_err(num),D48_block_err(num)
      double precision bgd_block(num),data(num)
      double precision dummy,dumy(num)
c
```

```
      double precision D47(nmax),dl47(nmax)
      double precision dl47_block(num),D47_block(num)
      double precision dl47_block_err(num),D47_block_err(num)
      double precision D47_cycle(num),dl47_cycle(num)
      double precision D47_cycle_err(num),dl47_cycle_err(num)
      double precision D47_block_bulk_err(num),dl47_block_bulk_err(num)
      double precision D47_block_nobg(num),dl47_block_nobg(num)
      double precision D47_block_nobg_err(num),dl47_block_nobg_err(num)
      double precision D47_block_bgl(num), D47_block_bgl_err(num)
      double precision D47_block_hgl(num), D47_block_hgl_err(num)
c
      double precision I44_smpl,I44_std,I45_smpl,I45_std,I46_smpl,
     &     I46_std,I47_smpl,I47_std,I48_smpl,I48_std
c
          double precision D47_bgl,D47_bgl_err,D47_hgl,D47_hgl_err
          double precision dl47_bgl,dl47_bgl_err,dl47_hgl,dl47_hgl_err
c
      character*45 fname
      character*15 sampleid
      character*11, Titles(30)
      logical lexist
```

```
!
! Read data into program from data file specified by user.
!
          print*,' '
          print*,' '
          print*,' '
      print*,'+-----------------------------------------------+'
      print*,'|              CO2 INDIUM                       |'
      print*,'|                                               |'
      print*,'|  Data reduction for UCLA MAT-253 D_47 in CO2   |'
      print*,'|     from both the 6-cup and the 2-cup         |'
      print*,'|             configurations                    |'
      print*,'|                                               |'
      print*,'|               July, 2012                      |'
      print*,'+-----------------------------------------------+'
5     print*,' '
      print*,'Enter data file name:'
      read(*,10) fname
!
!      fname='indium_input.dat'
!
```

```
10    format(A)
          open(unit=10,file=fname,status='old',err=5)
!
! READ HEADER
!
      read(10,10) sampleid
      print*,sampleid
          read(10,*) hgl_slope, hgl_int
          print*,hgl_slope, hgl_int
          read(10,*) hgl_s_err, hgl_i_err
          print*,hgl_s_err, hgl_i_err
          read(10,*) bgl_slope, bgl_int
          print*,bgl_slope,bgl_int
          read(10,*) bgl_s_err,bgl_i_err
          print*,bgl_s_err,bgl_i_err
          read(10,*) calib_slope, calib_int
          print*,calib_slope,calib_int
          read(10,*) calib_s_err, calib_i_err
          print*,calib_s_err,calib_i_err
      read(10,*) n_6_acid
      print*,n_6_acid
```

```
      read(10,*) n_2_acid
      print*,n_2_acid
      read(10,*) ncycles
      print*,ncycles
      read(10,*) ncyclesbg
!
! READ DATA according to number of analyses and number of cycles
! defined in the header.  Repeat whole procedure for each block i
!
      do 50 i=1,n_6_acid
!       print*,'Input for 6-cup block ',i
       do 12 l=1,ncycles
        read(10,*) (data_acid(l,j),j=1,10)
!         write(*,*) (data_acid(i,j),j=1,10)
12     continue
! ION CORRECTIONS FOR CO2 USING 6-CUP CONFIGURATION CYCLE BY CYCLE.
! Note that I47 and I46 for the two subroutines are not the same.
! In CO2_ion_corrections these are voltages collected from the 6-
! mass cup configuration.  For D47 these are the voltages collected
! using the 2-cup configuration for 46 and 47.  They have the same
! formal argument names for convenience, but will be different actual
```

```
! arguments when called.
!
! Start with ion correction for 6-cup configuration called n_6_acid
! times to calculate averages and standard deviations (external).
!
      do 15 l=1,ncycles
       I44_smpl=data_acid(l,1)
       I44_std=data_acid(l,6)
       I45_smpl=data_acid(l,2)
       I45_std=data_acid(l,7)
       I46_smpl=data_acid(l,3)
       I46_std=data_acid(l,8)
       I47_smpl=data_acid(l,4)
       I47_std=data_acid(l,9)
       I48_smpl=data_acid(l,5)
       I48_std=data_acid(l,10)
       call CO2_ion_corrections(I44_smpl,I44_std,I45_smpl,I45_std,
     &   I46_smpl,I46_std,I47_smpl,I47_std,I48_smpl,I48_std,
     &   d18O_smpl,d17O_smpl,d13C_smpl,D48_smpl)
       d18O(l)=d18O_smpl
       d17O(l)=d17O_smpl
```

```
      d13C(l)=d13C_smpl
      D48(l)=D48_smpl
15    continue
!
! Get mean values and errors for this block of 6-cup data. Convert
! standard deviations for cycles to standard errors.
!
      call xmean(ncycles,d18O,d18O_block(i))
      call stddev(ncycles,d18O_block(i),d18O,d18O_block_err(i))
          d18O_block_err(i)=d18O_block_err(i)/dsqrt(dble(ncycles))
      call xmean(ncycles,d17O,d17O_block(i))
      call stddev(ncycles,d17O_block(i),d17O,d17O_block_err(i))
      d17O_block_err(i)=d17O_block_err(i)/dsqrt(dble(ncycles))
      call xmean(ncycles,d13C,d13C_block(i))
      call stddev(ncycles,d13C_block(i),d13C,d13C_block_err(i))
      d13C_block_err(i)=d13C_block_err(i)/dsqrt(dble(ncycles))
      call xmean(ncycles,D48,D48_block(i))
      call stddev(ncycles,D48_block(i),d48,D48_block_err(i))
      D48_block_err(i)=D48_block_err(i)/dsqrt(dble(ncycles))
!
! Close loop for blocks of 6-cup data_cl_bg1!
```

```
50    continue
!
!
! MEAN VALUES for d18O, d17O, d13C and D48 for CO2 based on combining
! results for the blocks.
!
! Uncertainties are the uncertainties in the mean, basically a
! standard error but with the individual variances for each block
! considered.
!
      call xmean(n_6_acid,d18O_block,d18O_acid_mean)
      dn=dble(n_6_acid)
      d18O_acid_sigma=0.0D0
          do 60 i=1,n_2_acid
            d18O_acid_sigma=d18O_acid_sigma+(d18O_block_err(i)**2.0)/(dn)
60    continue
      d18O_acid_sigma=dsqrt(d18O_acid_sigma)
!
      call xmean(n_6_acid,d17O_block,d17O_acid_mean)
      d17O_acid_sigma=0.0D0
          do 65 i=1,n_2_acid
```

```
          d17O_acid_sigma=d17O_acid_sigma+(d17O_block_err(i)**2.0)/
     &     (dn)
65    continue
      d17O_acid_sigma=dsqrt(d17O_acid_sigma)
!
      call xmean(n_6_acid,d13C_block,d13C_acid_mean)
      d13C_acid_sigma=0.0D0
          do 70 i=1,n_2_acid
           d13C_acid_sigma=d13C_acid_sigma+(d13C_block_err(i)**2.0)/
     &     (dn)
70    continue
      d13C_acid_sigma=dsqrt(d13C_acid_sigma)
!
      call xmean(n_6_acid,D48_block,D48_acid_mean)
      D48_acid_sigma=0.0D0
          do 71 i=1,n_2_acid
           D48_acid_sigma=D48_acid_sigma+(D48_block_err(i)**2.0)/
     &     (dn)
71    continue
      D48_acid_sigma=dsqrt(D48_acid_sigma)
!
```

```
! CARBONATE d18O_SMOW and d18O_PDB from d18O_SMOW of CO2.
! Here we assume 25C equilibration of sample with phosphoric acid
! using the alpha of Friedman & O'Neil (1977). We use a ratio for
! 18O/16O SMOW that cancels in the final result. The shift from CO2
! to carbonate and from carbonate SMOW to PDB are both basically offsets
! in scale (rather than a stretching or shrinking), meaning the errors
! are unaffected.
!
    alpha_acid=1.01025D0
        R_acid=(d18O_acid_mean/1000.0D0+1.0D0)*0.00200514D0
        R_carb=R_acid/alpha_acid
        d18O_carb=1.0D03*(R_carb/0.00200514D0-1.0D0)
        d18O_carb_sigma=d18O_acid_sigma
        d18O_PDB =0.97006D0*d18O_carb-29.9832D0
        d18O_PDB_sigma=d18O_acid_sigma
!
!
! PROCESS 2-CUP DATA FOR MASSES 47 AND 46.  Loop 200 is for each
! block of data.  Calculations are made in their entirety for each
! block for proper propagation of errors.
!
```

```
! Start with reading data. Counters are as follows: i = blocks, l = cycles,
! j = ion beams, and k = random draws.  Do loop 200 is for blocks.
!
! START LOOP 200 FOR BLOCK
!
      do 200 i=1,n_2_acid
!
!       print*,'Input for 2-cup block ',i
        do 72 l=1,ncyclesbg
          read(10,*) (data_cl_bg1(l,j),j=1,4)
!           write(*,*) (data_cl_bg1(l,j),j=1,4)
72      continue
        do 73 l=1,ncycles
          read(10,*) (data_acid_cl(l,j),j=1,4)
!           write(*,*) (data_acid_cl(l,j),j=1,4)
73      continue
        do 74 l=1,ncyclesbg
          read(10,*) (data_cl_bg2(l,j),j=1,4)
!           write(*,*) (data_cl_bg2(l,j),j=1,4)
74      continue
!
```

```
! Calculate mean and uncertainties for the background measurements
! so they can be subtracted from the 46 and 47 ion signals.  These are
! the backgrounds for a single block.  In practice the background
! errors are tiny in comparison to the signal errors and are neglected.
!
      dn=dble(ncyclesbg)
! Smpl 46 bg1
      j=1
      do 82 l=1,ncyclesbg
        data(l)=data_cl_bg1(l,j)
82     continue
      call xmean(ncyclesbg,data,dum)
      smpl46_bg1=dum
      call stddev(ncyclesbg,smpl46_bg1,data,smpl46_bg1_err)
           smpl46_bg1_err=smpl46_bg1_err/dsqrt(dn)
! Smpl 47 bg1
      j=2
      do 83 l=1,ncyclesbg
        data(l)=data_cl_bg1(l,j)
83     continue
      call xmean(ncyclesbg,data,dum)
```

```
      smpl47_bg1=dum
      call stddev(ncyclesbg,smpl47_bg1,data,smpl47_bg1_err)
          smpl47_bg1_err=smpl47_bg1_err/dsqrt(dn)
! Std 46 bg1
      j=3
      do 84 l=1,ncyclesbg
        data(l)=data_cl_bg1(l,j)
84     continue
      call xmean(ncyclesbg,data,dum)
      std46_bg1=dum
      call stddev(ncyclesbg,std46_bg1,data,std46_bg1_err)
          std46_bg1_err=std46_bg1_err/dsqrt(dn)
! Std 47 bg1
      j=4
      do 85 l=1,ncycles
        data(l)=data_cl_bg1(l,j)
85     continue
      call xmean(ncyclesbg,data,dum)
      std47_bg1=dum
      call stddev(ncycles,std47_bg1,data,std47_bg1_err)
          std47_bg1_err=std47_bg1_err/dsqrt(dn)
```

```
!
! Smpl 46 bg2
      j=1
      do 86 l=1,ncyclesbg
        data(l)=data_cl_bg2(l,j)
86     continue
      call xmean(ncyclesbg,data,smpl46_bg2)
      call stddev(ncyclesbg,smpl46_bg2,data,smpl46_bg2_err)
          smpl46_bg2_err=smpl46_bg2_err/dsqrt(dn)
! Smpl 47 bg2
      j=2
      do 87 l=1,ncyclesbg
        data(l)=data_cl_bg2(l,j)
87     continue
      call xmean(ncyclesbg,data,smpl47_bg2)
      call stddev(ncyclesbg,smpl47_bg2,data,smpl47_bg2_err)
          smpl47_bg2_err=smpl47_bg2_err/dsqrt(dn)
! Std 46 bg2
      j=3
      do 88 l=1,ncyclesbg
        data(l)=data_cl_bg2(l,j)
```

```
88     continue
       call xmean(ncyclesbg,data,std46_bg2)
       call stddev(ncyclesbg,std46_bg2,data,std46_bg2_err)
            std46_bg2_err=std46_bg2_err/dsqrt(dn)
! Std 47 bg2
       j=4
       do 89 l=1,ncycles
         data(l)=data_cl_bg2(l,j)
89     continue
       call xmean(ncyclesbg,data,std47_bg2)
       call stddev(ncyclesbg,std47_bg1,data,std47_bg2_err)
            std47_bg2_err=std47_bg2_err/dsqrt(dn)
!
! At this point we have two backgrounds on either side of the 2-cup
! 47/46 measurements for this block.  We average these two backgrounds
! to arrive at a single background for 46 and for 47 to be subtracted
! from the data.
!
! SUBTRACT BACKGROUNDS FOR THIS BLOCK
!
       do 90 l=1,ncycles
```

```
        data_cl_bgcorr(l,1)=data_acid_cl(l,1)-
    &                   (smpl46_bg1+smpl46_bg2)/2.0D0
        data_cl_bgcorr(l,2)=data_acid_cl(l,2)-
    &                   (smpl47_bg1+smpl47_bg2)/2.0D0
        data_cl_bgcorr(l,3)=data_acid_cl(l,3)-
    &                   (std46_bg1+std46_bg2)/2.0D0
        data_cl_bgcorr(l,4)=data_acid_cl(l,4)-
    &                   (std47_bg1+std47_bg2)/2.0D0
90      continue
!
! Array data_cl_bgcorr(l,j) now contains four beam intensities for
! ncycles number of cycles for this block of data, corrected for backgrounds.
!
!
! CALCULATE CLUMPING PARAMETERS FOR THIS BLOCK OF DATA
BACKGROUND CORRECTED.
!
! Uncertainties from input d18O, d13C and 47CO2+/46CO2+ data are propagated
! using a Monte Carlo scheme for each cycle.  Final uncertainties for the
! block are taken from the cycle-to-cycle variability that includes
! propagation of uncertainties from all input parameters.
```

```
!
! Start loop for cycles
!
      do 105 l=1,ncycles
!
! d18O random draws for this cycle
        idum=-1
        call nrand(idum,nmax,d18O_acid_mean,d18O_acid_sigma,
     &       d18O_ran)
! d13C random draws for this cycle
        idum=-3
        call nrand(idum,nmax,d13C_acid_mean,d13C_acid_sigma,
     &       random2)
        do 94 k=1,nmax
          d13C_ran(k)=random2(k)
94      continue
!
! Ion correction for this cycle. Call to D47sub in this specific code
! includes the D47 of the reference gas being set to zero via the input
! file.  This is required if the absolute value of the sample is to be
! obtained from the "universal reference frame" calibration that utilizes
```

```
! D47 relative to reference gas as the x axis.  Otherwise, the absolute
! value for the sample D47 would have to come from the reference gas D47.
!
      I47_std=data_cl_bgcorr(l,4)
      I46_std=data_cl_bgcorr(l,3)
      I47_smpl=data_cl_bgcorr(l,2)
      I46_smpl=data_cl_bgcorr(l,1)
          do 100 k=1,nmax
            dummy=0.0D0
       d18O_smpl=d18O_ran(k)
       d13C_smpl=d13C_ran(k)
       call D47sub(d18O_smpl,d13C_smpl,I47_std,I46_std,
     &    I47_smpl,I46_smpl,R47_smpl_actual,R47_std_actual,
     &    R47_smpl,dummy)
       D47(k)=dummy
!
! This delta-47 is the sample relative to the reference gas. This is
! the parameter of interest for correcting for compositional non-linearity.
!
       dl47(k)=1000.0D0*(R47_smpl_actual/R47_std_actual-1.0D0)
!
```

```
100       continue  !Ends loop for Monte Carlo run for this data block
!
! Average estimates of D47 and d47 for this cycle.  Since the input
! uncertainty in the bulk isotopic composition was an uncertainty in
! the mean, the output stddev of the resulting values are a propagation
! of standard error, obviating the need to calculate std err from stdev.
!
              call xmean(nmax,D47,D47_cycle(l))
          call stddev(nmax,D47_cycle(l),D47,D47_cycle_err(l))
!          D47_cycle_err(l)=D47_cycle_err(l)/dsqrt(dble(ncycles))
!
              call xmean(nmax,dl47,dl47_cycle(l))
          call stddev(nmax,dl47_cycle(l),dl47,dl47_cycle_err(l))
!          dl47_cycle_err(l)=dl47_cycle_err(l)/dsqrt(dble(ncycles))
!
! End of calculations for this cycle
!
105     continue
!
! Average and standard error for these cycles, comprising a block.
! Uncertainty comes from adding the inter-cycle errors and the errors
```

```
! incurred from d18O and d13C alone in quadrature.  There will be some
! cross term as well, but for now this is assumed to be negligible.
!
      call xmean(ncycles,D47_cycle,D47_block(i))
!
! Standard error due to inter-cycle variability in measurements is simply
! standard deviation of the meausurements divided by sqrt of the number of
! cycles
!
      call stddev(ncycles,D47_block(i),D47_cycle,D47_block_err(i))
      D47_block_err(i)=D47_block_err(i)/dsqrt(dble(ncycles))
!
! Standard error due solely to uncertainties in d18O and d13C
! is obtained from the uncertainties in each cycle using a standard
! formula for uncertainty in the mean (std error)
!
      D47_block_bulk_err(i)=0.0D0
      do 110 l=1,ncycles
        D47_block_bulk_err(i)=D47_block_bulk_err(i)
     &              +D47_cycle_err(l)**2.0/dble(ncycles)
110     continue
```

```
      D47_block_bulk_err(i)=dsqrt(D47_block_bulk_err(i))
!
! Since d18O and d13C vs. inter-cycle variations are two independent
! sources of uncertainty in the mean, we add the standard errors in
! quadrature to arrive at the uncertainty in the mean for the block of
! cycles comprising this analysis.
!
      D47_block_err(i)=dsqrt(D47_block_err(i)**2.0
     &                +D47_block_bulk_err(i)**2.0)
!
! Repeat for d47...
!
      call xmean(ncycles,dl47_cycle,dl47_block(i))
!
      call stddev(ncycles,dl47_block(i),dl47_cycle,dl47_block_err(i))
      dl47_block_err(i)=dl47_block_err(i)/dsqrt(dble(ncycles))
!
      dl47_block_bulk_err(i)=0.0D0
      do 120 l=1,ncycles
        dl47_block_bulk_err(i)=dl47_block_bulk_err(i)
     &               +dl47_cycle_err(l)**2.0/dble(ncycles)
```

```
120     continue
!
       dl47_block_err(i)=dsqrt(dl47_block_err(i)**2.0
     &                 +dl47_block_bulk_err(i)**2.0)
!
! We now have raw D47 and d47 values for this block and their std errors in
! arrays D47_block(i), D47_block_err(i), dl47_block(i) and dl47_block_err(i).
!
            print*,'Block ',i,' background corrected:'
       print*,' D47 raw for this block = ',D47_block(i),'+/-',
     &   D47_block_err(i)
       print*,' d47 raw for this block = ',dl47_block(i),'+/-',
     &  dl47_block_err(i)
!
! D47 FOR THIS BLOCK, BACKGROUND CORRECTED, and its uncertainty based on the
! slope of the heated gas line.  Error in heated gas line slope is
! incorporated by standard propagation of errors along with errors in
! both d47 and D47 for this block.
!
            D47_block_bgl(i)=D47_block(i)-bgl_slope*dl47_block(i)
            D47_block_bgl_err(i)=(D47_block_err(i))**2.0+(bgl_slope**2.0)
```

```
     &  *(dl47_block_err(i)**2.0) + (dl47_block(i)**2)*(bgl_s_err**2.0)
       D47_block_bgl_err(i)=dsqrt(D47_block_bgl_err(i))
!
! We now have non-linearity (composition-dependent) corrected D47 for this
! block with its standard error stored in D47_block_bgl(i) and D47_block_bgl_err(i).
!
!
! REPEAT THE WHOLE CALCULATION WITH NO BACKGROUND CORRECTION OF
DATA.
!
! Start loop for cycles for no background corrected data calculations
!
       do 130 l=1,ncycles
!
! Ion correction for this cycle
!
          I47_std=data_acid_cl(l,4)
          I46_std=data_acid_cl(l,3)
          I47_smpl=data_acid_cl(l,2)
          I46_smpl=data_acid_cl(l,1)
c          d18O_smpl=d18O_acid_mean
```

```
c         d13C_smpl=d13C_acid_mean
             do 125 k=1,nmax
          d18O_smpl=d18O_ran(k)
          d13C_smpl=d13C_ran(k)
          call D47sub(d18O_smpl,d13C_smpl,I47_std,I46_std,
     &      I47_smpl,I46_smpl,R47_smpl_actual,R47_std_actual,
     &      R47_smpl,D47(k))
          dl47(k)=1000.0D0*(R47_smpl_actual/R47_std_actual-1.0D0)
125       continue  !Ends loop for Monte Carlo run for this data block
!
! Average estimates of D47 and d47 for this cycle
!
              call xmean(nmax,D47,D47_cycle(l))
         call stddev(nmax,D47_cycle(l),D47,D47_cycle_err(l))
         D47_cycle_err(l)=D47_cycle_err(l)/dsqrt(dble(ncycles))
!
              call xmean(nmax,dl47,dl47_cycle(l))
         call stddev(nmax,dl47_cycle(l),dl47,dl47_cycle_err(l))
         dl47_cycle_err(l)=dl47_cycle_err(l)/dsqrt(dble(ncycles))
!
! End of calculations for this cycle
```

```
!
130     continue
!
! Average and standard error for these cycles, comprising a block.
! Uncertainty comes from adding the inter-cycle errors and the errors
! incurred from d18O and d13C alone in quadrature.
!
       call xmean(ncycles,D47_cycle,D47_block_nobg(i))
!
! Standard error due to inter-cycle variability in measurements is simply
! standard deviation of the meausurements divided by sqrt of the number of
! cycles
!
       call stddev(ncycles,D47_block_nobg(i),D47_cycle,
     &       D47_block_err(i))
       D47_block_err(i)=D47_block_err(i)/dsqrt(dble(ncycles))
!
! Standard error due solely to uncertainties in d18O and d13C
! is obtained from the uncertainties in each cycle using a standard
! formula for uncertainty in the mean (std error)
!
```

```
      D47_block_bulk_err(i)=0.0D0
      do 135 l=1,ncycles
       D47_block_bulk_err(i)=D47_block_bulk_err(i)
     &              +D47_cycle_err(l)**2.0/dble(ncycles)
135   continue
!
! Since d18O and d13C vs. inter-cycle variations are two independent
! sources of uncertainty in the mean, we add the standard errors in
! quadrature to arrive at the uncertainty in the mean for the block of
! cycles comprising this analysis.
!
      D47_block_nobg_err(i)=dsqrt(D47_block_err(i)**2.0
     &              +D47_block_bulk_err(i)**2.0)
!
! Repeat for d47...
!
      call xmean(ncycles,dl47_cycle,dl47_block_nobg(i))
!
      call stddev(ncycles,dl47_block_nobg(i),dl47_cycle,
     &     dl47_block_err(i))
      dl47_block_err(i)=dl47_block_err(i)/dsqrt(dble(ncycles))
```

```
!
      dl47_block_bulk_err(i)=0.0D0
      do 140 l=1,ncycles
       dl47_block_bulk_err(i)=dl47_block_bulk_err(i)
   &              +dl47_cycle_err(l)**2.0/dble(ncycles)
140    continue
!
      dl47_block_nobg_err(i)=dsqrt(dl47_block_err(i)**2.0
   &               +dl47_block_bulk_err(i)**2.0)
!
! We now have raw D47 and d47 values for no background corrected version of
! this block and their std errors in arrays D47_block_nobg(i),
! D47_block_nobg_err(i), dl47_block-nobg(i) and dl47_block_nobg_err(i).
!
           print*,'Block ',i,' no background correction:'
      print*,' D47 raw for this block = ',D47_block_nobg(i),'+/-',
   &   D47_block_nobg_err(i)
      print*,' d47 raw for this block = ',dl47_block_nobg(i),'+/-',
   &  dl47_block_nobg_err(i)
!
```

```
! D47 FOR THIS BLOCK, NOT BACKGROUND CORRECTED, and its uncertainty based on
the
! slope of the non-background corrected heated gas line.  Error in heated
! gas line slope is incorporated by standard propagation of errors along with errors in
! both d47 and D47 for this block.
!
            D47_block_hgl(i)=D47_block_nobg(i)-hgl_slope*dl47_block_nobg(i)
            D47_block_hgl_err(i)=(D47_block_nobg_err(i))**2.0+(hgl_slope**2.0)
     &  *(dl47_block_nobg_err(i)**2.0) + (dl47_block_nobg(i)**2)
     &  *(hgl_s_err**2.0)
       D47_block_hgl_err(i)=dsqrt(D47_block_hgl_err(i))
!
! We now have non-linearity (composition-dependent) corrected D47 for this
! block with no background corrections and its standard error stored in
! D47_block_hgl(i) and D47_block_hgl_err(i).
!
!
! Repeat for next block of data...
!
! END LOOP 200 TO END THIS BLOCK OF DATA
!
```

```
200   continue
!
!
! UNIVERSAL REFERENCE FRAME CALUCLATIONS.
! Calculate D47 of CO2 clumping on a "universal" scale as
! proposed by Dennis et al. (2011).  This correction accounts for what
! the Caltech group refers to as stretching and what is a deviation in
! D47 for CO2 gases equilibrated at known T vs. the theoretical values
! of Wang et al. (2004).
!
! Errors in the mean are obtained by standard propagation of errors akin
! to dividing by sqrt of n but accounting for different uncertainties in
! measurements comprising the mean.
!
! First calculate results for the background-corrected data.
! Results stored in D47_bgl_u and D47_bgl_u_err. These are the CO2
! universal reference frame values and associated standard error.
!
        call xmean(n_2_acid,D47_block_bgl,D47_bgl)
        D47_bgl_err=0.0D0
        dn=dble(n_2_acid)
```

```
        do 205 i=1,n_2_acid
          D47_bgl_err=D47_bgl_err+(D47_block_bgl_err(i)**2.0)/(dn**2.0)
205   continue
        D47_bgl_err=dsqrt(D47_bgl_err)
!
     call xmean(n_2_acid,dl47_block,dl47_bgl)
        dl47_bgl_err=0.0D0
        dn=dble(n_2_acid)
        do 206 i=1,n_2_acid
          dl47_bgl_err=dl47_bgl_err+(dl47_block_err(i)**2.0)/
    &           (dn**2.0)
206   continue
        dl47_bgl_err=dsqrt(dl47_bgl_err)
!
     D47_bgl_u=calib_slope*D47_bgl+calib_int
     D47_bgl_u_err=(D47_bgl**2.0)*(calib_s_err**2.0)
    & +(calib_slope**2.0)*(D47_bgl_err**2.0) + calib_i_err**2.0
     D47_bgl_u_err=dsqrt(D47_bgl_u_err)
!
! Now repeat for the non-background corrected data, designated as hgl
! rather than bgl.
```

```
!
      call xmean(n_2_acid,D47_block_hgl,D47_hgl)
      D47_hgl_err=0.0D0
      dn=dble(n_2_acid)
      do 207 i=1,n_2_acid
        D47_hgl_err=D47_hgl_err+(D47_block_hgl_err(i)**2.0)/(dn**2.0)
207   continue
      D47_hgl_err=dsqrt(D47_hgl_err)
!
     call xmean(n_2_acid,dl47_block_nobg,dl47_hgl)
      dl47_hgl_err=0.0D0
      dn=dble(n_2_acid)
      do 208 i=1,n_2_acid
        dl47_hgl_err=dl47_hgl_err+(dl47_block_nobg_err(i)**2.0)/
    &           (dn**2.0)
208   continue
      dl47_hgl_err=dsqrt(dl47_hgl_err)
!
     D47_hgl_u=calib_slope*D47_hgl+calib_int
     D47_hgl_u_err=(D47_hgl**2.0)*(calib_s_err**2.0)
    & +(calib_slope**2.0)*(D47_hgl_err**2.0) + calib_i_err**2.0
```

```
      D47_hgl_u_err=dsqrt(D47_hgl_u_err)
!
! OUTPUT RESULTS.
!
! Print...
!
            print*,' '
            print*,'RESULTS +/- 1 STD ERR:'
      print*,'*(assumes acid digestion of carbonate at 25C):'
            print*,' '
            print*,'d18O SMOW       = ',d18O_acid_mean,'+/-',d18O_acid_sigma
            print*,'d18O carb SMOW  = ',d18O_carb,'+/-',d18O_carb_sigma
            print*,'d18O carb PDB   = ',d18O_PDB, '+/-',d18O_PDB_sigma
            print*,'d17O  SMOW      = ',d17O_acid_mean,'+/-',d17O_acid_sigma
            print*,'d13C  PDB       = ',d13C_acid_mean,'+/-',d13C_acid_sigma
            print*,'d47 bg corr     = ',dl47_bgl,'+/-',dl47_bgl_err
            print*,'D47 bg corr     = ',D47_bgl_u,'+/-',D47_bgl_u_err
            print*,'d47 no bg       = ',dl47_hgl,'+/-',dl47_hgl_err
            print*,'D47 no bg       = ',D47_hgl_u,'+/-',D47_hgl_u_err
!
! Create output file
```

```
!
      lexist=.false.
      inquire(file='indium_out.dat',exist=lexist)
           open(unit=13,file='indium_out.dat',access='append',
     & status='unknown')
      if(.not.lexist)then
        Titles(1)='d18O_SMOW'
        Titles(2)=' +/-'
        Titles(3)='d18O_carb'
        Titles(4)=' +/-'
        Titles(5)='d18O_PDB'
        Titles(6)=' +/-'
        Titles(7)='d17O_SMOW'
        Titles(8)=' +/-'
        Titles(9)='d13C_PDB'
        Titles(10)=' +/-'
        Titles(11)='d47_ref_bg'
        Titles(12)=' +/-'
        Titles(13)='D47_bg'
        Titles(14)=' +/-'
        Titles(15)='d47_ref'
```

```
      Titles(16)=' +/-'
      Titles(17)='D47 '
      Titles(18)=' +/-'
      Titles(19)='D47_bg_univ'
      Titles(20)=' +/-'
      Titles(21)='D47_univ'
      Titles(22)=' +/-'
      Write(13,800) (Titles(j),j=1,22)
800     format(1x,'sample_ID',11x,22(1x,A))
     endif
          write(13,900) sampleid,d18O_acid_mean,d18O_acid_sigma,d18O_carb,
    &  d18O_carb_sigma,d18O_PDB,d18O_PDB_sigma,d17O_acid_mean,
    &  d17O_acid_sigma,d13C_acid_mean,d13C_acid_sigma,
    &  dl47_bgl,dl47_bgl_err,D47_bgl,D47_bgl_err,dl47_hgl,dl47_hgl_err,
    &  D47_hgl,D47_hgl_err,D47_bgl_u,D47_bgl_u_err,
    &  D47_hgl_u,D47_hgl_u_err
900   format(1x,A,1x,22(1x,F11.4))
     close(unit=13)
!
! Close program
!
```

```
          print*,' '
          print*,'done...output in indium_out.dat'
      stop
      end
!
!*****************************************************************
          subroutine CO2_ion_corrections(I44_smpl,I44_std,I45_smpl,I45_std,
     & I46_smpl,I46_std,I47_smpl,I47_std,I48_smpl,I48_std,
     & d18O_smpl,d17O_smpl,d13C_smpl,D48_smpl)
!
! Performs usual Santrock et al. (1985) CO2 ion corrections based on
! input from 6-cup CO2 configuration on the UCLA MAT-253. Basic constants
! for the data reduction come from file CO2_parameters.in.
!
! D48_smpl is the delta value for measured 48CO2/44CO2 compared with the
! calculated stochastic value in per mil. This value is returned as a
! diagnostic for contamination of the CO2 sample.
!
! The calculations for 47CO2/44CO2 are not returned in this application
! because they are calculated using the 47CO2/46CO2 measurements using the
! peak hopping method developed at UCLA to avoid a wide cup on 47CO2+.
```

```
! If this program were to be used for a cup configuration with reliable
! 47CO2/44CO2 the list of arguments could be easily modified to return the
! D47 values calculated below.
!
! Inputs:
!
!               I44_smpl = ion current (voltage) for 44CO2+ for the sample gas
!                       .
!                       .
!           .
!
!               I48_std = ion current (voltage) for 48CO2+ for the std gas
!
! Outputs:
!
!               d18O_smpl = d18O of sample relative to SMOW
!               d17O_smpl = d17O of sample relative to SMOW
!               d13C_smpl = d13C of sample relative to PDB
!               D48_smpl  = d48CO2 of sample relative to stochastic
!
! EDY, June 19, 2011
```

```
!
!
      implicit double precision (a-h,o-z)
           double precision R18_SMOW,R17_SMOW,beta,R13_PDB,d18O_std,d13C_std,
     &     d18O_smpl,d13C_smpl,R18_std,R17_std,R18_smpl,R17_smpl,
     &     R45_smpl,R46_smpl,R45_std,R46_std,R47_std,R47_smpl
      double precision I44_smpl,I44_std,I45_smpl,I45_std,I46_smpl,
     &     I46_std,I47_smpl,I47_std,I48_smpl,I48_std,K
! ---------------------------------------------------------------------
! Input parameters for data reduction from file...
!
           open(unit=12,file='CO2_parameters.in',status='old')
            read(12,*) R18_SMOW
            read(12,*) R17_SMOW
            read(12,*) beta
            read(12,*) R13_PDB
            read(12,*) d18O_std
            read(12,*) d13C_std
            read(12,*) D47_std
           close(unit=12)
!
```

```
! ---------------------------------------------------------------------
! Calculate atomic ratios for standard
!
        R18_std=R18_SMOW*(d18O_std/1000.0D0 + 1.0D0)
        R17_std=R17_SMOW*(R18_std/R18_SMOW)**beta
        R13_std=R13_PDB*(d13C_std/1000.0D0 + 1.0D0)
!
! ---------------------------------------------------------------------
! Calculate stochastic isotopologue ratios for standard
!
        R45_std=R13_std+2.0D0*R17_std
        R46_std=2.0D0*R18_std+2.0D0*R13_std*R17_std+(R17_std)**2.0
        R47_std=R13_std*R17_std**2.0+2.0D0*R13_std*R18_std
    &       +2.0D0*R17_std*R18_std
     R48_std=R18_std**2.0+2.0D0*R13_std*R17_std*R18_std
!
! ---------------------------------------------------------------------
! Calculate actual 47CO2/44CO2 of standard from known D47_std
!
     R47_std_actual=R47_std*(D47_std/1000.0D0 +1.0D0)
!
```

```
! ------------------------------------------------------------------
! Calculate measured isotopologue ratios for standard from ion currents
!
    R45_std_meas=I45_std/I44_std
    R46_std_meas=I46_std/I44_std
    R47_std_meas=I47_std/I44_std
    R48_std_meas=I48_std/I44_std
!
! ------------------------------------------------------------------
! Calculate measured isotopologue ratios for sample from ion currents
!
    R45_smpl_meas=I45_smpl/I44_smpl
    R46_smpl_meas=I46_smpl/I44_smpl
    R47_smpl_meas=I47_smpl/I44_smpl
    R48_smpl_meas=I48_smpl/I44_smpl
!
! ------------------------------------------------------------------
! Calculate actual isotopologue ratios for sample
!
        R45_smpl=R45_std*(R45_smpl_meas/R45_std_meas)
        R46_smpl=R46_std*(R46_smpl_meas/R46_std_meas)
```

```
          R47_smpl_actual=R47_std_actual*(R47_smpl_meas/R47_std_meas)
          R48_smpl_actual=R48_std*(R48_smpl_meas/R48_std_meas)
!
! ---------------------------------------------------------------------
! Calculate atomic ratios for sample using Newton's method to find the
! root to equation 20 in Santrock et al. (1985).
!
      K=(R17_SMOW)/((R18_SMOW)**beta)
      R18_smpl=R46_smpl/2.0D0
      do 20 i=1,100
!       print*,'...iteration ',i,' R18_smpl = ',R18_smpl
       f=3.0*K**2.0D0*R18_smpl**(2.0*beta)-2.0D0*K*R45_smpl
     &*R18_smpl**beta-2.0D0*R18_smpl+R46_smpl
       fprime=3.0D0*(K**2.0)*2.0D0*beta*R18_smpl**(2.0D0*beta-1.0D0)
     &  -2.0D0*K*R45_smpl*beta*R18_smpl**(beta-1.0D0)-2.0D0
       if(abs(f).lt.1.0D-11) goto 21
       R18_smpl=R18_smpl-f/fprime
20     continue
21     continue
!
! R17_smpl from assumed fractionation law
```

```
!
      R17_smpl=K*R18_smpl**beta
!
! 13C/12C from correction for 12CO17O
!
      R13_smpl=R45_smpl-2.0D0*R17_smpl
!
! ----------------------------------------------------------------------
! Calculate stochastic R47 for sample from atomic ratios only
!
      R47_smpl=R13_smpl*R17_smpl**2.0+2.0D0*R13_smpl*R18_smpl
     &         +2.0D0*R17_smpl*R18_smpl
!
! ----------------------------------------------------------------------
! Calculate stochastic R48 for sample from atomic ratios only
!
      R48_smpl=R18_smpl**2.0+2.0D0*R18_smpl*R13_smpl*R17_smpl
!
! ----------------------------------------------------------------------
! Delta values of sample stochastic isotopologues to std
! stochastic isotopologues and d47 of actual sample to standard
```

```
!
        d45_smpl=1000.0D0*(R45_smpl/R45_std -1.0D0)
        d46_smpl=1000.0D0*(R46_smpl/R46_std -1.0D0)
        d47_smpl_std_stoch=1000.0D0*(R47_smpl/R47_std -1.0)
        d47_smpl_std=1000.0D0*(R47_smpl_actual/R47_std_actual -1.0D0)
        dsum = d45_smpl+d46_smpl
!
! ------------------------------------------------------------------
! Calculate D47 = measured 47CO2/44CO2 relative to stochastic
! 47CO2/44CO2 for the sample in per mil
!
    D47_smpl=1000.0D0*(R47_smpl_actual/R47_smpl -1.0D0)
!
! ------------------------------------------------------------------
! Calculate D48 = measured 48CO2/44CO2 relative to stochastic
! 48CO2/44CO2 for the sample in per mil
!
    D48_smpl=1000.0D0*(R48_smpl_actual/R48_smpl -1.0D0)
!
! ------------------------------------------------------------------
! Calculate delta values relative to SMOW for oxygen and PDB for carbon
```

```
! for the sample
!
    d18O_smpl=1000.0D0*(R18_smpl/R18_SMOW -1.0D0)
    d17O_smpl=1000.0D0*(R17_smpl/R17_SMOW -1.0D0)
    d13C_smpl=1000.0D0*(R13_smpl/R13_PDB -1.0D0)
!
! ---------------------------------------------------------------------
! Calculate raw delta-46/47 between sample and standard as a check for
! cup performance
!
    R47_46_smpl=R47_smpl_actual/R46_smpl
    R47_46_std=R47_std_actual/R46_std
    d47_46_smpl_std=1000.0D0*(R47_46_smpl/R47_46_std -1.0D0)
!
! Return to calling program
!
        return
        end
```

```
!
!*****************************************************************
        subroutine D47sub(d18O_smpl,d13C_smpl,I47_std,I46_std,
     &  I47_smpl,I46_smpl,R47_smpl_actual,R47_std_actual,
     &  R47_smpl,D47_smpl)
!
! Calculates D47 for CO2 gas samples from input reference and sample
! d18O_SMOW, d13C_PDB, D47_std and 47CO2+ and 46CO2+ ion currents for
! both the gas sample and the reference gas.
!
! This subroutine is required to reduce CO2 data on the UCLA MAT-253 using
! the peak-hopping technique that avoids the wide cup for 47CO2+.
!
! Basic constants for the data reduction come from file
! CO2_ion_corrections.in.
!
! Inputs:
!
!               d18O_smpl = d18O of sample gas relative to SMOW
!               d13C_smpl = d13C of sample gas relative to PDB
!               I47_std   = Ion current for 47CO2 of the reference gas
```

```
!                I47_smpl  = Ion current for 47CO2 of the sample gas
!                I46_std   = Ion current for 46CO2 of the reference gas
!                I46_smpl  = Ion current for 46CO2 of the sample gas
!
! where ion currents refer to voltages on the MAT-253.
!
! Outputs:
!
!                R47_smpl_actual = 47CO2/44CO2 of sample gas measured
!                R47_smpl        = 47CO2/44CO2 stochastic, calculated
!                D47_smpl        = 10^3*(R47_smple_actual/R47_smpl-1)
!
! where the last value is the D_47 for reporting.  Because of
! compositional non-linearity in measurements, the D_47 above must either
! be corrected for compositional effects where reference gas and sample
! gas are not identical in d47 or this value should be compared with a
! heated (i.e., scrambled) equivalent of the sample.
!
! EDY, June 19, 2011
!
!
```

```
!
!
      implicit double precision (a-h,o-z)
           double precision R18_SMOW,R17_SMOW,beta,R13_PDB,d18O_std,
     &  d13C_std,d18O_smpl,d13C_smpl,R18_std,R17_std,R18_smpl,R17_smpl,
     &  R45_smpl,R46_smpl,R45_std,R46_std,R47_std,R47_smpl
      double precision I47_std,I46_std,I47_smpl,I46_smpl
!
! Input parmaters from CO2_parameters.in
!
           open(unit=12,file='CO2_parameters.in',status='old')
            read(12,*) R18_SMOW
            read(12,*) R17_SMOW
            read(12,*) beta
            read(12,*) R13_PDB
            read(12,*) d18O_std
            read(12,*) d13C_std
            read(12,*) D47_std
           close(unit=12)
! ---------------------------------------------------------------------
! Calculate atomic ratios for standard
```

```
!
        R18_std=R18_SMOW*(d18O_std/1000.0D0 + 1.0D0)
        R17_std=R17_SMOW*(R18_std/R18_SMOW)**beta
        R13_std=R13_PDB*(d13C_std/1000.0D0 + 1.0D0)
!
! ------------------------------------------------------------------
! Calculate atomic ratios for sample
!
        R18_smpl=R18_SMOW*(d18O_smpl/1000.0D0 + 1.0D0)
        R17_smpl=R17_SMOW*(R18_smpl/R18_SMOW)**beta
        R13_smpl=R13_PDB*(d13C_smpl/1000.0D0 + 1.0D0)
!
! ------------------------------------------------------------------
! Calculate stochastic isotopologue ratios for standard
!
        R45_std=R13_std+2.0D0*R17_std
        R46_std=2.0D0*R18_std+2.0D0*R13_std*R17_std+(R17_std)**2.0
        R47_std=R13_std*R17_std**2.0+2.0D0*R13_std*R18_std
    &       +2.0D0*R17_std*R18_std
!
! ------------------------------------------------------------------
```

```
! Calculate actual 47CO2/44CO2 of standard
!
     R47_std_actual=R47_std*(D47_std/1000.0D0 +1.0D0)
!
! ---------------------------------------------------------------------
! Calculate actual 47CO2/46CO2 of standard
!
     R4746_std_actual=R47_std_actual/R46_std
!
! ---------------------------------------------------------------------
! Calculate stochastic isotopologue ratios for sample
!
          R45_smpl=R13_smpl+2.0D0*R17_smpl
          R46_smpl=2.0D0*R18_smpl+2.0D0*R13_smpl*R17_smpl+(R17_smpl)**2.0
          R47_smpl=R13_smpl*R17_smpl**2.0+2.0D0*R13_smpl*R18_smpl
     &       +2.0D0*R17_smpl*R18_smpl
!
! ---------------------------------------------------------------------
! Calculate actual 47CO2/44CO2 of sample from 47/46 ratios of sample
! and standard
!
```

```
      R4746_smpl_meas=I47_smpl/I46_smpl
      R4746_std_meas=I47_std/I46_std
      R4746_smpl_actual=
     &            R4746_smpl_meas*(R4746_std_actual/R4746_std_meas)
      R47_smpl_actual=R4746_smpl_actual*R46_smpl
      d4746_smpl_std=1000.0D0*(R4746_smpl_actual/R4746_std_actual-1.0D0)
!
! ------------------------------------------------------------------
! Delta values of sample stochastic isotopologues to std
! stochastic isotopologues
!
            d45_smpl=1000.0D0*(R45_smpl/R45_std -1.0D0)
            d46_smpl=1000.0D0*(R46_smpl/R46_std -1.0D0)
            d47_smpl_stoch=1000.0D0*(R47_smpl/R47_std -1.0D0)
            dsum = d45_smpl+d46_smpl
!
! ------------------------------------------------------------------
! Calculate D47 of sample, i.e. 47CO2/44CO2 relative to stochastic
! for the sample
!
      D47_smpl=1000.0D0*(R47_smpl_actual/R47_smpl -1.0D0)
```

```
!
! Return to calling program
!
          return
          end



!**********************subroutine xmean*******************************
      subroutine xmean(n,x,avg)
c
c Computes the mean of a set of values in array x. Integer n is the
c dimension of the array x containing the data to be averaged.
c
      integer n
      double precision x(n),avg
      rn=dble(n)
      avg=0.00D0
      do 10 i=1,n
        avg=avg+x(i)
10    continue
      avg=avg/rn
```

```
      return
      end



!************************subroutine stddev*****************************
      subroutine stddev(n,avg,x,sigma)
c
c Computes the standard deviation for a set of values in array x. The
c integer n is the dimension of the array x containing the data.
c The returned standard deviation is in variable sigma.
c
      integer n
      double precision x(n),sigma,avg
      rn=real(n)
      sqdiff=0.00
      do 10 i=1,n
        sqdiff=sqdiff+(x(i)-avg)**2.0
10    continue
      temp=sqdiff/(rn-1.00)
      sigma=sqrt(temp)
      return
```

```
      end
*****************************function ran1***********************************
      function ran1(IDUM)
c
c Returns a uniform random deviate between 0.0 and 1.0. Set IDUM to any
c negative value to initialize or reinitialize the sequence. Routine comes
c from Numerical Recipes (Press et al. , 1986, p. 196) and is a portable
c replacement (and improvement over) system routines.
c
      save
      dimension r(97)
      parameter (M1=259200,IA1=7141,IC1=54773,RM1=1./M1)
      parameter (M2=134456,IA2=8121,IC2=28411,RM2=1./M2)
      parameter (M3=243000,IA3=4561,IC3=51349)
      data iff /0/
      if(IDUM.lt.0.or.iff.eq.0)then
        iff=1
        IX1=MOD(IC1-IDUM,M1)
        IX1=MOD(IA1*IX1+IC1,M1)
        IX2=MOD(IX1,M2)
        IX1=MOD(IA1*IX1+IC1,M1)
```

```
      IX3=MOD(IX1,M3)
      do 11 j=1,97
        IX1=MOD(IA1*IX1+IC1,M1)
        IX2=MOD(IA2*IX2+IC2,M2)
        r(j)=(float(IX1)+float(IX2)*RM2)*RM1
11     continue
      IDUM=1
    endif
    IX1=MOD(IA1*IX1+IC1,M1)
    IX2=MOD(IA2*IX2+IC2,M2)
    IX3=MOD(IA3*IX3+IC3,M3)
    j=1+(97*IX3)/M3
    if(j.gt.97.or.j.lt.1)pause
    ran1=r(j)
    r(j)=(float(IX1)+float(IX2)*RM2)*RM1
    return
    end
**************************subroutine urand**********************************
    subroutine urand(idum,n,rlow,rhigh,x)
c--------------------------------------------------------------------------
c URAND gives an array of n random numbers x from a uniform distribution
```

```
c with boundaries rlow and rhigh. Random numbers between 0 and 1 are
c provided by function RAN1. Arguments are:
c
c          n     =  number of random ``draws'' from distribution
c
c       rlow     =  lower bound of uniform distribution
c
c      rhigh     =  upper bound of uniform distribution
c
c          x     =  n-dimensional array of random numbers
c                   drawn from distribution (rlow,rhigh)
c
c       idum     =  negative integer to intitialize random number
c                   generator ran1
c
c-------------------------------------------------------------------------
      integer n,idum
      double precision x(n),rlow,rhigh
      do 10 i=1,n
        r=ran1(idum)
        x(i)=dble(r)*(rhigh-rlow)+rlow
```

```
10    continue
      return
      end
**************************subroutine nrand**********************************
      subroutine nrand(idum,n,rmean,stdev,x)
c-----------------------------------------------------------------------
c NRAND gives an array of n random numbers x from a normal distribution
c defined by parameters rmean (mean) and stdev (standard deviation). The
c routine utiizes function RAN1 to generate random numbers
c between 0 and 1. The algorithm for the integrated probability density
c function for a Gaussian distribution used here is described by Harbaugh
c and Bonham-Carter (1970, Computer Simulation in Geology, Wiley, p. 69,
c 82-84).
c
c Arguments are:
c
c          n     =  number of random ``draws'' from distribution
c
c       rmean    =  mean for parent Gaussian distribution
c
c       stdev    =  standard deviation for parent Gaussian distribution
```

```
c
c          x    =  n-dimensional array of real random numbers
c                  drawn from distribution (rmean,stdev)
c
c         idum   =  negative integer to initialize random number
c                  generator ran1
c
c--------------------------------------------------------------------------
      integer n,idum
      double precision x(n),rlow,rhigh,rsum,stdev,rmean
      do 10 i=1,n
        rsum=0.0D0
        do 5 j=1,12
          r=dble(ran1(idum))
          rsum=rsum+r
5       continue
        x(i)=(rsum-6.0D0)*stdev+rmean
10    continue
      return
      end
```

A-2 References

Dennis K. J., Affek H. P., Passey B. H., Schrag D. P. and Eiler J. M. (2011) Defining an absolute reference frame for 'clumped' isotope studies of CO_2. *Geochim. Cosmochim. Acta* **75**, 7117–7131.

Friedman I. and O'Neil J.R. (1977) *Compilation of stable isotope fractionation factors of geochemical interest* **440** USGPO.

Huntington K.W., Eiler J.M., Affek H.P., Guo W., Bonifacie M., Yeung L.Y., Thiagarajan N., Passey B.H., Tripati A., Daëron M. and Came R. (2009) Methods and limitations of 'clumped' CO_2 isotope (Δ_{47}) analysis by gas-source isotope ratio mass spectrometry. *J. Mass Spectrom*. **44**, 1318–1329.

Santrock J., Studley S. A. and Hayes J. M.(1985) Isotopic analyses based on the mass spectrum of carbon dioxide. *Anal. Chem.* **57**, 1444–1448.

Wang Z., Schauble E.A. and Eiler J. M. (2004) Equilibrium thermodynamics of multiply

substituted isotopologues of molecular gases. *Geochim. Cosmochim. Acta* **68**, 4779–4797.